

NOAA Technical Memorandum NMFS-SEFC-6



OBSERVATIONS OF TEMPERATURE, CURRENT, AND WIND VARIATIONS OFF THE CENTRAL EASTERN COAST OF FLORIDA DURING 1970 AND 1971

Thomas D. Leming
August 1979

U.S. DEPARTMENT OF COMMERCE
National Oceanic and Atmospheric Administration
National Marine Fisheries Service
Southeast Fisheries Center
National Fisheries Engineering Laboratory
NSTL Station, Mississippi 39529

NOAA Technical Memorandum NMFS-SEFC-6



OBSERVATIONS OF TEMPERATURE, CURRENT, AND WIND VARIATIONS OFF THE CENTRAL EASTERN COAST OF FLORIDA DURING 1970 AND 1971

Thomas D. Leming
August 1979

U.S. DEPARTMENT OF COMMERCE
Juanita M. Kreps, Secretary
National Oceanic and Atmospheric Administration
Richard A. Frank, Administrator
National Marine Fisheries Service
Terry L. Leitzell, Assistant Administrator for Fisheries

This TM series is used for documentation and timely communication of preliminary results, interim reports, or similar special purpose information. Although the memos are not subject to complete formal review, editorial control, or detailed editing, they are expected to reflect sound professional work.

PREFACE

The major portion of this technical memorandum constituted a thesis submitted to the faculty of the University of Miami in partial fulfillment of the requirements for the degree of Master of Science.

OBSERVATIONS OF TEMPERATURE, CURRENT, AND WIND VARIATIONS OFF THE
CENTRAL EASTERN COAST OF FLORIDA DURING 1970 AND 1971. (JUNE, 1979)

THOMAS D. LEMING*

ABSTRACT

Results of an approximately monthly series of XBT transects during 1971 near Cape Canaveral revealed a pronounced seasonal difference in thermal structure over the continental shelf. Temperature sections were averaged to portray four major seasonal conditions: winter-spring, summer, fall, and winter. The coastal waters were strongly vertically stratified during summer and nearly isothermal in winter. Typical horizontal temperature gradients at 100 m depth averaged $7.5^{\circ}/8$ km and $1.0^{\circ}/8$ km for summer and winter, respectively. This was interpreted as due to increased strength and onshore movement of the Florida Current during the summer months, which was accompanied by intrusion of cold ($<18^{\circ}\text{C}$) water along the bottom onto the shelf. Following offshore retreat of the Florida Current, cold water lenses 80 km long, 10 km wide, and 5 m thick remained over the bottom in the mid-shelf zone (20 to 40-m depth).

Long term measurements of surf temperature, bottom temperatures at 20 m, and wind stress revealed fluctuations over a wide band of time scales from 2 to 23 days and longer. All temperature records during summer contained negative temperature anomalies which were associated with upwelling favorable wind stress. Spectrum analyses for two seasonally different (winter/summer), overlapping records (approximately $4\frac{1}{2}$ months long) of bottom temperature, surf temperature, and wind stress showed that temperature was significantly coherent with the alongshore wind stress for both seasons at a period of 11.5 days. Fluctuations at that period were interpreted as continental shelf waves. During winter, temperature was also found to be significantly coherent with the wind stress at 3 to 4-day and 5 to 6-day periods. The summer temperatures were coherent with the stress near the 3-day period. Phase relations between temperature and wind stress were highly frequency dependent for both seasons; however, in the 3 to 4-day period band and at the 11.5-day period, the phase between temperature and the alongshore wind stress was consistent with that expected from upwelling due to wind-driven Ekman divergence at the coastal boundary.

Short term (one month) measurements of wind stress, bottom (20 m) currents, and temperatures during June to July 1970 revealed an oscillatory northwestward - southeastward flow with periodicities of 3 to 10 days, consistent with bottom Ekman cross-shelf flow driven by alongshore interior flow. Typical onshore-offshore and alongshore velocities were 3 to 4 cm/sec and 6 to 7 cm/sec, respectively. Onshore flow was generally associated with decreasing temperature and upwelling favorable wind stress. An apparent upwelling "event" during late July 1971 was evident in four bottom-mounted thermograph records as well as the surf temperature. From the horizontal sea-surface temperature field, the surface temperature depression was confined to a narrow coastal zone north of Cape Canaveral. The width of the apparent upwelling zone (\approx

*National Fisheries Engineering Laboratory
NSTL Station, MS 39529

17 km) was approximately the estimated local Rossby deformation radius. A vorticity analysis suggested that the apparent asymmetry of the upwelling could be induced by the change in vorticity along a streamline in flow (both northward and southward) around Cape Canaveral.

A 50-hour current and temperature profiling anchor station was maintained near the shelfbreak (102-m depth) off Cape Canaveral during late July 1971. Mean velocity profiles showed that the flow was nearly aligned with the local bathymetry. The mean alongshore velocity had a subsurface maximum of 184 cm/sec at a depth of 20 m, near the top of the thermocline in the mean temperature profile. The perturbation velocity fields suggested that: 1) The onshore-offshore flow was nearly depth-independent and fluctuated with an apparent half-period of at least 36 to 40 hours; 2) The alongshore flow contained both the 36 to 40 hour fluctuation and an apparently longer time scale of half-period at least 48 to 50 hours; 3) Both components exhibited near-inertial motion in the upper 30 to 50 m. The perturbation temperature field was consistent with onshore-offshore advection of the horizontal temperature gradient associated with the Florida Current and geostrophic adjustment to the alongshore flow variations. Estimates of the gradient Richardson Number suggested that the flow was unstable in the strongly sheared upper mixed layer (15 m). Maximum values of Ri occurred in the middle of the water column (20 to 70 m) and in the bottom 10 m when the alongshore flow was at a minimum in those zones.

An empirical orthogonal function (EOF) analysis of the velocity data revealed that the first EOF's accounted for about 87% of the variance in u and 61% in v . The second EOF for v accounted for 29% of the variance and had a temporal variation similar to the first EOF for u which indicated an apparent 3 to 4-day period. The vertical structure of these two EOF's was consistent with that predicted by Wang and Mooers (1976) for the first mode topographic Rossby wave for intermediate stratification. The expected upwelling over the shelfbreak during onshore flow was strongly suggested by the upward bowing of isotherms in an XBT section made just prior to the anchor station.

ACKNOWLEDGEMENTS

I would like to thank Dr. J. P. Geisler and Dr. John Van Leer for their criticism, suggestions, and assistance with administrative requirements. I owe special thanks to Dr. Christopher N. K. Mooers for his patience, encouragement, and guidance.

I would also like to thank Dr. Andrew J. Kemmerer, Director of the National Fisheries Engineering Laboratory, for providing the opportunity to complete this study. Mr. Hillman J. Holley provided considerable assistance with computer programming. Many hours of valuable discussions were spent with Dr. David Brooks.

TABLE OF CONTENTS

	<u>PAGE</u>
1.0 INTRODUCTION AND OBJECTIVES	1
1.1 Florida Current Effects	1
1.2 Data Acquisition and Rationale	6
1.3 Thesis Objectives	12
1.4 Organization	13
2.0 THERMAL FIELD	15
2.1 Mean Conditions	15
2.2 Temporal and Spatial Variability	21
2.3 Short Term Variation and Alongshore Extent of Summer Intrusions	26
3.0 TEMPERATURE AND WIND TIME SERIES ANALYSIS	32
3.1 Data Processing	32
3.1.1 Bottom Temperature	32
3.1.2 Surf Temperature	33
3.1.3 Wind Stress	33
3.2 General Characteristics of Time Domain	33
3.3 The Frequency Domain	39
3.3.1 Sample Statistics	40
3.3.2 Cross-Spectrum Analysis: W71	46
3.3.3 Cross-Spectrum Analysis: S71	51
3.3.4 Phase Relations	55
4.0 CURRENT AND TEMPERATURE STRUCTURE AT SHELFBREAK	56
4.1 Data Acquisition and Processing	56
4.2 Mean Velocity and Temperature Profiles	57
4.3 Temporal Variations of Velocity and Temperature	61
4.4 Temporal Variations of the Perturbation Velocity and Temperature	70
4.5 Stability Estimates	75
4.6 Empirical Orthogonal Functions	79
5.0 SPECIFIC EVENTS	87
5.1 Temperature, Currents, and Winds - Summer, 1970	87
5.2 An Apparent Upwelling Event - A Closer Look	93
5.2.1 Time Variations	93
5.2.2 Horizontal Variations	96
5.2.3 Effects of Cape Canaveral	99

TABLE OF CONTENTS

	<u>PAGE</u>
6.0 SUMMARY AND CONCLUSIONS	106
BIBLIOGRAPHY	167
<u>APPENDIX</u>	
A Spectrum Analysis of Selected Wind Stress and Temperature Records	115
A.1 Data Analyzed	115
A.2 April to July 1970	115
A.3 November 1970 to January 1971	120
A.4 March to May 1971	127
A.5 July to August 1971	134
B Results Significant to Calico Scallop	144
B.1 Current Effects	144
B.2 Temperature Effects	146
C Individual XBT Sections	151
D Tabularized Daily Surf Temperature and Daily Mean Bottom Temperatures	161

LIST OF ILLUSTRATIONS

<u>FIGURE</u>	<u>TITLE</u>	<u>PAGE</u>
1.1	Plan view of Florida Straits and South-Atlantic Bight with locations referred to in text. The general study area is shaded.	2
1.2	Study area with location of data acquisition sites.	7
2.1	Averaged temperature section along Transect 3 for January, March, and April 1971.	16
2.2	Averaged temperature section along Transect 3 for May, June, July, and August 1971.	17
2.3	Temperature section along Transect 3 for November 1971.	18
2.4	Temperature section along Transect 3 for December 1971.	19
2.5	Time-depth temperature contours for inner shelf, mid-shelf, and shelfbreak stations along Transect 3. The depth scale for the shelfbreak station is one-half that for the inner and mid-shelf stations. Asterisks indicate months with no date.	22
2.6	Intersection with bottom of 18°C isotherm by month from XBT. Numbers refer to month of year (1971).	24
2.7	Intersection with bottom of 15°C isotherm by month from XBT. Numbers refer to month of year (1971).	25
2.8	Temperature section along Transect 3 run between 2235 EDT, 23 July and 0250 EDT, 24 July 1971. The 18°C isotherm is dashed for emphasis.	27
2.9	Temperature section along Transect 3 run between 1107 EDT and 1508 EDT, 26 July 1971. The 18°C isotherm is dashed for emphasis.	28
2.10	Bottom temperature from XBT measurements for 23 to 25 July 1971. Contour interval is 1°C. Solid lines indicate the XBT transects used.	30
3.1	Low pass filtered wind stress vectors, surf temperature, and bottom temperature (BY1, BY2) for 1970 and 1971. Wind stress vectors are plotted daily while temperatures are 8-hourly. Vertical lines indicate major temperature events in the record referred to in the text.	35
3.2	Low-passed onshore-offshore (USTR) and alongshore (VSTR) wind stress components, surf temperature at Daytona Beach (SFT), and bottom temperature at BY1 for W71; 5 January to 18 May 1971.	41

<u>FIGURE</u>	<u>TITLE</u>	<u>PAGE</u>
3.3	Low-passed onshore-offshore (USTR) and alongshore (VSTR) wind stress components, surf temperature at Daytona Beach, and bottom temperature at BY2 for S71; 21 March to 20 August 1971.	42
3.4	Autospectra for USTR, VSTR, SFT, and BY1; W71. Normalization factors are given in parentheses. $N = 399$ $\Delta t = 8$ hours, $M = 69$, $BW_e = 0.027$ cpd, $DOF = 14.5$.	47
3.5	Coherence squared and phase for SFT vs. USTR and VSTR, BY1 vs. USTR and VSTR, and for SFT vs. BY1; W71. $N = 399$, $\Delta t = 8$ hours, $M = 69$, $BW_e = 0.027$ cpd, $DOF = 14.5$.	48
3.6	Autospectra for USTR, VSTR, SFT, and BY2; S71. Normalization factors are given in parentheses. $N = 455$, $\Delta t = 8$ hours, $M = 69$, $BW_e = 0.027$ cpd, $DOF = 16.5$.	52
3.7	Coherence squared and phase for SFT vs. USTR and VSTR, BY2 vs. USTR and VSTR, and for SFT vs. BY2; S71. $N = 455$, $\Delta t = 8$ hours, $M = 69$, $BW_e = 0.027$ cpd, $DOF = 16.5$.	53
4.1	Mean profiles of temperature (\bar{T}), onshore (-) - offshore (+) velocity (\bar{U}) and alongshore velocity (\bar{V}) from 50 hour anchor station (36 hours for temperature). Coordinate system has been rotated 10° counter-clockwise from true north. $\bar{U} (+10^\circ)$ and $\bar{U} (-10^\circ)$ are average profiles for a further $\pm 10^\circ$ coordinate rotation. Horizontal bars indicate the 95% confidence limits for the estimate of the mean.	58
4.2	Time-depth contours of the onshore (-) - offshore (+) component (u) of velocity for the 50 hour anchor station. The standard contour interval is 10 cm/sec with departures indicated by dashed contours. Negative values (onshore flow) are shaded. Blank areas are gaps in the data due to the profiling current meter's failure to reach the bottom.	62
4.3	Time-depth contours of the alongshore component (v) of velocity for the 50 hour anchor station. The standard contour interval is 20 cm/sec with departures indicated by dashed contours. Negative values (south-southeastward flow) are shaded. Blank areas are gaps in the data due to the profiling current meter's failure to reach the bottom.	63
4.4	Temperature section along Transect 3 run between 1107 EDT and 1508 EDT, 26 July 1971. Vertical line at the shelfbreak indicates location of anchor station.	65

<u>FIGURE</u>	<u>TITLE</u>	<u>PAGE</u>
4.5	Time-depth contours of temperature for anchor station. The XBT recorder failed after 36 hours. The standard contour interval is 1.0°C with departures indicated by dashed contours.	67
4.6	Comparison of calculated alongshore geostrophic velocity (dotted line) with measured mean profile from 50 hour anchor station (solid line). Geostrophic velocity is established between XBT stations 57 and 59 (Fig. 4.4). Both profiles are referenced to zero surface velocity. Horizontal bars indicate the 95% confidence limits for the estimate of the measured mean.	69
4.7	Time-depth contours of the perturbation onshore-offshore component (u) of velocity for the 50 hour anchor station. The standard contour interval is 10 cm/sec with departures indicated by dashed contours. Negative anomalies are shaded. Blank areas are gaps in the data due to the profiling current meter's failure to reach the bottom.	71
4.8	Time-depth contours of the perturbation alongshore (v) component of velocity for the 50 hour anchor station. The standard contour interval is 20 cm/sec with departures indicated by dashed contours. Negative anomalies are shaded. Blank areas are gaps in the data due to the profiling current meter's failure to reach the bottom.	72
4.9	Time-depth contours of perturbation temperature for the anchor station. The XBT recorder failed after 36 hours. The standard contour interval is 0.5°C with departures indicated by dashed contours. Negative anomalies are shaded.	73
4.10	Mean profiles of static stability ($\overline{N^2}$), velocity shear (\overline{S}), and gradient Richardson Number (Ri) for the anchor station.	77
4.11	Time-depth contours of the gradient Richardson Number (Ri) for the anchor station. Contours are for $R_i = 0.25, 0.5, 1.0, 10.0$ and 100.0 . Areas where $R_i \leq 0.25$ are shaded and $R_i \geq + 1.0$ striped.	78
4.12	Empirical orthogonal functions (EOF) I, II, and III for the u and v velocity components. Percent of variance accounted for by each EOF is indicated.	82
4.13	Time variation of first two empirical orthogonal functions (EOF-I, II) for the u and v velocity components.	83

<u>FIGURE</u>	<u>TITLE</u>	<u>PAGE</u>
5.1	Daily mean temperature at BY1, onshore-offshore (USTR) and alongshore (VSTR) wind stress components, and semi-daily mean onshore-offshore (U) and alongshore (V) bottom current components at BY2 for the period of 28 May to 1 July 1970.	88
5.2	Progressive vector diagram for bottom current at BY2; 28 May to 1 July 1970. Each point represents semi-daily mean. Circled points are labeled with date. Horizontal axis scale is exaggerated by a factor of two relative to vertical axis.	90
5.3	Approximate onshore-offshore and alongshore bottom current displacement amplitudes at BY2, and daily mean bottom temperature at BY1 for 28 May to 1 July 1970. Displacements are from semi-daily mean current components.	92
5.4	Daily mean values for USTR, VSTR, SFT, BY1, BY2, CM1 and CM2 for 26 June to 23 July 1971. Data for USTR, VSTR, SFT, BY1 and BY2 are extended to 5 August to show temperature depression. Dashed diagonal lines indicate assumed correspondence of temperature minima.	94
5.5	Surface temperature during XBT survey for 23 to 25 July 1971: R/V VENTURE Cruise 7102. Dots indicate station locations. Also indicated are locations of measurements for USTR, VSTR, SFT, BY1, BY2, CM1 and CM2.	97
5.6	Streamlines for idealized flow around Cape Canaveral with signs of terms in equation (2): (a) southward flow (b) northward flow. Points P, Q, and M are referred to in text.	103
A.1	Low-passed u and v wind stress components (USTR, VSTR) and bottom temperature (BY1) for 1 April to 11 July 1970.	116
A.2	Autospectra for USTR, VSTR, and BY1; 1 April to 11 July 1970, Normalization factors are given in parentheses. $N = 303$, $\Delta t = 8$ hours, $M = 54$, $BW_e = 0.035$ cpd, $DOF = 14.0$.	119
A.3	Coherence squared and phase for BY1 vs. USTR and VSTR; 1 April to 11 July 1970. $N = 303$, $\Delta t = 8$ hours, $M = 54$, $BW_e = 0.035$ cpd, $DOF = 14.0$.	121
A.4	Low-passed u and v wind stress components (USTR, VSTR), and bottom temperatures at BY1 and BY2 for 16 November 1970 to 18 January 1971.	122

<u>FIGURE</u>	<u>TITLE</u>	<u>PAGE</u>
A.5	Autospectra for USTR, VSTR, BY1 and BY2; 16 November 1970 to 18 January 1971. Normalization factors are given in parentheses. $N = 189$, $\Delta t = 8$ hours, $M = 33$, $BW_e = 0.057$ cpd, $DOF = 14.3$.	125
A.6	Coherence squared and phase for BY1 and BY2 vs. USTR and VSTR, and BY2 vs. BY1; 16 November 1970 to 18 January 1971. $N = 189$, $\Delta t = 8$ hours, $M = 33$, $BW_e = 0.057$ cpd, $DOF = 14.3$.	126
A.7	Low-passed u and v wind stress components (USTR, VSTR), surf temperature (SFT), and bottom temperature at BY1 and BY2 for 21 March to 18 May 1971.	128
A.8	Autospectra for USTR, VSTR, SFT, BY1 and BY2; 21 March to 18 May 1971. Normalization factors are given in parentheses. $N = 174$, $\Delta t = 8$ hours, $M = 21$, $BW_e = 0.089$ cpd, $DOF = 20.7$.	131
A.9	Coherence squared and phase for SFT and BY1 vs. USTR and VSTR; 21 March to 18 May 1971. $N = 174$, $\Delta t = 8$ hours, $M = 21$, $BW_e = 0.089$ cpd, $DOF = 20.7$.	132
A.10	Coherence squared and phase for BY2 vs. USTR and VSTR, SFT vs. BY1 and BY2, and BY2 vs. BY1; 21 March to 18 May 1971. $N = 174$, $\Delta t = 8$ hours, $M = 21$, $BW_e = 0.089$ cpd, $DOF = 20.7$.	133
A.11	Low passed u and v wind stress components (USTR, VSTR), surf temperature at Daytona Beach (SFT), and bottom temperatures at BY1 and BY2 for 1 July to 18 August 1971.	135
A.12	Autospectra for USTR, VSTR, SFT, BY1 and BY2; 1 July to 18 August 1971. $N = 144$, $\Delta t = 8$ hours, $M = 27$, $BW_e = 0.069$ cpd, $DOF = 13.3$.	139
A.13	Coherence squared and phase for SFT and BY1 vs. USTR and VSTR; 1 July to 18 August 1971. $N = 144$, $\Delta t = 8$ hours, $M = 27$, $BW_e = 0.069$ cpd, $DOF = 13.3$.	140
A.14	Coherence squared and phase for BY2 vs. USTR and VSTR; SFT vs. BY1 and BY2; and BY2 vs. BY1: 1 July to 18 August 1971. $N = 144$, $\Delta t = 8$ hours, $M = 27$, $BW_e = 0.069$ cpd, $DOF = 13.3$.	141
C.1	Vertical XBT temperature sections, 25-27 January 1971.	150
C.2	Vertical XBT temperature sections, 11-12 March 1971.	151
C.3	Vertical XBT temperature sections, 15-17 April 1971.	152
C.4	Vertical XBT temperature sections, 20-21 May 1971.	153

<u>FIGURE</u>	<u>TITLE</u>	<u>PAGE</u>
C.5	Vertical XBT temperature sections, 28-29 June 1971.	154
C.6	Vertical XBT temperature sections, 24-26 July 1971.	155
C.7	Vertical XBT temperature sections, 30-31 August 1971.	156
C.8	Vertical XBT temperature sections, 2-3 November 1971.	157
C.9	Vertical XBT temperature sections, 1-2 December 1971.	158

LIST OF TABLES

<u>NUMBER</u>	<u>TITLE</u>	<u>PAGE</u>
1.1	Data acquisition logistics including time line for each data unit used.	8
1.2	Cruise number, date and transects covered for XBT surveys. Transect numbers refer to those shown in Figure 1.2.	10
3.1	Statistics for low-pass filtered onshore-offshore (USTR) and alongshore (VSTR) wind stress components, surf temperature (SFT), and bottom temperature (BY1, BY2) for the two data subsets W71 and S71.	44
3.2	Correlation coefficients and lag adjustment for onshore-offshore (USTR) and alongshore (VSTR) wind stress components, surf temperature (SFT), and bottom temperature at BY1, BY2 for W71, S71.	45
4.1	Approximated temperature-salinity relationship for geostrophic velocity computations. Values are based on results given by Parr (1937).	68
4.2	Empirical orthogonal function variance.	81
A.1	Statistics for low-passed u and v wind stress components (USTR, VSTR) and bottom temperature at BY1 for 1 April to 11 July 1970. Record length = 303 points. $\Delta t = 8$ hours.	118
A.2	Statistics for low-passed u and v wind stress components (USTR, VSTR) and bottom temperatures at BY1, BY2 for 16 November 1970 to 18 January 1971. Record length = 189 points. $\Delta t = 8$ hours.	125
A.3	Statistics for low-passed u and v wind stress components (USTR, VSTR), surf temperature at Daytona Beach (SFT), and bottom temperatures at BY1 and BY2 for 21 March to 18 May 1971. Record length = 174. $\Delta t = 8$ hours.	129
A.4	Statistics for low-passed u and v wind stress components (USTR, VSTR), surf temperature at Daytona Beach (SFT), and bottom temperature at BY1 and BY2 for 1 July to 18 August 1971. Record length = 144. $\Delta t = 8$ hours.	137
B.1	Percentage distribution of the daily mean bottom temperature observations by temperature interval for BY1; 27 August 1970 to 24 August 1971.	147

LIST OF TABLES

<u>NUMBER</u>	<u>TITLE</u>	<u>PAGE</u>
D.1	Daily surf temperature (°C) at Sun Glow Fishing Pier, Daytona Beach, Florida for 1971.	160
D.2	Daily mean bottom temperatures (°C) at BY1 for 1970. Missing data are due to instrument loss or malfunction.	161
D.3	Daily mean bottom temperatures (°C) at BY1 for 1971. Missing data are due to instrument loss or malfunction.	162
D.4	Daily mean bottom temperatures (°C) at BY2 for 1970 and 1971. Missing data are due to instrument loss or malfunction.	163
D.5	Daily mean bottom temperatures (°C) at CM1 and CM2 during June, July, 1971.	164

1. INTRODUCTION AND OBJECTIVES

The occurrence of anomalously low sea-surface temperatures during the summer months along the central and northern east coast of Florida was first reported by Green (1944), and then confirmed by Wagner (1957). Taylor and Stewart (1959) analyzed coastal water temperature records from U.S. Coast and Geodetic Survey tide stations. They found that the summer occurrences of low water temperatures were associated with reduced sea level and upwelling favorable winds. The greatest temperature anomalies ($6\text{ }^{\circ}\text{C}$) appeared between Daytona Beach and Canova Beach. The anomalies never occurred at stations north of Fernandina Beach and only rarely south of Canova Beach (Fig. 1.1).

Stone and Azarovitz (1968) also reported unusually low surface water temperatures during the summer. Utilizing surface temperature data from U.S. Coast Guard Airborne Radiation Thermometer (ART) flights, the authors discovered an unusually cold patch of surface water off St. Lucie Inlet (Fig. 1.1) on 20 June 1968. The temperature depression, compared to the same data from the previous year, was about $7\text{ }^{\circ}\text{C}$. The authors speculated that the anomaly resulted from upwelling favorable winds produced by tropical storms "Abby" and "Brenda" as they crossed the southern portion of Florida during the first three weeks of June, 1968.

1.1 Florida Current Effects

The possible effects of Florida Current meanders and eddies on the shelf circulation near Cape Canaveral were largely ignored in these previous studies. Bumpus (1964) conducted hydrographic studies in the area during March and April, and August 1962. Vertical sections of tempera-

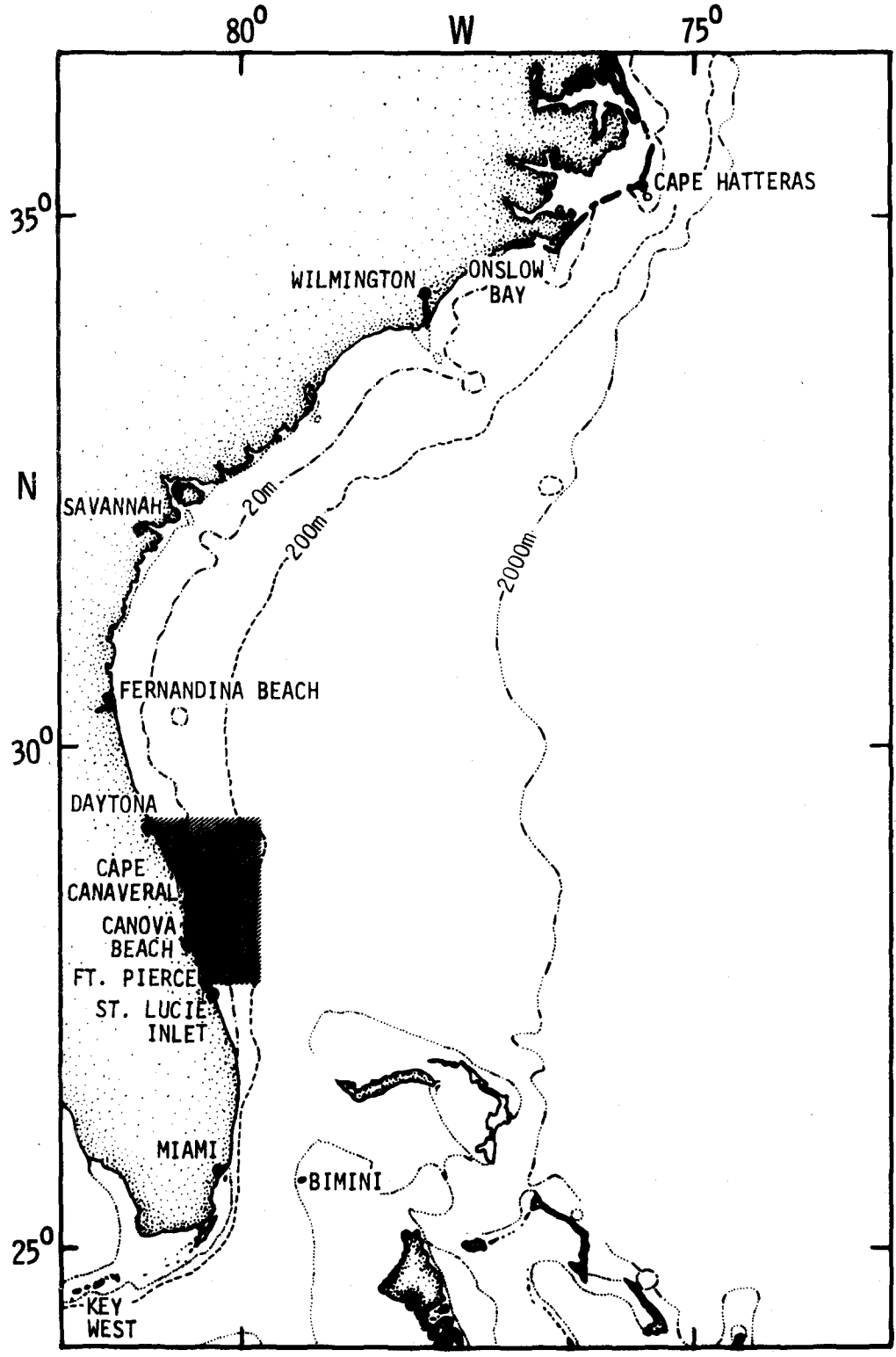


Figure 1.1. Plan view of Florida Straits and South-Atlantic Bight with locations referred to in text. The general study area is shaded.

ture and salinity were made on several transects normal to the coast. Results indicated that the coastal waters were relatively well-mixed, both horizontally and vertically, in temperature and salinity during the winter to spring season. The August sections showed, however, an intense vertical stratification over the shelf which was primarily temperature dependent. These results are very similar to the horizontal and vertical temperature and salinity distributions found over the continental shelf off Onslow Bay, North Carolina (Fig. 1.1) by several investigators (Bumpus, 1955; Bumpus and Pierce, 1955; Webster, 1961; Blanton, 1971; Stefánsson, Atkinson and Bumpus, 1971). These authors proposed that the circulation and hydrographic properties over the shelf off Onslow Bay may be dominated, especially during summer, by horizontal variations in the axial position of the Gulf Stream. Webster (1961) stated that Gulf Stream meanders off Onslow Bay with horizontal amplitudes of 10 km were apparently related to the onshore component of the wind stress.

The meandering of the Gulf Stream and Florida Current has been the subject of many recent studies. Mysak and Hamon (1969) found southward propagating sea level disturbances along the North Carolina coast which they believed to be barotropic continental shelf waves forced by atmospheric pressure fluctuations, with periods of 3 to 10 days. Mooers and Brooks (1977) examined sea level and thermistor string temperature data between Miami and Bimini. They found that, for fluctuation time scales of several days to monthly, the ocean fields were strongly coupled to the local wind stress. Brooks and Mooers (1977a) developed a model for the propagation of barotropic continental shelf waves (CSW) in a horizontally sheared barotropic current. Results indicated that southward propagating CSW's occur with periods of 10 to 14 days, wavelengths of 180 to 200 km,

and a phase speed of about 17 cm/sec for the first mode. Brooks and Mooers (1977b) examined annual records of sea level, oceanic temperature, winds and atmospheric pressure in the Florida Straits. They found that a significant fraction of the subinertial frequency fluctuations of the Florida Current occurred at periods of 7 to 10 days in winter and 12 to 14 days in summer. These fluctuations were strongly coupled to both components of the local wind stress. The sea level array along the east coast of Florida confirmed the existence of southward propagating disturbances with alongshore coherence scales of 300 to 400 km. Düing, Mooers and Lee (1977) analyzed current meter records from the Miami Terrace and found the predominant low frequency fluctuations of the Florida Current to occur at time scales of 2 to 3, 4 to 5, and 8 to 25 days. Brooks (1978) demonstrated that sea level fluctuations in Onslow Bay were strongly coupled to atmospheric forcing in the 2.5 to 3.5 day and 10 day and greater period bands. The wavelength and southwestward propagation phase speed for the first mode, zero group speed shelf wave (2.5 to 3.5 day period) were about 420 km and 150 km/day, respectively. The observed sea level phase lags in Onslow Bay (Brooks, 1978) and off Florida (Brooks and Mooers, 1977b) indicated that the CSW's travelled faster than expected from the theory.

Interpretations of meanders are not based totally on continental shelf wave theory. Orlandi (1969) considered the stability effects of bottom topography on a two-layer jet. The model results indicated that baroclinic instabilities may occur which differ markedly for simulated conditions upstream and downstream from Cape Hatteras. The most unstable disturbance upstream (south) of Cape Hatteras had a wavelength of about 220 km and a period of 10 pendulum days. Wavelength and period for the

most unstable wave downstream of Cape Hatteras were 365 km and 37.4 pendulum days, respectively. Orlanski and Cox (1973) expanded on the baroclinic instability theory with a three dimensional numerical model. In agreement with the two-layer model, the current was found to be baroclinically unstable for typical Gulf Stream parameters. Typical wavelengths of 100 to 400 km were found. Niiler and Mysak (1971) developed a model for the propagation of barotropic oscillations imbedded in an intense, laterally-sheared, western boundary current. The most unstable waves were found to propagate northward with wavelengths of about 150 km and periods of about 10 days.

Small diameter, northward propagating, cyclonic edge eddies of the Florida Current were found to occur in southeast Florida coastal waters at intervals of 1 to 2 days (Lee, 1975). Typical eddy dimensions were 10 km in the east-west direction and 20 to 30 km north-south. Characteristic northward translation speeds were about 25 cm/sec. Eddies appeared to be associated with horizontal wave-like meanders of the Florida Current with time scales ranging from 2 to 10 days (Lee and Mayer, 1977).

In addition, seasonal fluctuations occur in the Gulf Stream due to changes in the large-scale North Atlantic circulation (Fuglister, 1951). Schmitz and Richardson (1969) found that the seasonal transport fluctuations were as much as 1/3 the mean transport. Niiler and Richardson (1973) found a pronounced seasonal variation with the maximum transport occurring during June.

This review is not meant to be complete; however, significant variations in the Florida Current near Miami are very similar to those in the South-Atlantic Bight area. Furthermore, these fluctuations were shown to

have a controlling influence on the shelf circulation system off North Carolina. It seems reasonable to assume that similar processes may occur over the Florida shelf near Cape Canaveral.

1.2 Data Acquisition and Rationale

The data presented in this thesis are from a program initiated in 1970 by the National Marine Fisheries Service (NOAA). The purpose of the study was to investigate the life history and biology of the calico scallop (Argopecten gibbus), a species discovered to be commercially abundant in the coastal waters off Cape Canaveral, Florida. One program goal was to relate changes of environmental variables (primarily temperature and currents) to calico scallop spawning, growth, and mortality. The data acquisition effort was designed as a habitat (i.e., the bottom) monitoring project and not as an investigation of physical oceanographic processes. Thus, most of the long term measurements of temperature and currents were from bottom-mounted instruments.

The study area and data acquisition sites are shown in Figure 1.2. The shelf width ranges from about 20 km off Ft. Pierce Inlet to about 75 km near Daytona Beach. The shelfbreak (edge) is at a depth of about 100 m. Following is a description of each data unit. A time line for each data unit is presented in Table 1.1.

1. Horizontal and Vertical Temperature

A series of approximately monthly expendable bathythermograph (XBT) transects were made over one year during 1971. Five standard transects were established (Transects 1 to 5, Fig. 1.2) beginning inshore at about the 20 m isobath and extending offshore to the 300 m isobath. Typical horizontal station spacing was about 5 km and 15 km in the offshore and

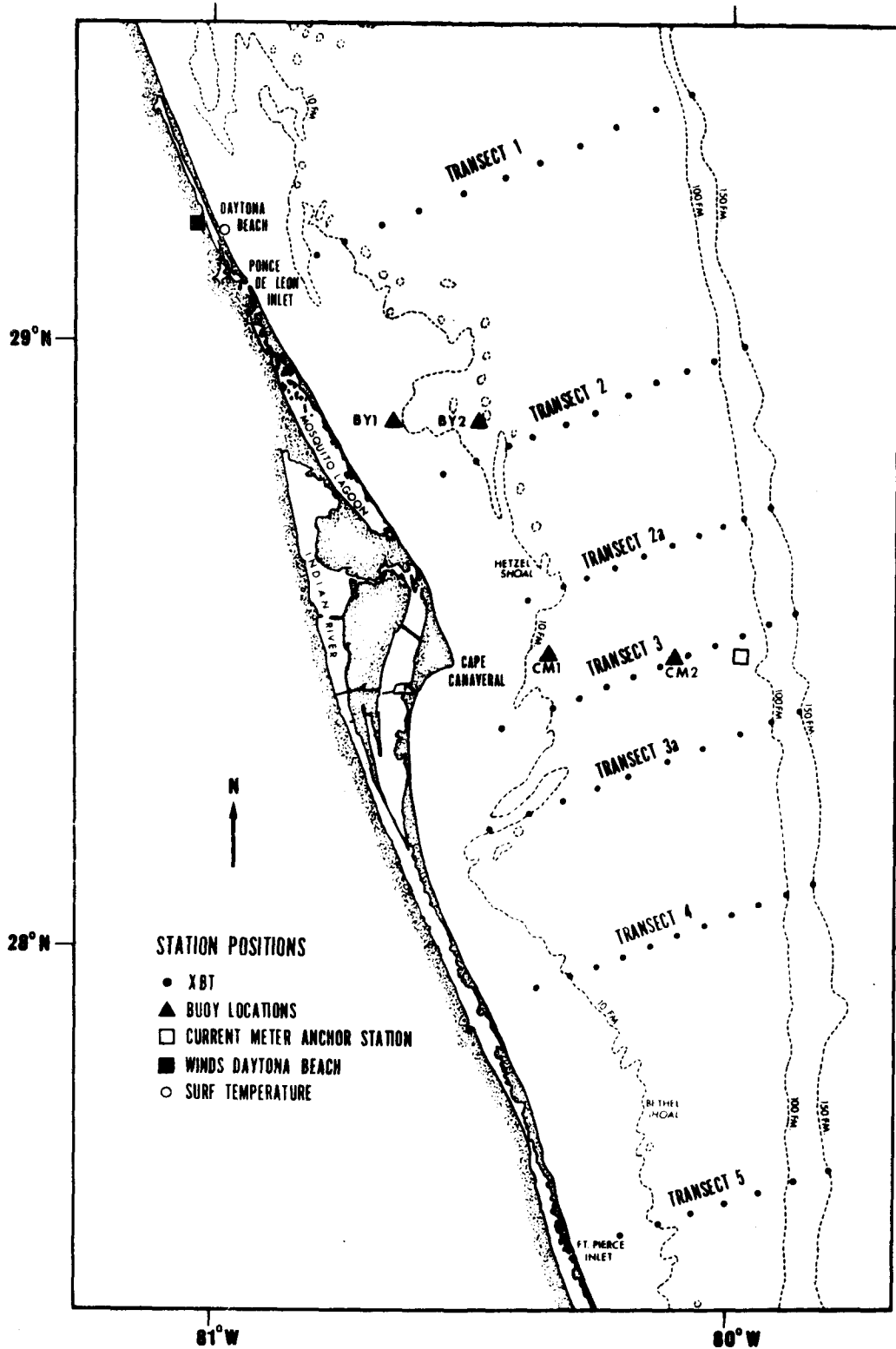


Figure 1.2. Study area with location of data acquisition sites.

alongshore directions respectively. Two supplementary transects (2a and 3a) were occupied during the June and July cruises, respectively. Transect 2a was also occupied in January. Not all transects were successfully run every month because of foul weather, equipment failures and vessel scheduling difficulties. The dates and transects actually occupied for each cruise are given in Table 1.2. All XBT lowerings were calibrated by bucket thermometer and the traces adjusted accordingly.

2. Bottom Temperature and Current

Two biological buoy sites were established (BY1, BY2; Fig. 1.2) to monitor scallop biology, water temperature and currents. Locations, water depths, and record periods, are given in Table 1.1. Record gaps are due either to instrument failure or loss.

Braincon model 531 recording thermographs, with a sampling interval of 20 minutes, were mounted on biological study cages or tripods about 1 m above the bottom. Each instrument was calibrated in a temperature bath before emplacement. All were found to be within the manufacturer's specifications of $\pm 0.3^{\circ}\text{C}$ accuracy and a thermal response of 10 minutes to 95% of full value. The timing mechanism was an Accutron clock with estimated accuracy of ± 2 seconds per day. Two additional buoys were implanted (CM1, CM2; Fig. 1.2) during the June XBT cruise. Each site contained a thermograph and a Geodyne model 102-0 film recording current meter mounted in a tripod approximately 1 m from the bottom. The current meter at CM1 was retrieved flooded, and the interval timer failed on the current meter at CM2; therefore, the thermograph record lengths are shown as CM1 and CM2 in Table 1.1. From 28 May to 1 July 1970 simulta-

TABLE 1.2. Cruise number, date and transects covered for OXT surveys. Transect numbers refer to those shown in Figure 1.2.

<u>Ship</u>	<u>Cruise Number</u>	<u>Date</u>	<u>Transects</u>
R/V BOWERS	7101	25-27 Jan 71	2a, 3, 4, 5
R/V BOWERS	7102	11-12 Mar 71	1, 2, 3, 4, 5
R/V BOWERS	7103	15-17 Apr 71	1, 2, 3, 4, 5
R/V BOWERS	7104	20-21 May 71	1, 2, 3, 4, 5
R/V VENTURE	7101	28-29 Jun 71	2a, 3, 3a
R/V VENTURE	7102	24-26 Jul 71	2, 3 (twice), 3a, 4, 5
R/V BOWERS	7105	30-31 Aug 71	1, 2, 3, 4, 5
R/V BOWERS	7106	02-03 Nov 71	1, 2, 3, 4
R/V VIRGINIA KEY	7102	01-02 Dec 71	2, 3, 4, 5

neous records of bottom temperature at BY1 and bottom current at BY2 were obtained (Table 1.1).

3. Surface Water Temperature

A full year (1971) of surf temperature data, measured daily at the Sun Glow fishing pier, Daytona Beach, were acquired from the National Climatic Center (NCC), Asheville, N.C. The approximate location is shown in Figure 1.2 and the record length is given in Table 1.1.

4. Winds

Wind data from the Daytona Beach airport (Fig. 1.2) also were acquired from the NCC. Wind speed and direction, recorded every 3 hours, were keypunched and recorded on magnetic tape for further analysis. The station location and record duration are given in Table 1.1.

5. Current and Temperature Profile

During the July XBT cruise, an anchor station was established near the offshore end of Transect 3 (Fig. 1.2). A profiling current meter system developed at the University of Miami (Dúing and Johnson, 1972) was used to measure the vertical distribution of horizontal current speed and direction every 90 minutes over a 50-hour period. Expendable bathythermograph measurements of the vertical temperature profile were made simultaneously; however, the XBT recorder failed after 36 hours. Water depth at the anchor station was 102 m.

During the 1971 summer cruises, repeated attempts were made to obtain salinity concurrently with vertical temperature measurements. Two different self-contained STD instruments were used and neither operated

properly. Due to funding constraints, no further salinity measurements were possible.

1.3 Thesis Objectives

The general objectives of this thesis address the following questions:

1. What are the mean vertical and horizontal thermal conditions in the coastal waters near Cape Canaveral?
 - a. What are the seasonal variations?
 - b. To what extent does the Florida Current control the thermal field over the shelf and when?
2. What are the predominant time scales present in bottom temperature records?
 - a. Can these temperature variations be related to fluctuations of the local wind stress and/or the Florida Current?
 - b. Do the temperature records indicate an apparent coastal upwelling (cooling) during the summer?
 - c. What are the seasonal variations of predominant time scales of the temperature records?
3. What is the mean vertical structure of temperature and horizontal currents occurring near the shelfbreak off Cape Canaveral?
 - a. What are the short term temporal variations of these variables?
 - b. Can the thermal and velocity variations be logically related?
4. What is the general character of specific events in the temperature record?

- a. Can large negative temperature anomalies during the summer be explained by wind-driven coastal upwelling or other processes?
5. How well can these measurements be explained by existing theory and previous observations?
6. What is the significance of the observations to the calico scallop fishery?
7. What are some recommendations for future experiments in the area?

1.4 Organization

The data analyses in this thesis deal with numerous different data types acquired at different locations and various times. Reasons for the somewhat sporadic data set character were alluded to in Chapter 1.2. Therefore, to avoid confusion, each chapter will introduce the particular data considered with a discussion of the data preparation and handling. The thesis is divided into six chapters which are briefly summarized below:

Chapter 1. Introduction and Objectives.

Chapter 2. The results of approximately monthly XBT surveys during 1971 are presented. First, the horizontal and vertical mean thermal fields are depicted as composite sections for four primary time periods: winter - early spring, summer fall, and early winter. Specific temperature sections are then used to depict the temporal changes in thermal structure throughout the year with emphasis on intrusions of offshore water during the summer months.

Chapter 3. Bottom temperature, surf temperature, and wind stress for two seasonally different, overlapping records are analyzed by standard

time series techniques to determine the temporal fluctuation scales and their relationships. Additional shorter time series are analyzed and results presented in Appendix A.

Chapter 4. Results of a 50-hour current and temperature profiling anchor station (July 1971) at the shelfbreak are presented. Mean profiles, time-depth variations, and results of an empirical orthogonal function analysis of the currents are discussed.

Chapter 5. Specific events (large, abrupt changes) in the bottom temperature records, primarily during summer, are examined in more detail combining results from the XBT surveys, wind stress measurements, and one bottom current record (June, 1970) of short duration. An attempt is made to generalize the character of these events in light of other observational and theoretical work.

Chapter 6. The results of the research are summarized and conclusions presented. The objectives stated in Chapter 1.3 are then addressed, and recommendations are presented for future work. Results considered significant to the calico scallop are discussed in Appendix B. Vertical temperature sections for every XBT Transect are presented in Appendix C.

2. THE THERMAL FIELD

2.1 Mean Conditions

Since Transect 3 (Fig. 1.2) was the only XBT section occupied on every cruise (Table 1.2), the temperatures from this transect were used to develop composite temperature plots. The data for the individual cruises were plotted, then grouped for those months for which the thermal structure was most similar. The results from the January, March, and April cruises were averaged to form a mean temperature section. Similarly, a mean temperature section was constructed from XBT sections for the May, June, July and August cruises. However, the thermal structure found in November was strikingly dissimilar to that of December; therefore, those two sections were plotted individually. The results are shown in Figures 2.1 to 2.4.

The mean section for January, March and April was representative of temperature conditions for late winter and early spring (Fig. 2.1). The inner shelf area was nearly isothermal at about 20°C. The thermal field over the outer shelf and slope was stratified with the isotherms sloping nearly linearly downward in the offshore direction. This tilted thermal structure was associated with the internal mass field of the Florida Current. The bottom temperature decreased offshore from about 19.8°C at station 1 to 16.8°C at station 7 near the shelfbreak (75 m depth). The horizontal temperature gradient at 100 m between stations 8 and 10 was $\frac{\Delta T}{\Delta X} \approx \frac{4^\circ\text{C}}{8 \text{ km}}$. Except perhaps for the nearshore area (stations 1 and 2), the entire shelf thermal structure was influenced by the sloping isotherms associated with the Florida Current.

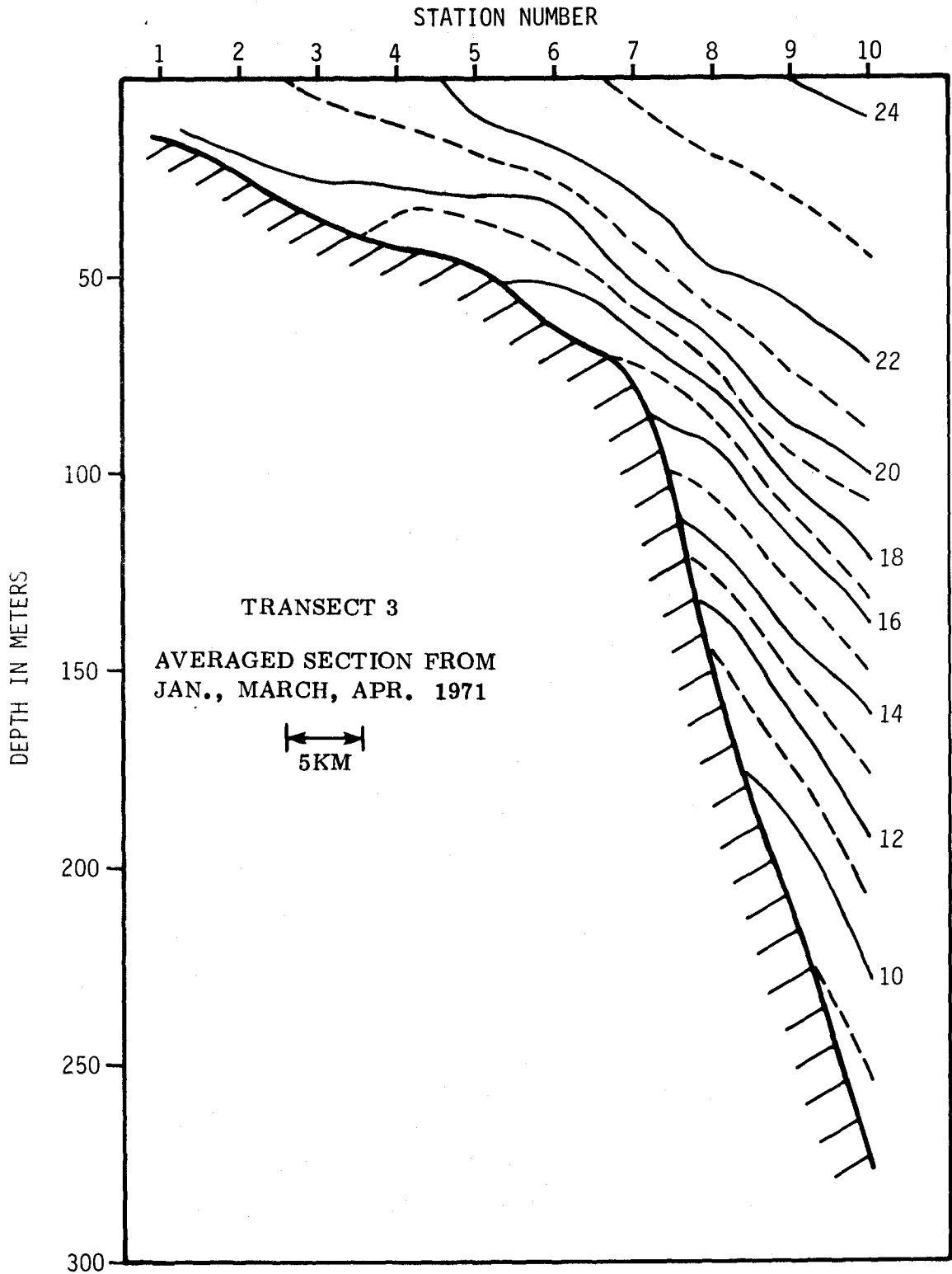


Figure 2.1. Averaged temperature section along Transect 3 for January, March, and April 1971.

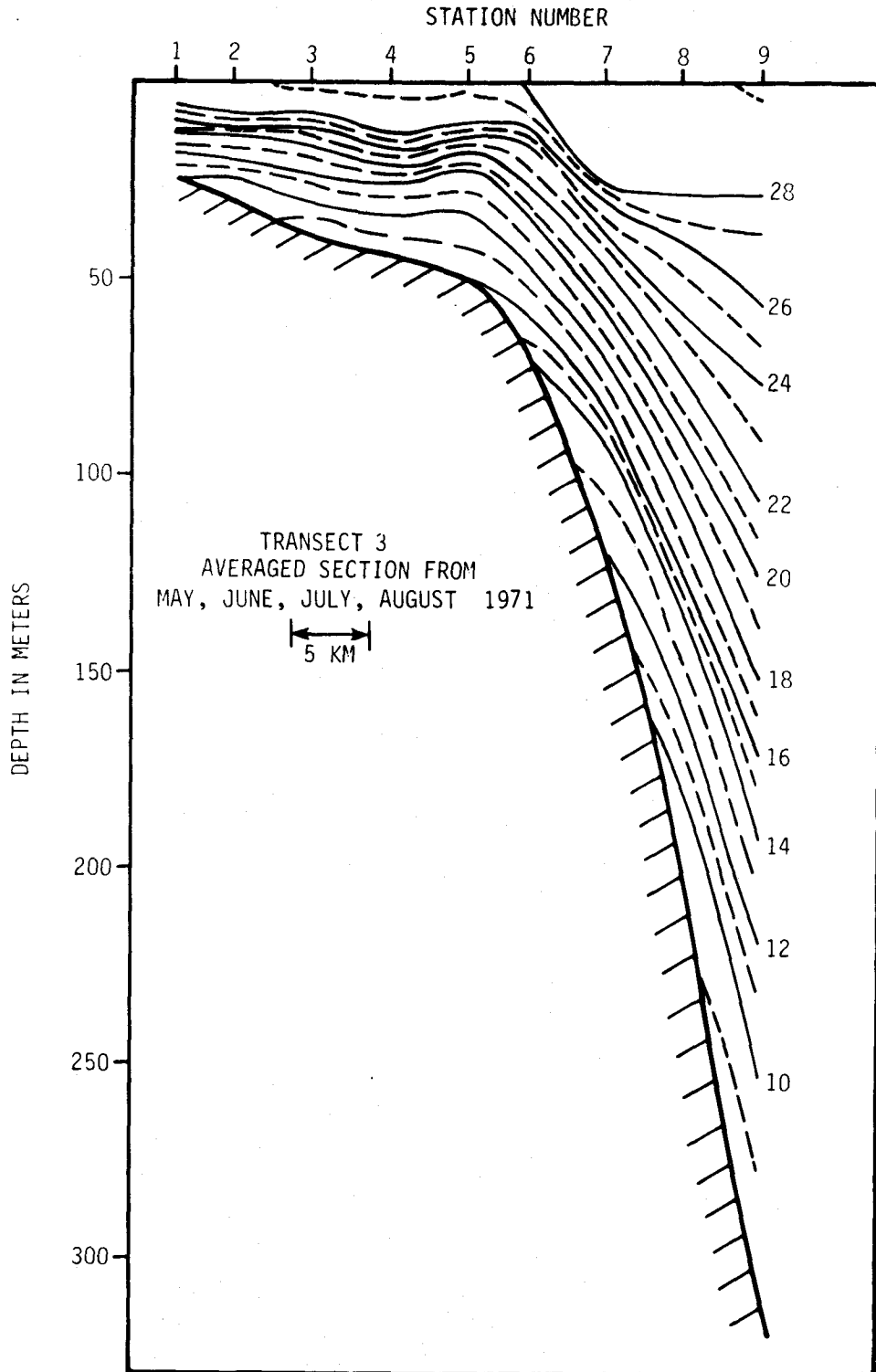


Figure 2.2. Averaged temperature section along Transect 3 for May, June, July, and August 1971.

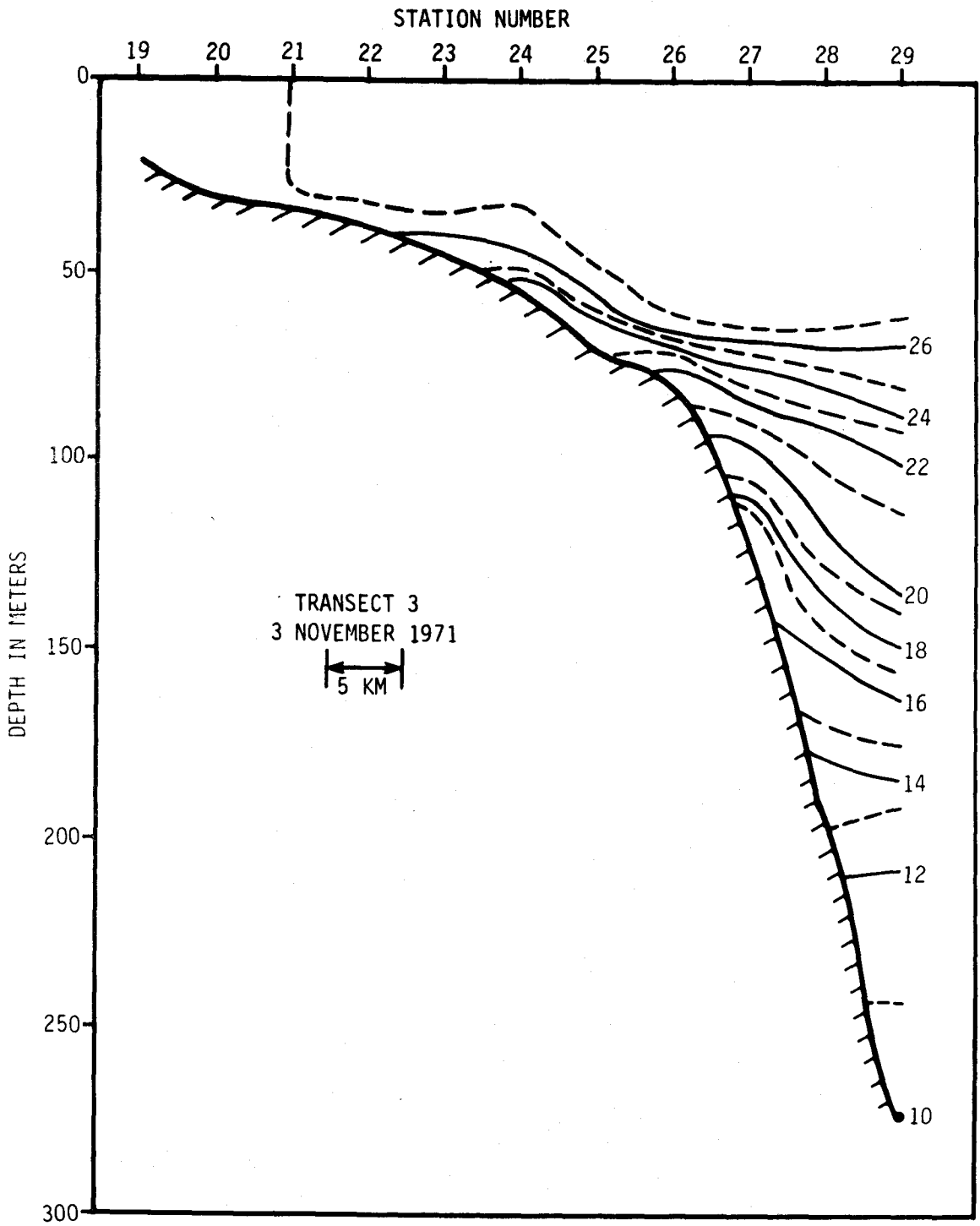


Figure 2.3. Temperature section along Transect 3 for November 1971.

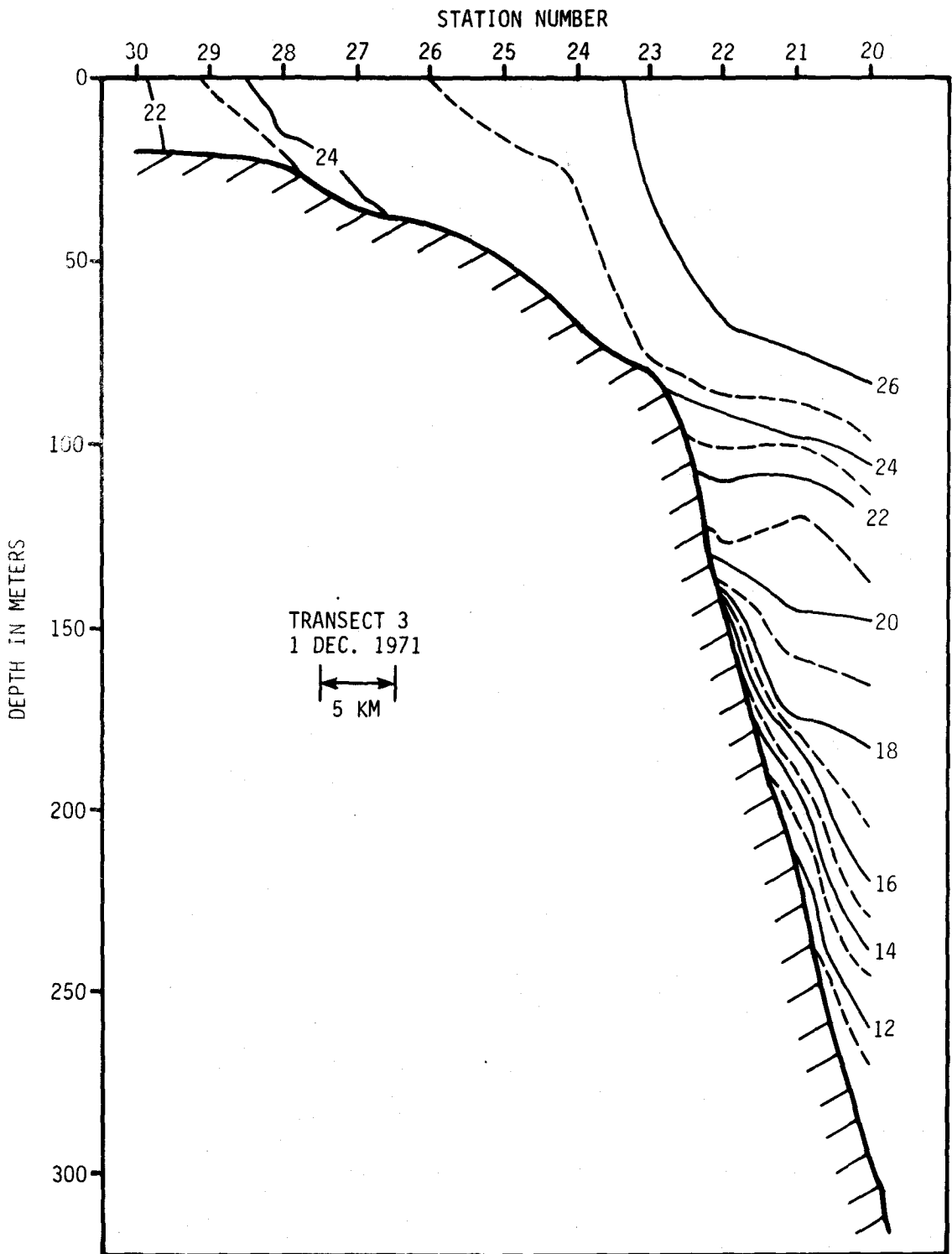


Figure 2.4. Temperature section along Transect 3 for December 1971.

Thermal conditions typical for the summer period are shown in Figure 2.2. In contrast to winter-spring, the entire shelf area was now very strongly vertically stratified. The surface temperature over the shelf was about 27°C due to seasonal heating. The bottom temperatures over the shelf were, however, colder (16°-18°C) than those found during the winter-spring period (17°-20°C). The isotherms seaward of the shelfbreak sloped downward much more strongly than those for the winter-spring section (Fig. 2.1). The horizontal temperature gradient at 100 m between stations 7 and 9 was $\frac{\Delta T}{\Delta X} \approx \frac{7.5^\circ\text{C}}{8 \text{ km}}$ or about twice the value found for the winter-spring period. This indicates that the Florida Current had moved closer to shore and/or increased in strength during the summer months. These results are consistent with the summer maximum in Florida Current transport reported by Niiler and Richardson (1973). Evidence for cold water intrusion onto the Miami Slope and Terrace during summer was discussed by Lee and Mooers (1977).

The temperature structure found during November (Fig. 2.3) had changed drastically from the summer conditions. The entire shelf shoreward of the 50 m isobath was essentially isothermal at 27°C. The slope of the isotherms was much weaker than expected for the thermal structure of the Florida Current. The horizontal temperature gradient at 100 m between stations 27 and 29 was $\frac{\Delta T}{\Delta X} \approx \frac{2^\circ\text{C}}{8 \text{ km}}$, or half that found for winter-spring conditions. The total heat content over the shelf was much greater than during the summer months. Apparently, the Florida Current had shifted offshore.

The thermal field during December (Fig. 2.4) reflected a transition from fall to winter conditions. Seasonal cooling and possibly intrusion

of cooler northern water produced nearly vertically isothermal conditions over the entire shelf. The temperature increased offshore at all depths. This was the only time of the year when the bottom temperature gradient over the shelf was positive in the offshore direction, with the bottom temperature increasing from about 21.7°C at 20 m water depth to 24.5°C at the shelfbreak. Isotherms sloped strongly downward below 140 m, indicating that the Florida Current had shifted closer to shore.

The horizontal temperature gradient at 100 m between stations 20 and 22 was about $\frac{\Delta T}{\Delta X} = \frac{1^\circ\text{C}}{8 \text{ km}}$, the smallest magnitude for any season.

2.2 Temporal and Spatial Variability

Results of the previous section indicate apparent anomalies existed in the temperature field, primarily during the summer. To more closely examine the time and space fluctuation of the vertical temperature structure, the temperature fields at three stations from Transect 3 were contoured in the time-depth domain (Fig. 2.5). The stations labeled inner shelf, mid-shelf, and shelf-break are the first, fourth, and seventh stations, respectively, along Transect 3 in Figure 1.2. Note that the vertical scale of the shelfbreak station is one-half that for the other two stations.

During winter, the shelf stations were isothermal and the shelf-break slightly stratified until mid-March; the time of minimum temperature. The normal seasonal heating cycle was apparent at all stations. In late March and early April at the offshore station, cold (18°C) water began to move onshore near the bottom. The onshore progression of this cold water intrusion interrupted the seasonal heating and continued to the inner shelf station in late July to early August. The offshore

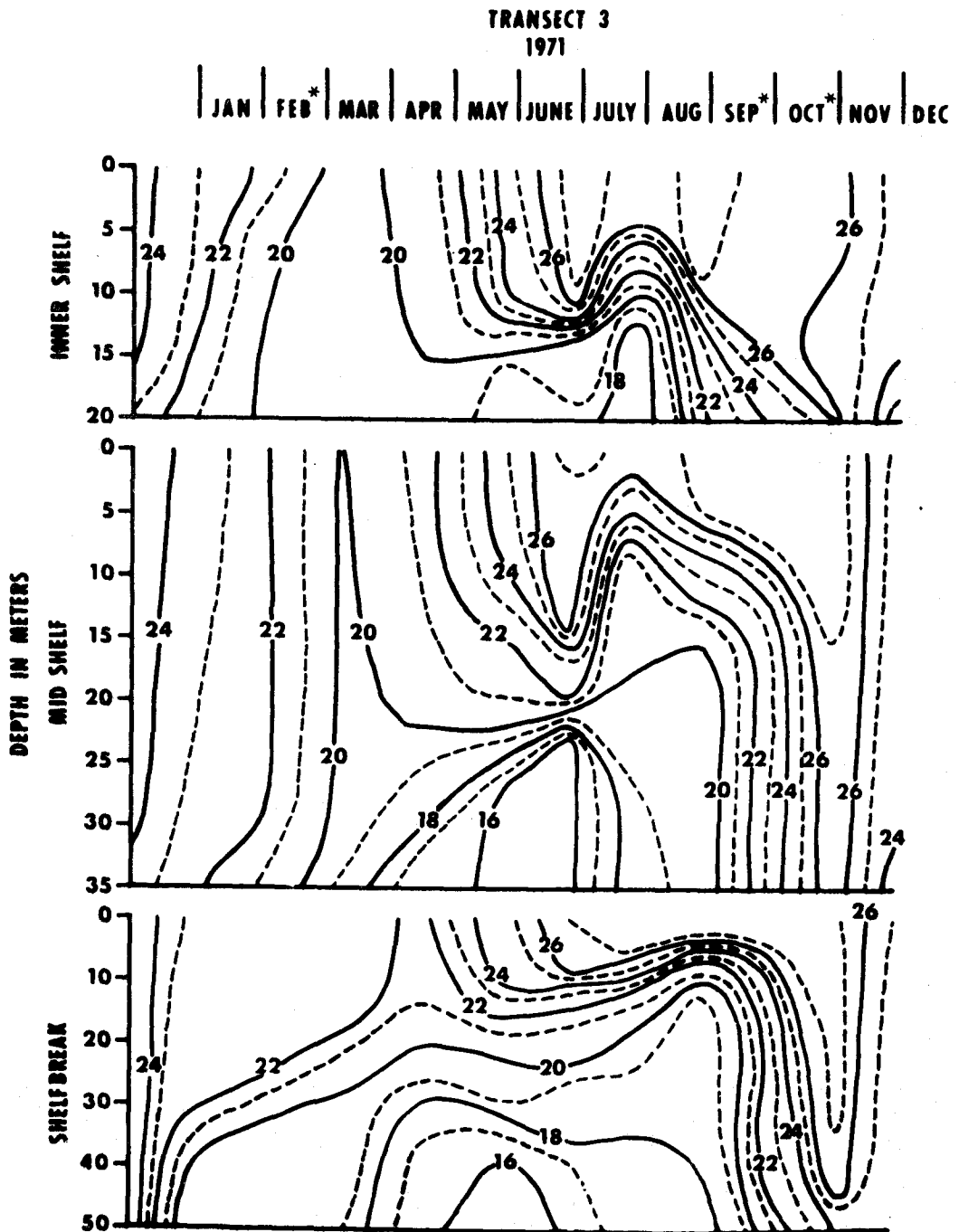


Figure 2.5. Time-depth temperature contours for inner shelf, mid-shelf and shelfbreak stations along transect 3. The depth scale for the shelfbreak station is one-half that for the inner and mid-shelf stations. Asterisks indicate months with no data.

movement of the colder water was then rapid and essentially disappeared from the shelf by late September. These effects may not be due entirely to local onshore-offshore motion. Alongshore advection from the north may also be important. The results suggest that cold, deep offshore water had flooded the near-bottom layer over the shelf area during the summer months. In fact, at all stations the lowest bottom temperatures for the year were recorded between May and July. These results are qualitatively identical to those found by Stefánsson, et al. (1971, Figure 4A) off Onslow Bay. The authors proposed that the intrusion of subsurface Caribbean Water onto the shelf was at least partly wind-controlled by upwelling favorable northeastward winds during the summer.

The onshore movement of the cold water mass was accompanied by some upward vertical mixing. However, even at the inner shelf station, the temperature depression at the surface was small, less than 1°C . This station was located only about 7 km from the coast. Thus, if upwelling to the surface occurred, it must have been confined to a very narrow coastal band. The existence of a narrow band for coastal upwelling has been predicted by theoretical considerations (e.g.; O'Brien and Hurlburt, 1972; Allen, 1973) and confirmed experimentally (Smith, 1974). This aspect is considered further in Chapter 5.2.

The intersection with the bottom of the 18°C and 15°C isotherms (Figs. 2.6, 2.7) showed that the general onshore movement of cold water during the summer was evident along the entire shelf. The 18°C isotherm along the bottom from November through March was generally found at or offshore of the 30 fm (55 m) isobath (Fig. 2.6). In contrast, during May to July, the same isotherm intersected the bottom near and inshore

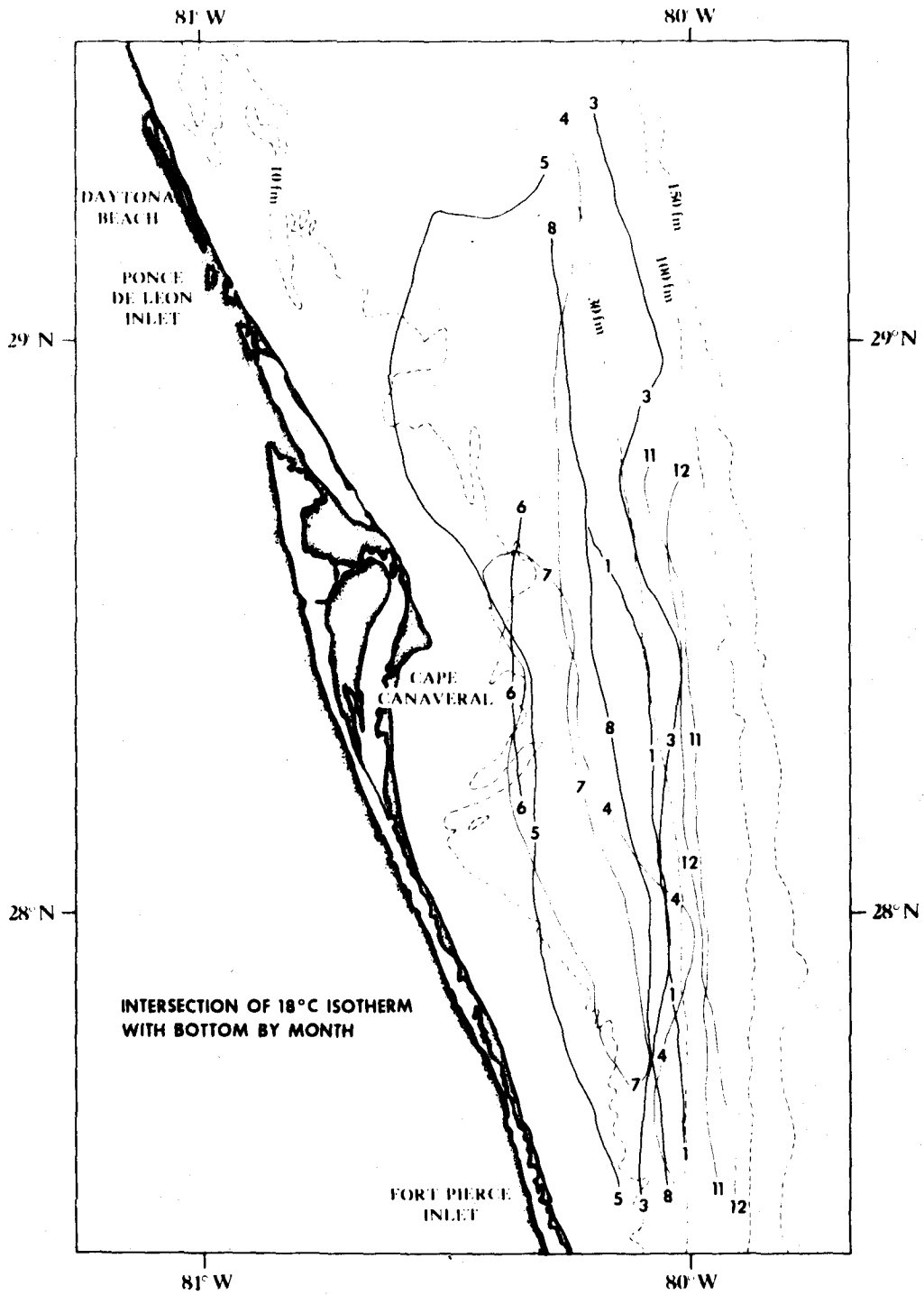


Figure 2.6. Intersection with bottom of 18°C isotherm by month from XBT. Numbers refer to month of year (1971).

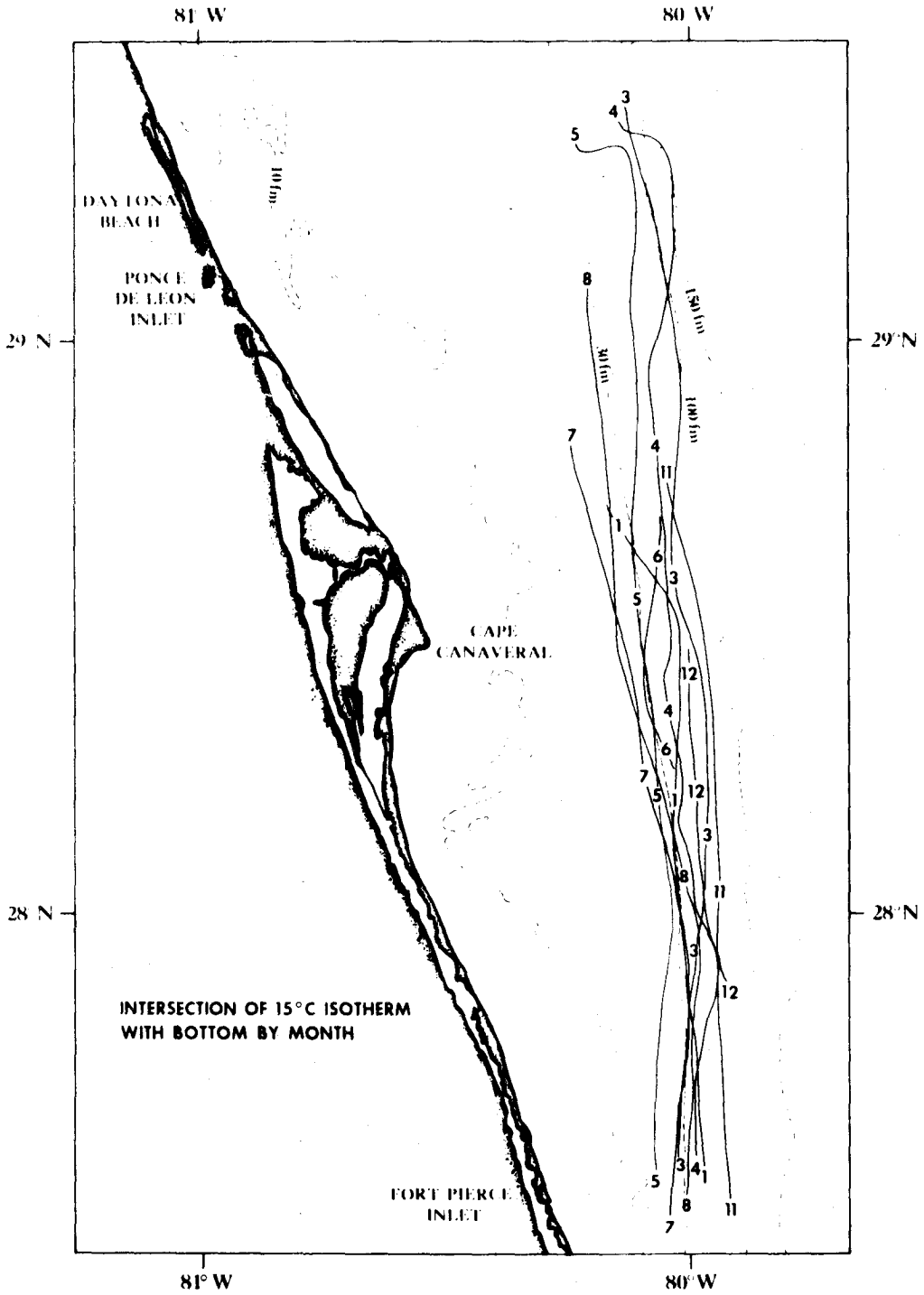


Figure 2.7. Intersection with bottom of 15°C isotherm by month from XBT. Numbers refer to month of year (1971).

of the 10 fm (18 m) isobath. The cross-shelf excursion of the bottom intersection of the 15°C contour (Fig. 2.7) was less than for 18°C, but the onshore movement during the summer was evident. In fact, the 15°C temperature was found inshore of the 30 fm (55 m) isobath only May to August. It may be significant that the 30 fm (55 m) depth is considered to be the maximum depth for the commercial calico scallop fishery and 15°C may be lethal to the animal (G. Miller, personal communication).

2.3 Short Term Variation and Alongshore Extent of Summer Intrusions

Large fluctuations in the horizontal and vertical temperature structure occurred on time scales much shorter than the monthly survey intervals. During the July cruise, Transect 3 was run first from 2235 EDT on 23 July to 0250 EDT on 24 July, and again from 1107 to 1508 EDT on 26 July, or about 61 hours later. The results are shown in Figures 2.8 and 2.9. During 23 to 24 July (Fig. 2.8), a pool of cold (<18°C) water was left along the bottom as the 18°C isotherm apparently retreated offshore. On the second pass on 26 July (Fig. 2.9), the 18°C isotherm again moved in over the shelf from offshore and the inshore position retreated somewhat, intersecting the bottom at about 25 m. The much steeper slope of the isotherms offshore from the shelfbreak for the 26 July section suggests that the Florida Current intensified and moved onshore from 23 and 24 July to 26 July. In addition, large vertical movement of the isotherms occurred between stations 5 and 7 for the 23 to 24 July section and 53 to 55 for the 26 July section. For example, when the Florida Current had apparently moved offshore, the 20°C isotherm at station 6 (Fig. 2.8) was about 10 m deep. After the onshore excursion, it was 25 m deep at that location (Fig. 2.9). The pattern of this change reflected the general trend of the downward sloping iso-

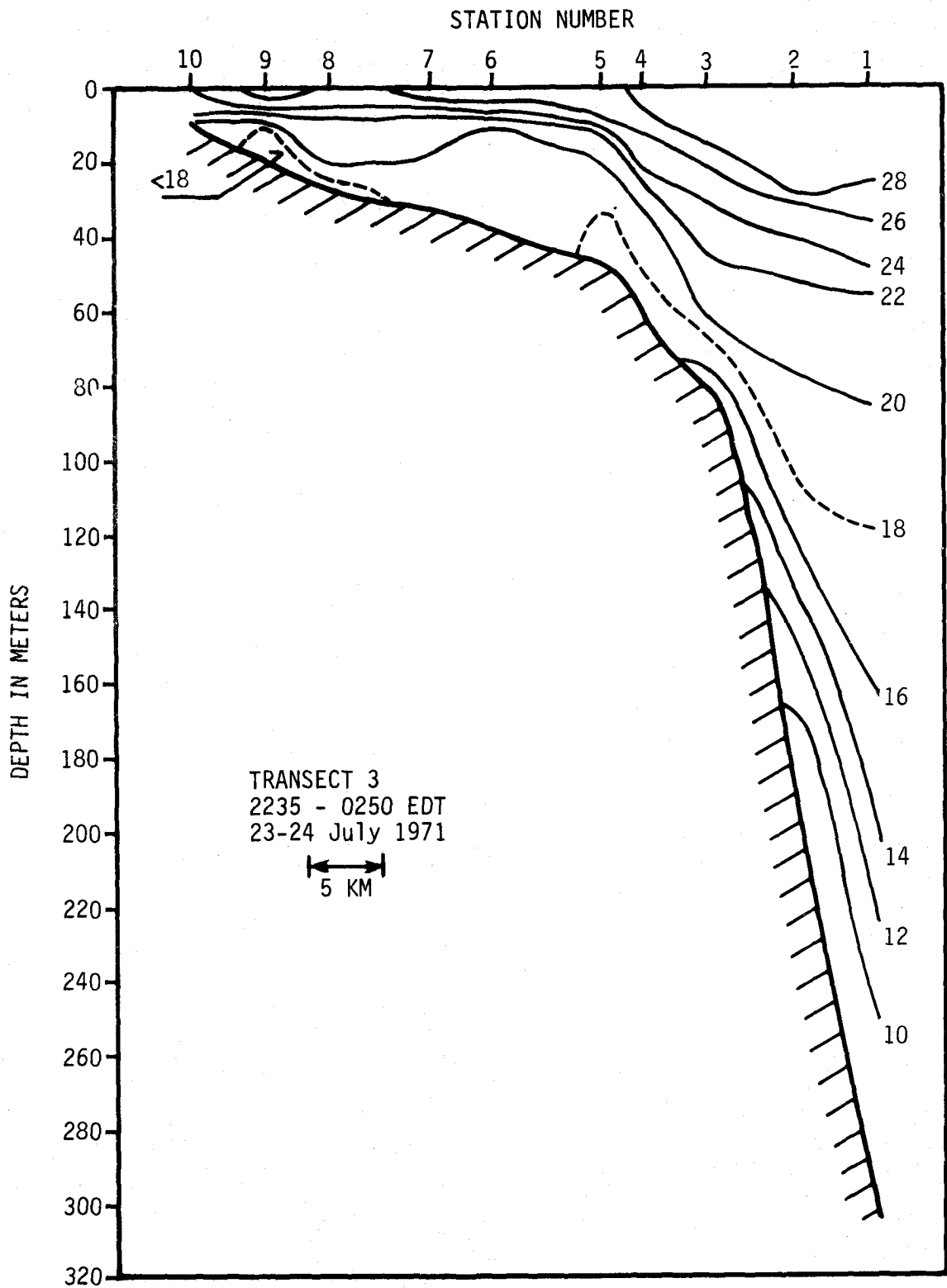


Figure 2.8. Temperature section along Transect 3 run between 2235 EDT, 23 July and 0250 EDT, 24 July 1971. The 18°C isotherm is dashed for emphasis.

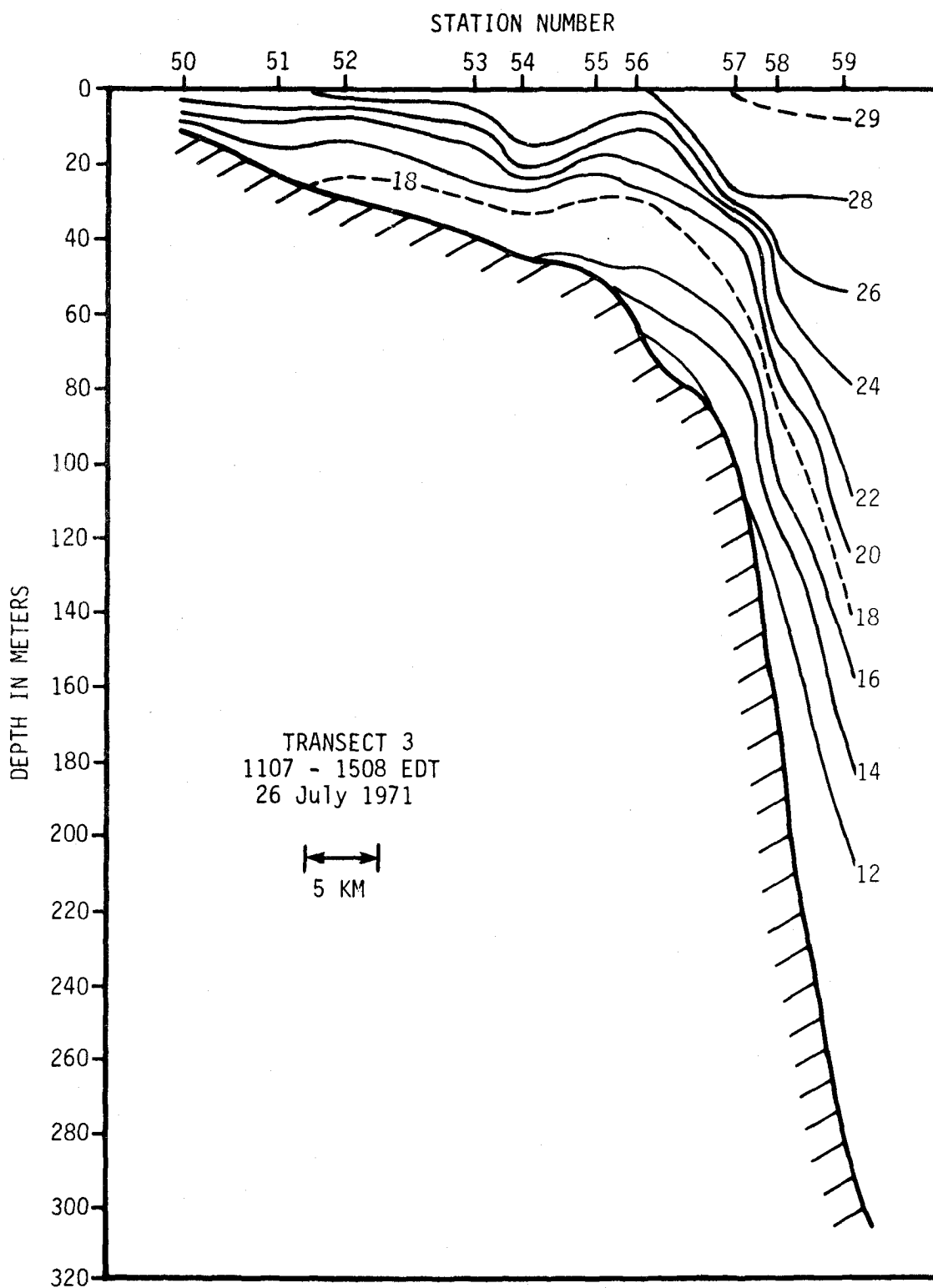


Figure 2.9. Temperature section along Transect 3 run between 1107 EDT and 1508 EDT, 26 July 1971. The 18°C isotherm is dashed for emphasis.

therms in the offshore direction. That is, when the Florida Current moved toward shore, the upper layers tended to increase in temperature while colder water was introduced along the bottom. The upward bowing of the isotherms over the shelfbreak for the onshore movement (Fig. 2.9) indicates possible bottom-trapped upwelling.

During 23 to 24 July, after the apparent maximum shoreward extent of the onshore motion, some indication of surface penetration by upwelling was evident. The effect was limited to inshore of stations 7 and 8, a distance of about 18 km from the coast (Fig. 2.8). The indication again is that any coastal upwelling to the surface occurs in a very narrow coastal band. The alongshore extent of the cold water intrusions is indicated by the bottom temperature field during the July cruise (Fig. 2.10). The data for Transect 3 on 23 to 24 July were used with Transects 2a, 3a, 4 and 5 to construct this plot. The cold water pool ($<18^{\circ}\text{C}$) extended along the coast for a distance of about 80 km. This suggests that the onshore-offshore movement occurred coherently over an alongshore distance of at least that distance. The average onshore-offshore width was about 10 km and the mean height above the bottom was about 5 m. For these dimensions, the total volume was about $2 \times 10^9 \text{ m}^3$. Large cut-off pools of cold water also have been observed off the North Carolina coast by Blanton (1971), and Stefánsson, et al. (1971). These authors reported that cold lenses over the mid-shelf area in Raleigh, Onslow, and Long Bays were semi-permanent features during summer months. However, this does not appear to be typical off Cape Canaveral. More recent time series of temperature and currents in the coastal waters of the South-Atlantic Bight (Atkinson 1977; Blanton and Pietrafesa, 1978)

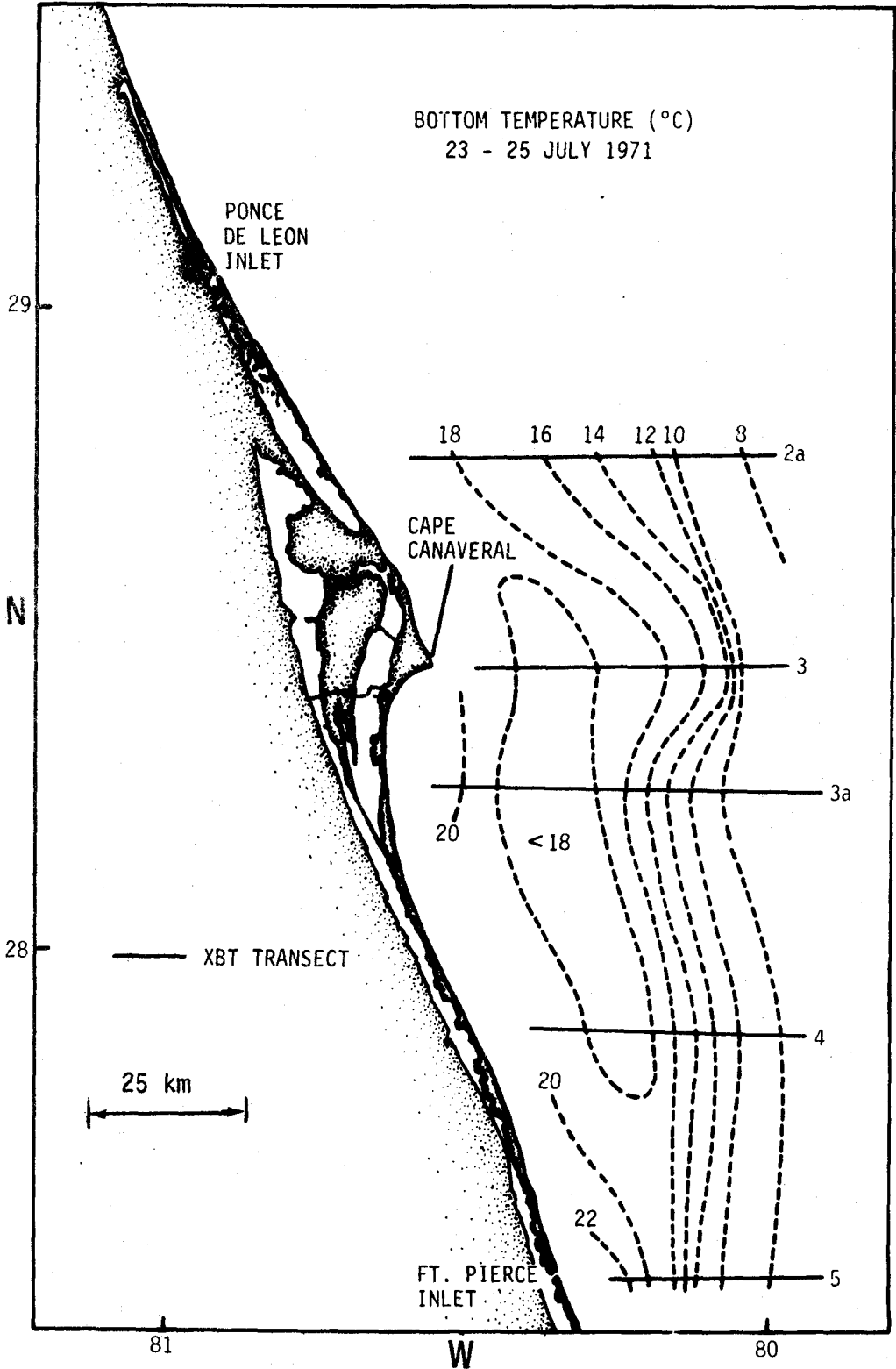


Figure 2.10. Bottom temperature from XBT measurements for 23 to 25 July 1971. Contour interval is 1°C. Solid lines indicate the XBT transects used.

and over the shelf and slope off Miami (Lee and Mooers, 1977) suggest that such lenses are periodic or intermittent rather than permanent features.

Typical temperature sections for winter to early spring, summer, fall, and early winter revealed that the strength and onshore-offshore migration of the Florida Current had a major influence on the thermal structure of the shelf waters. The annual cycle suggested that the Florida Current was at maximum strength and closest to shore during the summer months. It apparently shifted offshore during the fall and winter. During the summer, cold water was introduced into the lower layer over the shelf which may have penetrated to the surface in a narrow (≈ 18 km) coastal band. In addition, large pools of cold ($<18^{\circ}\text{C}$) water were found in the bottom layer over the mid-shelf as a result of an apparent offshore movement of the Florida Current. These cold lenses extended along the coast for at least 80 km, with a cross-shelf width of about 10 km and vertical extent of 2 to 7 m. The total volume of about $2 \times 10^9 \text{ m}^3$ was apparently formed and removed on a time scale of 2 to 3 days.

3. TEMPERATURE AND WIND TIME SERIES ANALYSIS

3.1 Data Processing

The time series analysis in this section and in Appendix A treats four basic data sets: 1) bottom temperature at buoy site 1 (BY1), 2) bottom temperature at buoy site 2 (BY2), 3) surf temperature at Daytona Beach (SFT) and, 4) wind stress computed from wind speed and direction recorded at the Daytona Beach airport. The locations for the data sets are shown in Figure 1.2. Following is a brief discussion of the editing and data processing for each data set.

3.1.1 Bottom Temperature

The bottom temperatures at the biological buoy sites (BY1, BY2) were recorded at twenty minute intervals on film. The film was digitized by the instrument manufacturer and the data returned on paper tape. The temperature values were then keypunched and transferred to magnetic tape. The total number of usable data points acquired was about 5×10^4 . This thesis is concerned primarily with low frequency fluctuations in the coastal waters; therefore, tidal and inertial period variations in the data were removed by digital filtering of the records. The original data were low-pass filtered by convolution with a Lanczos taper. The energy response for the filter selected was -1 dB at 55 hours (0.44 cycles/day), -6 dB (half-amplitude point) at 48 hours (0.5 cycles/day), and -20 dB at 40 hours (0.6 cycles/day). After filtering, the data were sub-sampled at 8-hour intervals. The time span for each data set is shown in Table 1.1. For convenience, daily mean bottom temperatures are tabularized in Appendix D.

3.1.2 Surf Temperature

The surf temperature data set for 1971 was obtained from the National Climatic Center (NOAA). Daily temperature recordings at 0700 local time were made at the Sun Glow fishing pier, Daytona Beach. The original data were recorded in whole Fahrenheit degrees; thus, upon conversion to Celsius degrees, there is a quantization error of $\pm 0.56^\circ$. The daily values were then filtered with a digital filter having the same response characteristics as that described in 3.1.1. After filtering, the daily values were linearly interpolated to 8-hour intervals to be compatible with the bottom temperature records. For convenience, daily surf temperatures are tabularized in Appendix D.

3.1.3 Wind Stress

The National Climatic Center also provided wind speed and direction sampled every three hours at the Daytona Beach airport (Fig. 1.2) for 1970 and 1971. The wind stress components were computed using a quadratic drag law with a drag coefficient of 1.5×10^{-3} . The general trend of the isobaths and coastline near Cape Canaveral is about 10° west of true north. The coordinate system for the wind stress components was rotated 10° counterclockwise yielding offshore (u positive) and alongshore (v positive toward north-northwest) stress components. The three-hourly stresses were linearly interpolated to two-hourly values. The data were convolved with a Lanczos taper with the same response characteristics as used for the bottom and surf temperatures. Each stress component data set was then sub-sampled at the 8-hour interval.

3.2 General Characteristics of Time Domain

The filtered bottom temperature, surf temperature, and wind stress

vectors are plotted as a function of time for 1970 and 1971 in Figure 3.1. Note the factor of two difference in the scales for the surf and bottom temperatures. For clarity, the filtered stress vectors are plotted daily while the temperatures are plotted at the 8-hour sampling rate. The following general features are evident in Figure 3.1.

1. The bottom temperature records for both BY1 and BY2 show striking interruptions of a normal seasonal heating and cooling cycle. Maximum and minimum bottom temperatures of 27.2°C and 16.2°C were recorded in October 1970 and February 1971, respectively, as might be expected on a seasonal basis. However, a bottom temperature of 16.8°C was recorded at BY1 during May and July 1971. These cold water intrusions during the summer confirm the results of the XBT measurements discussed in Chapter 2. Abrupt temperature decreases were also apparent in June and July 1970, and June and August 1971. Typically, these summer temperature anomalies were characterized by a decrease of 4 to 6°C within 3 to 5 days.
2. In contrast to the negative temperature anomalies for bottom temperatures during summer, positive anomalies occurred during December 1970 to March 1971. It is not clear, however, whether the winter minimum was governed by seasonal cooling or by advection.
3. During the winter, the offshore buoy (BY2) temperature was consistently warmer than that of the inshore buoy (BY1). Conversely, BY2 was generally cooler than BY1 during summer.
4. The most energetic temperature fluctuations at BY1 from April to June 1970 were somewhat cyclic with an apparent period of 20 to 30

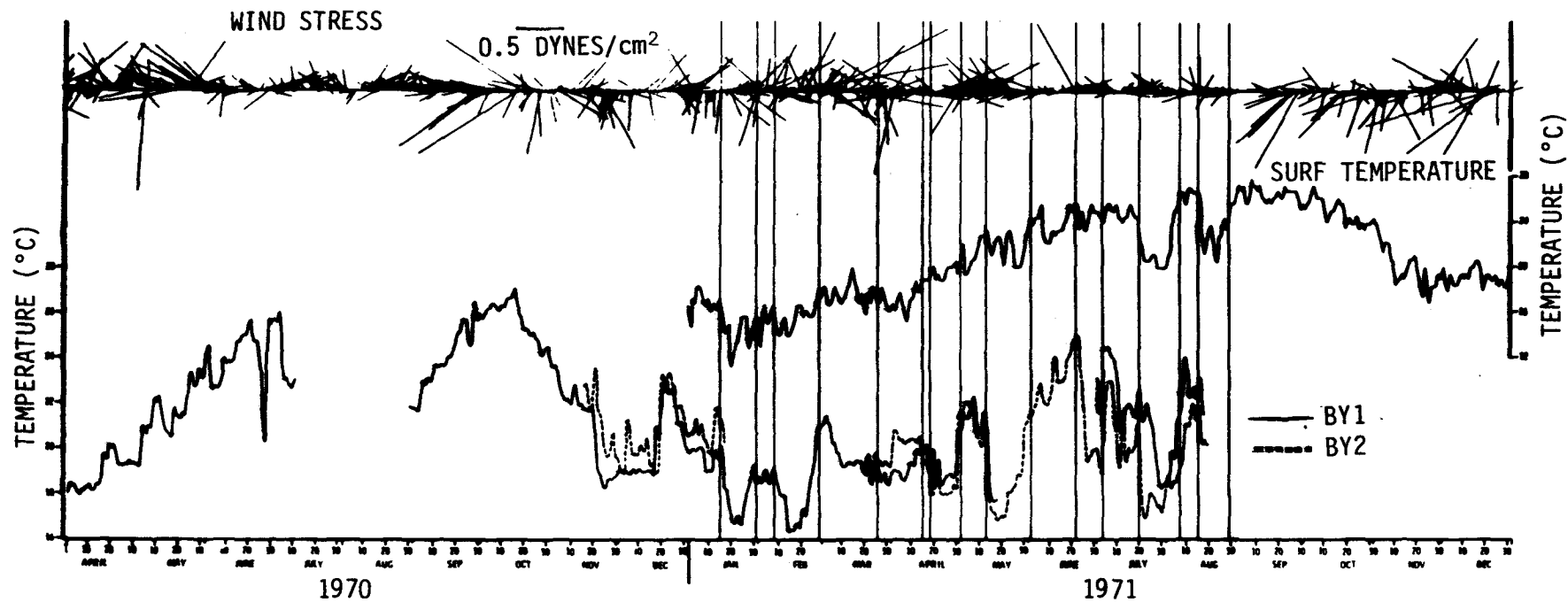


Figure 3.1. Low pass filtered wind stress vectors, surf temperature, and bottom temperature (BY1, BY2) for 1970 and 1971. Wind stress vectors are plotted daily while temperatures are 8-hourly. Vertical lines indicate major temperature events in the record referred to in that text.

days. The bottom temperature record in general, however, suggested that many of the major temperature fluctuations were apparently aperiodic and superimposed on the annual cycle.

5. For those time periods when data for both BY1 and BY2 were available, the records were generally similar, i.e. oscillating nearly in phase. This was especially true during July to August 1971.
6. Oscillations with periods of several days to a week were apparent at both BY1 and BY2. The amplitudes of these fluctuations were, however, small compared to the large amplitude, apparently aperiodic components and the seasonal cycle.
7. The surf temperature had a seasonal cycle with a minimum (11.3°C) and maximum (27.7°C) occurring in January and September 1971, respectively.
8. The surf temperature record contained more high frequency information than the bottom temperature records. Some of this variation may have been due to air temperature fluctuations which did not affect the bottom temperatures. A certain amount of noise in the record, however, can be attributed to the $\pm 0.6^{\circ}$ uncertainty introduced by the conversion from whole degrees Fahrenheit.
9. Nearly all of the major "events" in the bottom temperature record were observed in the surf temperature record. For clarity, these have been bracketed by vertical lines.
10. The wind stress vectors clearly demonstrated the seasonal influence of the major weather systems affecting this area. During the win-

ter, the winds are strong and highly variable, alternating from northward to southward on time scales of about one week. The strong southward stresses are associated with large, spatially coherent extratropical cyclones, usually followed by an outbreak of sub-Arctic cold air masses in this area (Partagas and Mooers, 1974). The transition from winter to summer conditions is characterized by a strengthening of the Bermuda-Azores high pressure ridge. The winds decreased in amplitude and were generally steady northwestward or northeastward until July. Brooks (1975) showed that a minimum in the monthly latitudinal excursion of the high pressure ridge occurred in July for both 1970 and 1971. He also demonstrated that the excursion of the ridge axis during June 1970 and July 1971 had approximately fortnightly and monthly periods, respectively. The change from summer to fall was accompanied by an increase in stress, directed predominantly onshore from mid-August to mid-September. The transition to winter conditions, with associated strong southward stresses, began in early October.

11. The relationship of events in the bottom and surf temperatures records to the local wind stress was, in many instances, consistent with simple coastal upwelling theory. Positive alongshore stress induces an offshore Ekman flux in the upper layer compensated by onshore flow in the lower layer. Consequently, the onshore flow is associated with lower temperature at the bottom and at the surface very near the coast. Negative alongshore stress has the opposite effect and is associated with increasing temperatures. The latter effect was especially apparent during April to July 1970 and January to April 1971.

12. During periods of relatively uninterrupted increase in the bottom temperatures, such as early September to mid-October 1970 and mid-May to mid-June 1971, the wind stress was predominately onshore.
13. The large negative temperature anomalies in the summer of 1971 appeared to be more directly related to the onshore-offshore component of the wind stress than to the alongshore component. Although the relationship was not straightforward, decreasing (increasing) temperatures were associated with offshore (onshore) stress.

It is questionable that the large, non-seasonal fluctuations of the temperature fields can be completely explained by simple coastal upwelling driven by the local wind stress. The wind stress rarely exceeded 1 dyne/cm² even during winter and typical summer values were 0.1 to 0.3 dynes/cm². These stresses are at least an order of magnitude less than those typical for coastal upwelling areas (Smith, 1968). The lack of large wind stress values may be compensated by the long duration of upwelling favorable winds, however, especially during the summer.

Wind stress conditions conducive to coastal upwelling occurred frequently with no apparent response in the temperature data. This fact, coupled with the large amplitude of the non-seasonal temperature fluctuations and the results of Chapter 2 suggest that onshore-offshore migration of the Florida Current was the primary forcing function. The Florida Current meanders may be wind-driven, however, confusing the results. The extent to which the fluctuation of the wind stress and temperature fields can be correlated and their frequency content are discussed in the next section and in Appendix A.

3.3 The Frequency Domain

A spectrum analysis of various bottom temperature, surf temperature and wind stress data subsets is given in Appendix A. The results of that analysis suggest that the surf and bottom temperature records were dominated by very low frequency fluctuations (periods greater than 20 days) or by aperiodic or episodic events. Higher frequency temperature fluctuations (2 to 18 day periods) were found to be significantly coherent with the wind stress, especially in the spring and summer months. In addition, a strong correlation existed between the temperature records and the onshore-offshore stress during the summer consistent with simple upwelling theory. The alongshore stress was generally positive, and positive offshore stress was significantly correlated with decreasing surf and bottom temperatures.

The seasonal effects were examined by patching the bottom temperature record from BY2 from 18 May to 1 July 1971 to the BY1 record from 22 August 1970 to 18 May 1971 and 1 July 1971 to 27 August 1971 to give a total record length of 373 days. A least squares fit of the annual component was calculated for this data set. The annual component accounted for about 52% of the total variance in the bottom temperature record. This amount of variance removal was about the same accounted for when linear trends were removed from the shorter temperature records presented in Appendix A.

The analysis in this section concentrates on two overlapping, but seasonally different, data sets.

1. Low pass filtered surf temperature (SFT), bottom temperature at BY1, and the onshore-offshore and alongshore wind stress components (USTR,

VSTR) for the period 5 January to 18 May 1971; hereafter referred to as W71. The number of data points was 399 with $\Delta t = 8$ hours for a 133 day record.

2. Low pass filtered surf temperature (SFT), bottom temperature at BY2, and the onshore-offshore and alongshore wind stress components (USTR, VSTR) for 21 March to 20 August 1971; hereafter referred to as S71. The number of data points was 455 with $\Delta t = 8$ hours for a 151.6 day record.

Standard time series analysis techniques are used throughout. Spectrum and cross-spectrum computations were made by Fourier transformation of the correlation functions (Blackman and Tukey, 1958; Jenkins and Watts, 1968). Linear trends were removed before the spectrum calculations.

3.3.1 Sample Statistics

The onshore-offshore and alongshore components of wind stress (USTR, VSTR), surf temperature (SFT), and bottom temperature (BY1, BY2) for W71 and S71 are shown in Figures 3.2 and 3.3, respectively. The more frequent occurrence of relatively large wind stress values for W71 compared to S71 reflects the passage of winter cold fronts. During the summer, the winds were generally lighter and less variable as discussed in Chapter 3.2. For W71, the surf temperature (SFT) was generally about 2° to 4°C colder than the bottom temperature at BY1 (Fig. 3.2). As spring warming continued the SFT gradually became greater than BY1. In addition, a much higher frequency content was evident in SFT than in BY1. This likely reflected the day-to-day air temperature changes which did not penetrate to the bottom. In contrast to the winter conditions, the

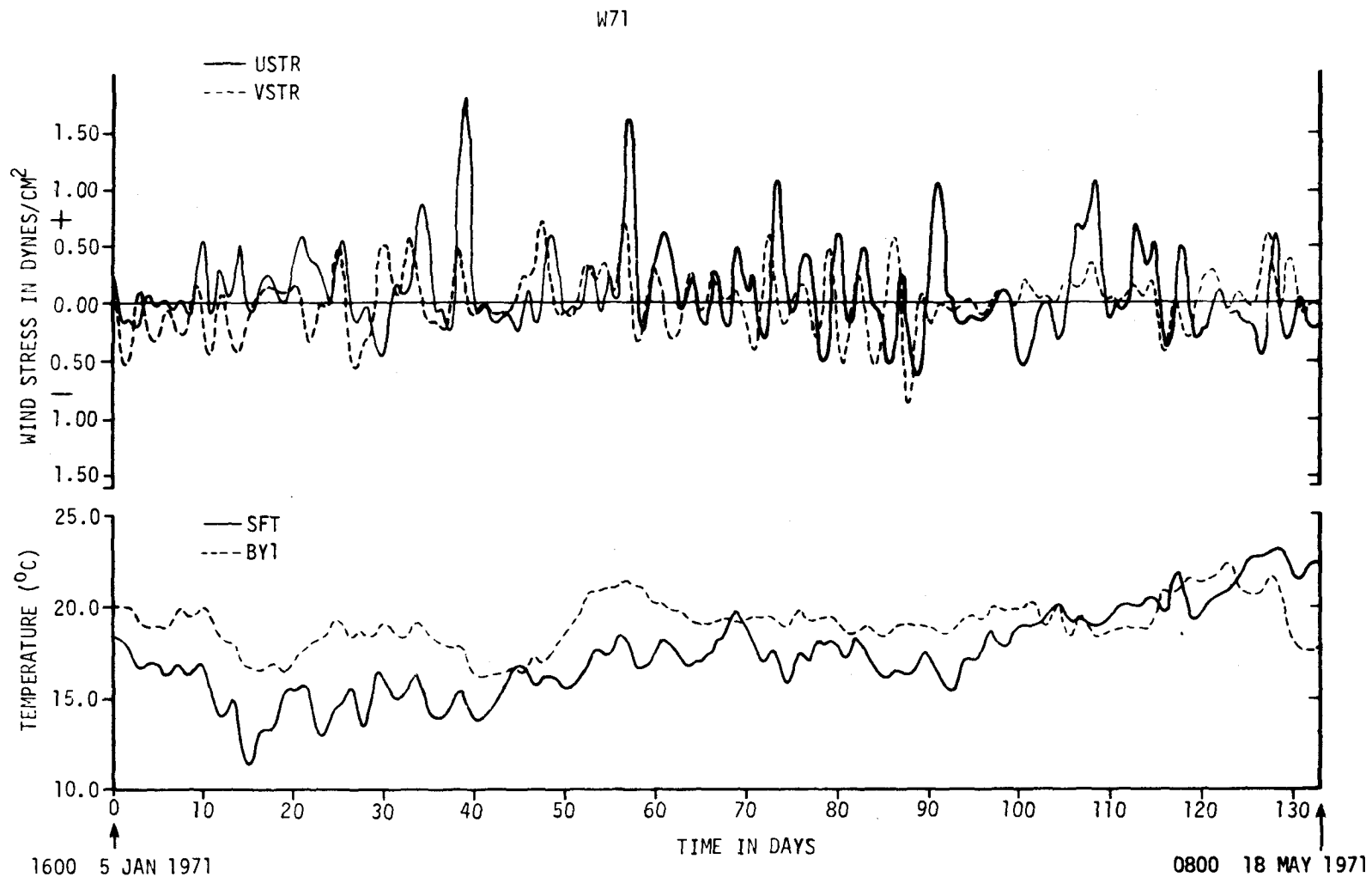


Figure 3.2. Low-passed onshore-offshore (USTR) and alongshore (VSTR) wind stress components, surf temperature at Daytona Beach (SFT), and bottom temperature at BY1 for W71; 5 January to 18 May 1971.

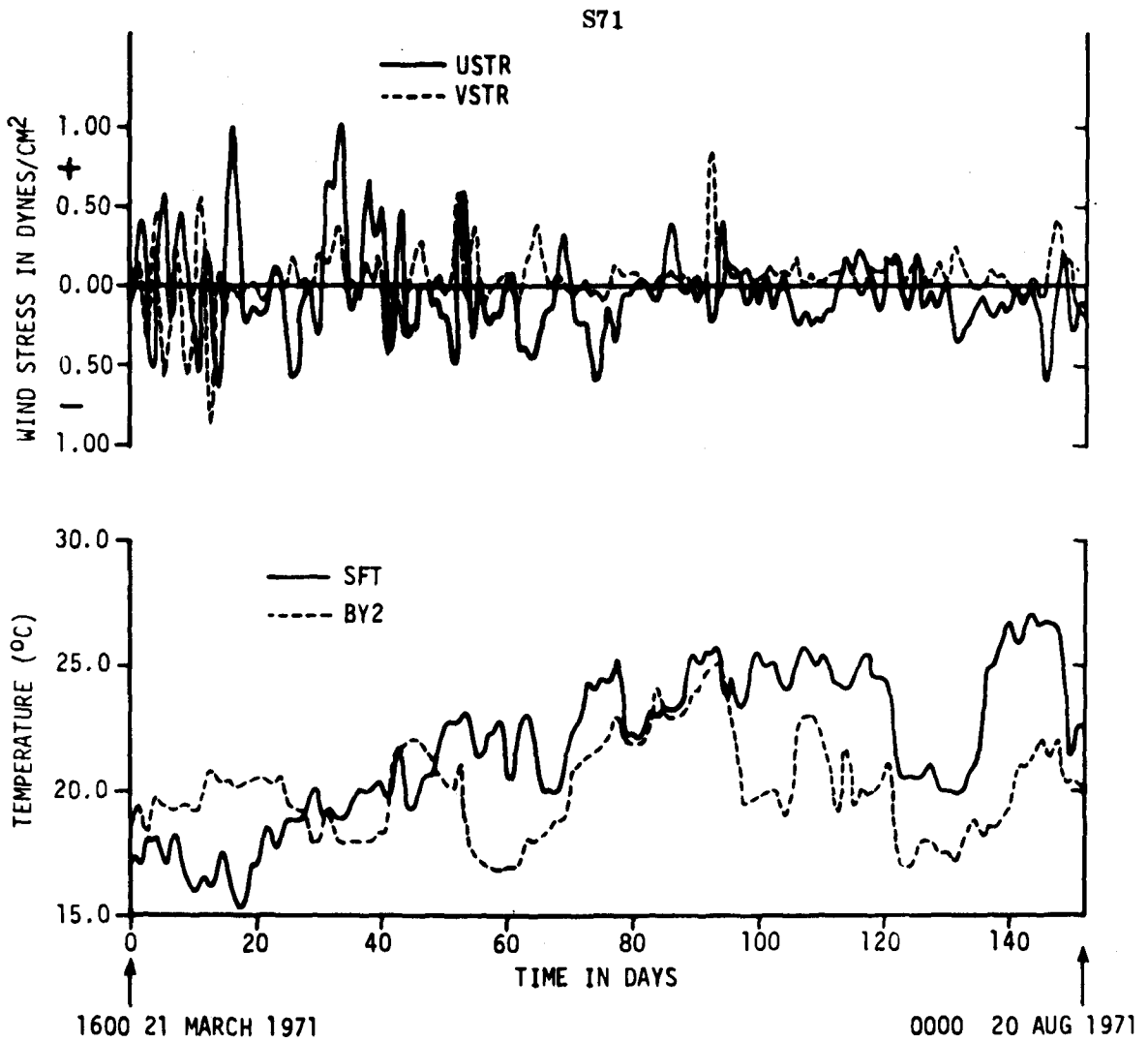


Figure 3.3. Low-passed onshore-offshore (USTR) and alongshore (VSTR) wind stress components, surf temperature at Daytona Beach (SFT), and bottom temperature at BY2 for S71; 21 March to 20 August 1971.

visual correlation between SFT and BY2 is greater in summer, especially for the abrupt temperature drops which occurred near days 54, 94, 121, and 148. All of these events were associated with a local maximum in the alongshore (upwelling favorable) wind stress followed by a local maximum in the offshore stress (Fig. 3.3).

The first order statistics for the W71 and S71 data sets are given in Table 3.1. The mean wind stress for W71 was higher than that for S71, and the wind stress was considerably more variable as reflected in the magnitude of standard deviations. The mean wind stress for S71 was close to zero for both components. For both data sets, the onshore-offshore component of wind stress had the largest positive value, and the alongshore component the largest negative value. The maximum and minimum surf temperatures occurred during S71 and W71, respectively; however, the difference between the maximum and minimum was almost identical (11.9°C) for both seasons. The standard deviation for BY2, however, suggests more vigorous fluctuations occurred at that site during the summer (S71) than at BY1 during the winter (W71).

The overall correlation coefficients for wind stress components vs. surf and bottom temperature and surf temperature vs. bottom temperature were computed (Table 3.2). The coefficients were calculated after detrending and making a lag adjustment correction for the maximum absolute value of the cross correlation function. The time delay associated with the lag adjustment is indicated in Table 3.2. Those coefficients which were significantly different from zero at the 99% level and at the 95% (but not 99%) level are also indicated in Table 3.2. The correlation coefficients between wind stress and temperature were all low; however,

TABLE 3.1. Statistics for low-pass filtered onshore-offshore (USTR) and alongshore (VSTR) wind stress components, surf temperature (SFT), and bottom temperature (BY1, BY2) for the two data subsets W71 and S71.

W71					S71				
VARIABLE	5 JANUARY TO 18 MAY 1971				VARIABLE	21 MARCH TO 20 AUGUST 1971			
	N = 399 $\Delta t = 8$ HOURS					N = 455 $\Delta t = 8$ HOURS			
	MAX	MIN	MEAN	STD. DEV.		MAX	MIN	MEAN	STD. DEV.
USTR (dynes/cm ²)	1.81	-0.67	0.10	0.37	USTR (dynes/cm ²)	1.04	-0.67	-0.04	0.28
VSTR (dynes/cm ²)	0.73	-0.91	0.14	0.25	VSTR (dynes/cm ²)	0.86	-0.91	0.04	0.18
SFT (°C)	23.2	11.3	17.3	2.4	SFT (°C)	27.1	15.3	21.8	3.0
BY1 (°C)	22.3	16.3	19.1	1.3	BY2 (°C)	25.0	16.8	20.1	1.9

TABLE 3.2. Correlation coefficients and lag adjustment for onshore-offshore (USTR) and alongshore (VSTR) wind stress components, surf temperature (SFT), and bottom temperature at BY1, BY2 for W71, S71.

W71				S71			
1	2	CORRELATION COEFFICIENT	TIME LAG IN DAYS*	1	2	CORRELATION COEFFICIENT	TIME LAG IN DAYS*
USTR VS.	{ SFT	-.26**	+1.6	USTR VS.	{ SFT	-.16	+1.3
	{ BY1	-.15	+9.0		{ BY2	+.16	-8.0
VSTR VS.	{ SFT	+.25**	+13.6	VSTR VS.	{ SFT	+.24**	-3.0
	{ BY1	+.18	+4.6		{ BY2	-.14	+3.6
SFT VS.	{ BY1	+.63***	+1.0	SFT VS.	{ BY2	+.43***	-0.3

*POSITIVE INDICATES COLUMN 1 LEADS COLUMN 2

**SIGNIFICANT AT 95% LEVEL

***SIGNIFICANT AT 99% LEVEL

they were statistically significant at the 95% level for USTR and VSTR vs. SFT (W71), and for VSTR vs. SFT (S71). The low values for S71 are somewhat surprising considering the strong correlations found between the onshore-offshore component (USTR) and surf and bottom temperatures during July to August 1971 (Table A.4). The correlation between SFT and BY1 for W71 was moderately high (+.63) and significant at the 99% level. That for SFT and BY2 (S71) was much lower (+.43) than expected from the results of Chapter A.5 (but significant at 99% level) where the correlations between surf and bottom temperatures during July to August 1971 were very high ($>+0.8$). This discrepancy may be due to the longer record length for S71 which contained a broader spectrum of fluctuation scales.

3.3.2 Cross-Spectrum Analysis: W71

Autospectra, cross-spectra, coherence-squared, and phase were calculated for the data sets for W71. The calculations were made for a record length of 399 (N), a time interval of $\Delta t = 8$ hours with 69 lags (M), an equivalent computational bandwidth (BW_e) of 0.027 cycles/day (cpd), and approximately 14.5 degrees of freedom (DOF). Twenty-four spectrum estimates were computed for the 0.0 to 0.5 cpd frequency band. The normalized autospectra for USTR, VSTR, SFT and BY1 are shown in Figure 3.4. The coherence squared and phase for SFT and BY1 vs. USTR and VSTR, and for SFT vs. BY1 are shown in Figure 3.5. Significant coherence-squared between records is defined as equal to or exceeding the 95% confidence level. The following conclusions are drawn from these calculations:

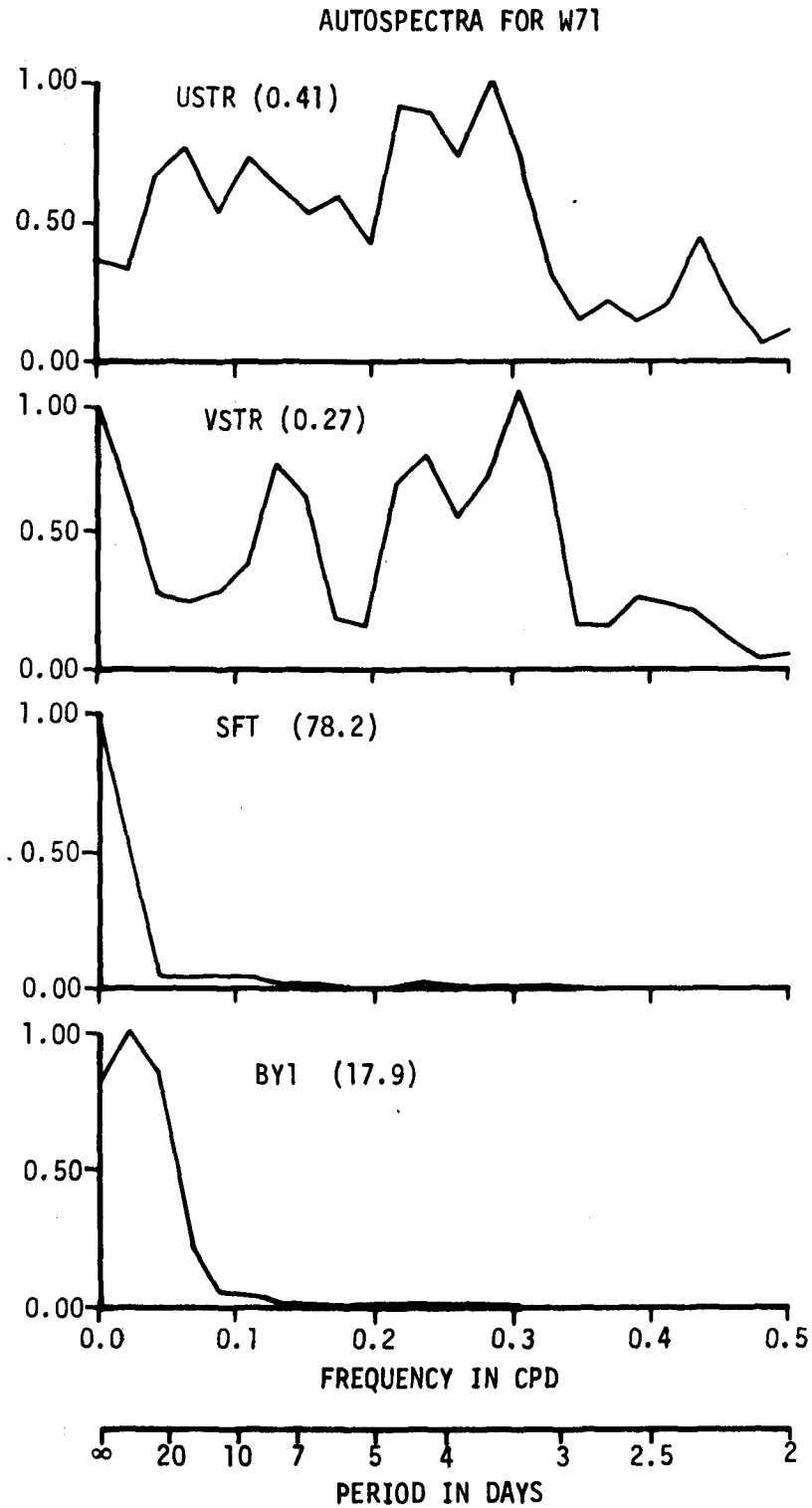


Figure 3.4. Autospectra for USTR, VSTR, SFT, and BY1; W71. Normalization factors are given in parentheses. $N = 399$, $t = 8$ hours, $M = 69$, $BW_e = 0.027$ cpd, $DOF = 14.5$.

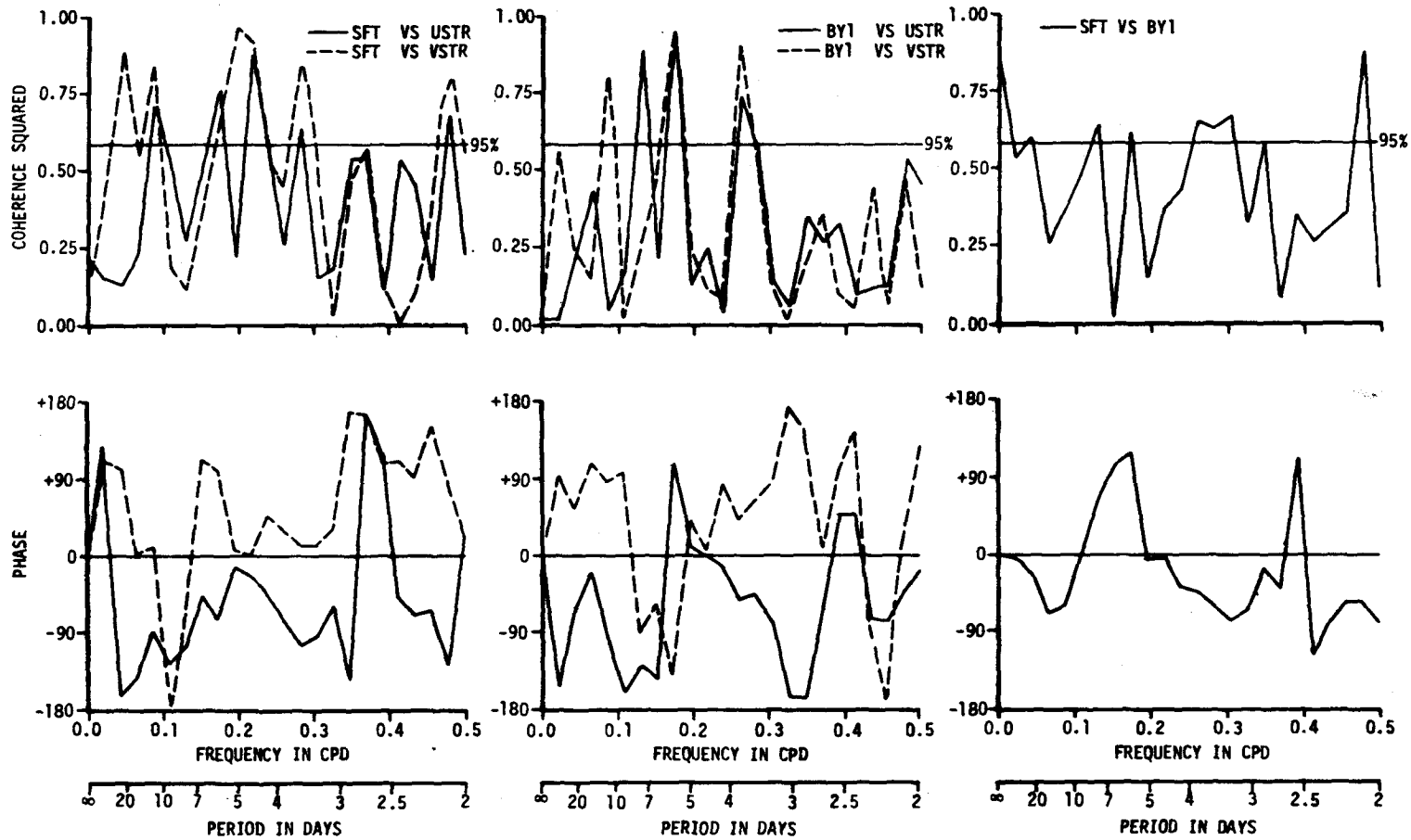


Figure 3.5. Coherence squared and phase for SFT vs. USTR and VSTR, BY1 vs. USTR and VSTR, and for SFT vs. BY1; W71. $N = 399$, $\Delta t = 8$ hours, $M = 69$, $BW_e = 0.027$ cpd, $DOF = 14.5$.

1. The autospectra for the onshore-offshore (USTR) and alongshore (VSTR) wind stress components (Fig. 3.4) were quite different. The USTR spectrum was spread over a wide band of frequencies from about 0.03 to 0.40 cpd with a maximum at 0.283 cpd ($T = 3.5$ days). There was a secondary peak at a period of 2.3 days. The VSTR spectrum had a significant peak centered at a period of about one week and a broad band of high energy between 0.2 to 0.3 cpd with a maximum at a period of 3.3 days. The peak at the weekly period was probably associated with the approximately weekly passage of cold fronts through the area (Partagas and Mooers, 1975).
2. The spectrum (Fig. 3.4) for SFT was almost totally "red," similar to the others for the surf temperature shown in Appendix A. About 98% of the energy content was accounted for at frequencies below about 0.04 cpd.
3. The spectrum for BY1 (Fig. 3.4) was essentially dominated by frequencies less than about 0.08 cpd.
4. The SFT was coherent at the 95% level with both wind stress components at periods of 11.5, 5.8, 4.6, 3.5, and 2.1 days (Fig. 3.5). At the 11.5 day period, the surf temperature was in phase with the alongshore stress and led the offshore stress by about 2.9 days. At the 4.6 day period, the surf temperature and both stress components were nearly in phase, while the phase relation at the 3.5 day period was nearly the same as for the 11.5 day band. At the 2.1 day period, the alongshore stress led the surf temperature by about 0.5 days and the offshore stress lagged the temperature by about 0.8 days. Significant coherence existed between SFT and VSTR at a pe-

riod of 23 days with the stress leading the temperature by about 5.1 days.

5. The bottom temperature at BY1 was coherent with both wind stress components at periods of 5.8 and 3.8 days (Fig. 3.5). At the 5.8 day period the offshore stress led the temperature by about 1.8 days and the alongshore stress lagged the temperature by about 2.4 days. At 3.8 days, the temperature was nearly in phase with the offshore stress and lagged the alongshore stress by about 75° . The BY1 temperature was also coherent with the alongshore stress at the 11.5 day period. In contrast to the in-phase relation between SFT and VSTR at that period, the alongshore stress led the BY1 temperature by 90° (2.9 days). As will be seen in Chapter 3.3.4, the phase relations between SFT and VSTR at 23 days, BY1 and both stress components at 3.8 days, and BY1 vs. VSTR at 11.5 days were consistent with those expected from onshore Ekman compensation flow due to upwelling favorable winds.
6. The coherence between the two temperature records (SFT, BY1) was significant at periods of 2.1, 3.2 to 3.8, 5.8, 7.6, and 23 days (Fig. 3.5). For the shorter periods ($T < 3.8$ days) the phase was negative indicating that SFT led BY1. The phase was also negative at the 23 day period. For the 5.8 and 7.6 day periods, BY1 led SFT.

In general, the spectrum analysis has shown that most of the energy in the temperature records occurred at very low frequencies. There were, however, significant coherences between the temperature records and the wind stress components at higher frequencies. The periods most commonly associated with significant coherence were 2.1, 11.5, and 23

days, and bands of 3.2 to 3.8 and 4.5 to 7.8 days. These periods are similar to those which several investigators have determined are predominant in temperature, sea level, and current fluctuations in the Florida Current regime (Schott and Dúing, 1976; Brooks and Mooers, 1977 a; Dúing, Mooers, and Lee, 1977).

3.3.3 Cross-Spectrum Analysis: S71

The auto- and cross-spectrum calculations for the S71 data set were performed with a record length of 455 points (N), a time interval (Δt) of 8 hours, a maximum of 69 lags (M), for an equivalent effective bandwidth (BW_e) of 0.027 cpd and 16.5 degrees of freedom (DOF). Twenty-four spectrum estimates were computed for the 0.0 to 0.5 cycle/day frequency band. The normalized autospectra for USTR, VSTR, SFT and BY2 are shown in Figure 3.6. The coherence squared and phase for SFT and BY2 vs. USTR and VSTR, and for SFT vs. BY2 are shown in Figure 3.7. The following conclusions are drawn from these calculations:

1. The USTR spectrum for S71 (Fig. 3.6), in contrast to that for W71 (Fig. 3.4), showed a shift in the maximum to the low frequency range of 0.07 to 0.04 cpd. A similar maximum energy band during the summer was found by Brooks (1975) for winds at Miami. In addition, the USTR spectrum (S71) was much less broad banded than for W71, with distinct peaks at periods near 7.6, 5.1, and 3.5 to 3.8 days.
2. The VSTR spectrum (Fig. 3.6) had a broad peak centered at a period of about 3.3 days with secondary peaks at 2.6 and 6.6 days.
3. As in all previous cases (W71 and Appendix A), the temperature spec-

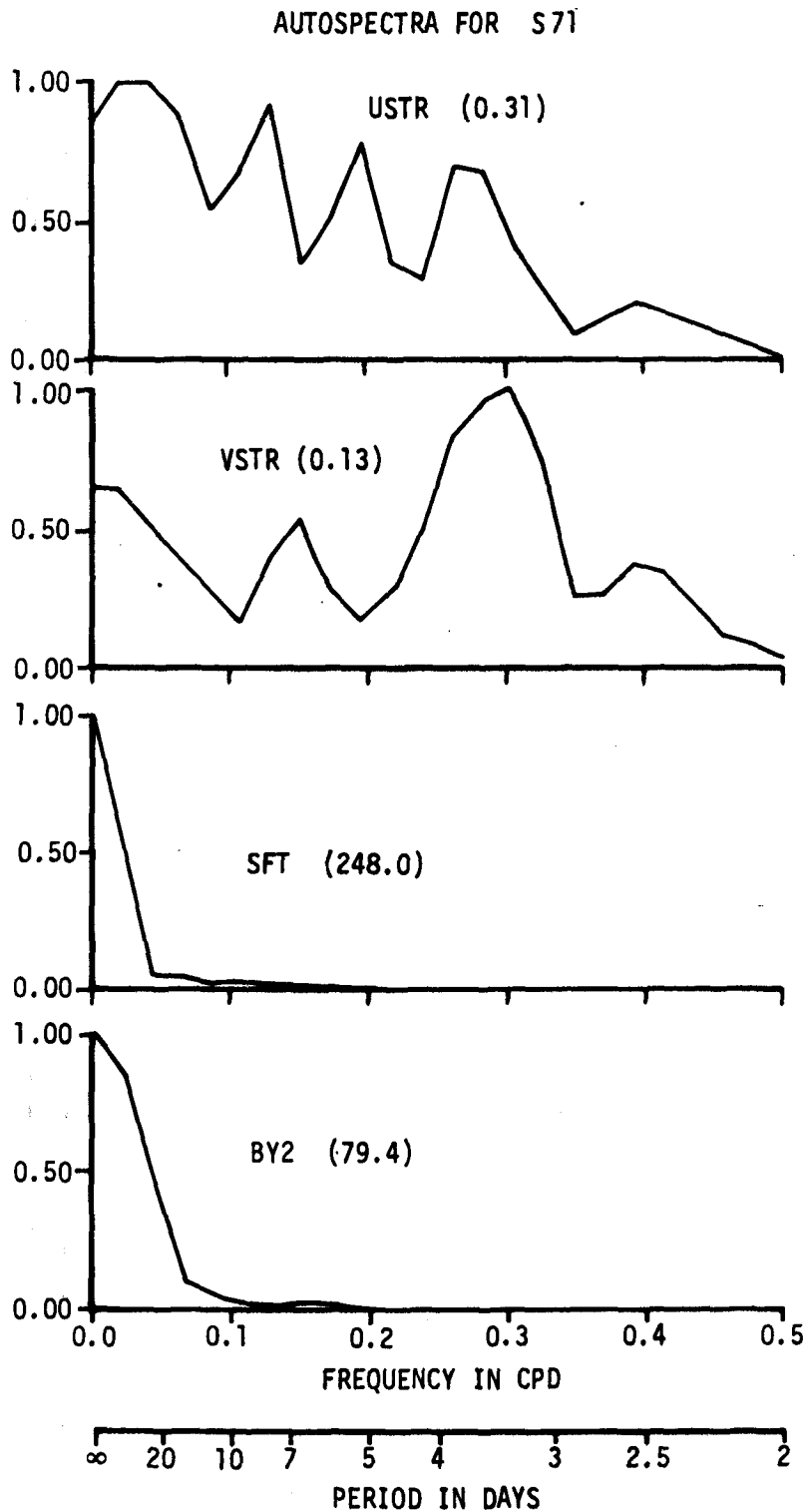


Figure 3.6. Autospectra for USTR, VSTR, SFT, and BY2; S71. Normalization factors are given in parentheses. $N = 455$, $t = 8$ hours, $M = 69$, $BW_e = 0.027$ cpd, $DOF = 16.5$.

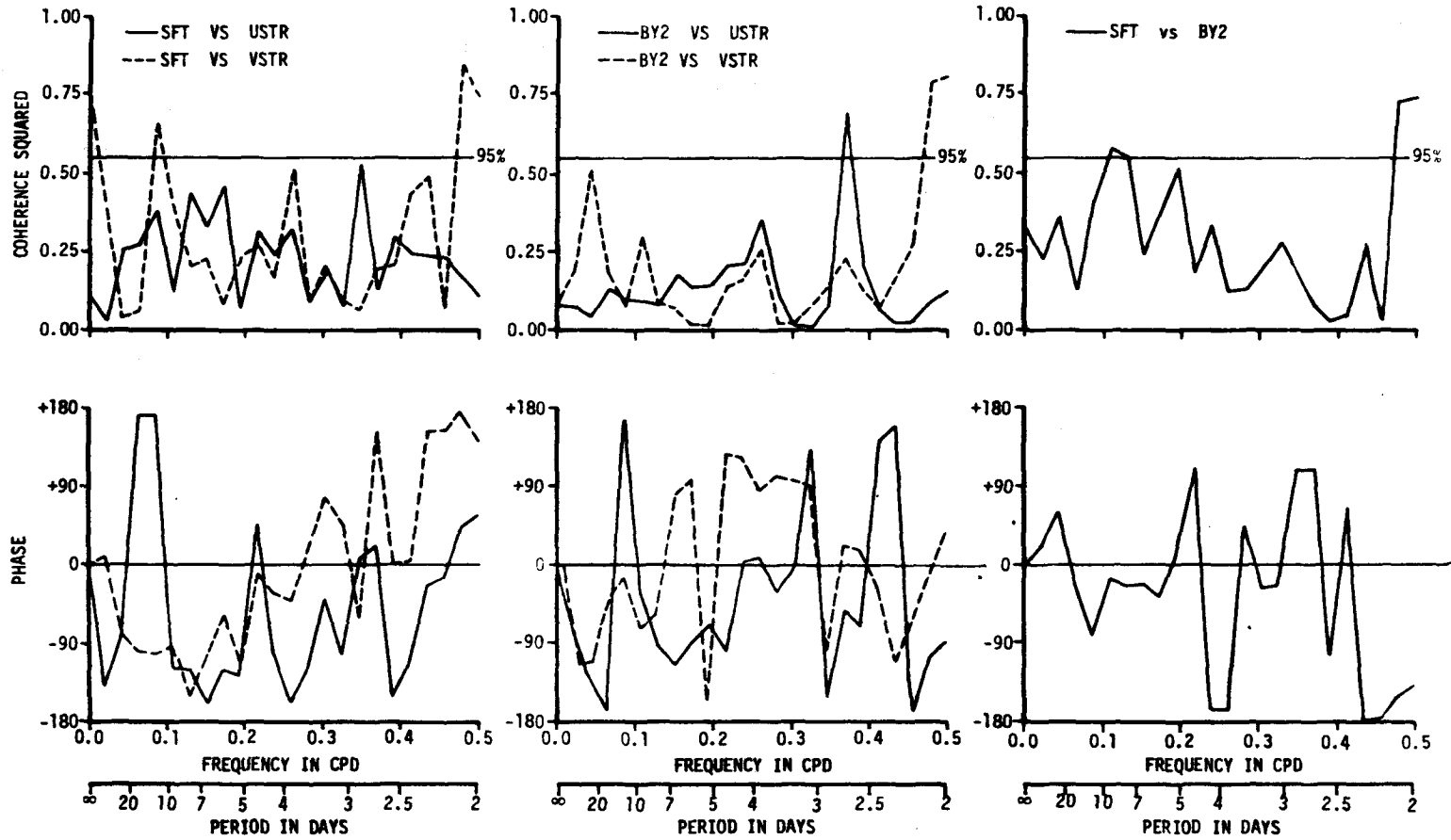


Figure 3.7. Coherence squared and phase for SFT vs. USTR and VSTR, BY2 vs. USTR and VSTR, and for SFT vs. BY2; S71. $N = 455$, $\Delta t = 8$ hours, $M = 69$, $BW_e = 0.027$ cpd, $DOF = 16.5$.

tra had no pronounced peaks and energy concentrated at very low frequencies (<0.6 cpd).

4. In contrast to the results for the W71 record (with significant coherence at many frequencies), the coherence squared between SFT and the wind stress components for S71 was significant only for SFT vs. VSTR at periods of 2.1 and 11.5 days (Fig. 3.7). At the 2.1 day period, the alongshore stress and the temperature were nearly out of phase. Conversely, at the 11.5 day period, the surf temperature led VSTR by about 2.8 days. For the W71 data set, the surf temperature was essentially in phase with the alongshore stress at the 11.5 day period. None of these phase relationships were consistent with that predicted by simple Ekman theory (see Chap. 3.4.4).
5. The bottom temperature at BY2 was significantly coherent with USTR at a frequency of 0.37 cpd ($T = 2.7$ days). At this frequency, the temperature led the stress by about 50° (Fig. 3.7). BY2, as well as SFT, was also significantly coherent with the alongshore stress at the 2.1 day period, but BY2 was essentially in phase with VSTR.
6. The two temperature records (SFT vs. BY2) were significantly coherent at the 2.1 day period and also for a small period band between 7.6 and 9.2 days (Fig. 3.7). At the 2.1 day period, the surf temperature led the bottom temperature. For the longer period band, they were nearly in phase.

The general results for S71 calculations suggest that the temperatures were consistently coherent with the alongshore wind stress at a period of about 2.1 days. In addition, coherence between the surf

temperature and the alongshore stress at a period of 11.5 days appeared to be a persistent feature for both winter and summer records. This result is consistent with the findings of Dúing, et al. (1977) which showed that the seasonal change in atmospheric variables did not affect v-component current amplitudes (measured in the Florida Current) in the 10- to 13-day band. They concluded that these oscillations were due to continental shelf waves which respond to well-defined atmospheric forcing events and occur in wave packets of typically four to six cycles, regardless of the season.

3.3.4 Phase Relations

Results of the cross-spectrum analyses indicated that the phase relationships between the temperature and the wind stress were consistent with those expected from coastal upwelling theory for the 3- to 4-day and 11.5 day periods. For a simple wind-driven coastal Ekman divergence, a compensation onshore flow occurs below the surface Ekman layer. The divergence at the coastal boundary in turn results in upward vertical velocity into the surface layer. For a simple time dependent wind stress independent of x and y , the compensation onshore-offshore velocity will be out of phase with the alongshore stress and lag the onshore-offshore stress by 90° (e.g., Kundu, et al.; 1975). The phase between recorded temperature at a particular depth and the stress depends on the sign of the horizontal and vertical temperature gradients. For typical conditions off Cape Canaveral, both are assumed positive. In that case, the expected phase between the recorded temperatures and the stress is such that the temperature is in phase with the onshore-offshore stress and lags the alongshore stress by 90° .

4. CURRENT AND TEMPERATURE STRUCTURE AT SHELFBREAK

Evidence indicates that onshore-offshore motion of the Florida Current, together with wind-forcing, dominates the circulation and hydrography over the shelf area. For this reason, during the July 1971 cruise, measurements were made of the vertical structure of currents and temperature near the shelfbreak. The purpose was to establish the offshore boundary conditions typical of mid-summer for this area.

4.1 Data Acquisition and Processing

The R/V VENTURE was anchored in a water depth of 102 m at 2100 EDT, 27 July 1971 near the shelfbreak directly offshore from Cape Canaveral along Transect 3 (Fig. 1.2). A profiling current meter system, developed at the University of Miami's Rosenstiel School of Marine and Atmospheric Sciences, was used. An Aanderaa current meter was mounted in a slightly negatively buoyant float and allowed to descend through the water column along a plastic coated cable suspended from the ship. Hence, the current meter float was largely detached from the ship, minimizing the influence of ship motion (Düing and Johnson, 1972).

The anchor station was occupied for a period of 50 hours. This record length was selected to allow averaging to eliminate effects from semidiurnal, diurnal, and inertial motions. The local inertial period is 25.1 hours. Current meter lowerings were made every 90 minutes and were accompanied by an XBT cast. The XBT recorder failed, however, after 36 hours. The mean descent time for the current meter was about 20 minutes.

The raw current meter data were corrected for horizontal motion of the instrument using an assumed wire shape of a quarter sine wave (Düing and Johnson, 1971). The vector component data were then interpolated to 5 meter depth intervals with a three point polynomial interpolation scheme. The interpolated value was calculated first using two points above and one point below the standard depth, then one point above and two points below. The results of the two were then averaged to obtain the value for each component at the standard depths. Finally, the coordinate system was rotated ten degrees counterclockwise for alignment with the isobaths. The XBT data were digitized to the same 5 meter intervals.

4.2 Mean Velocity and Temperature Profiles

The profiles of temperature (\bar{T}), onshore-offshore velocity component (\bar{u}), and alongshore velocity component (\bar{v}) are shown in Figure 4.1. The temperature mean was calculated for the 36 hour record while the mean velocity components were for the total 50 hour period. The 95% confidence limits on the mean were calculated at each depth for the three profiles according to:

$$Y_L = \bar{y} \pm tS_{\bar{y}} \text{ and } S_{\bar{y}} = \frac{S}{\sqrt{N}}$$

where

Y_L = limits of the mean value

\bar{y} = sample mean value

N = degrees of freedom = number of samples (n)-1

t = value of the Student's t distribution for 95% probability level and N degrees of freedom.

S = sample standard deviation

$S_{\bar{y}}$ = standard error of the mean

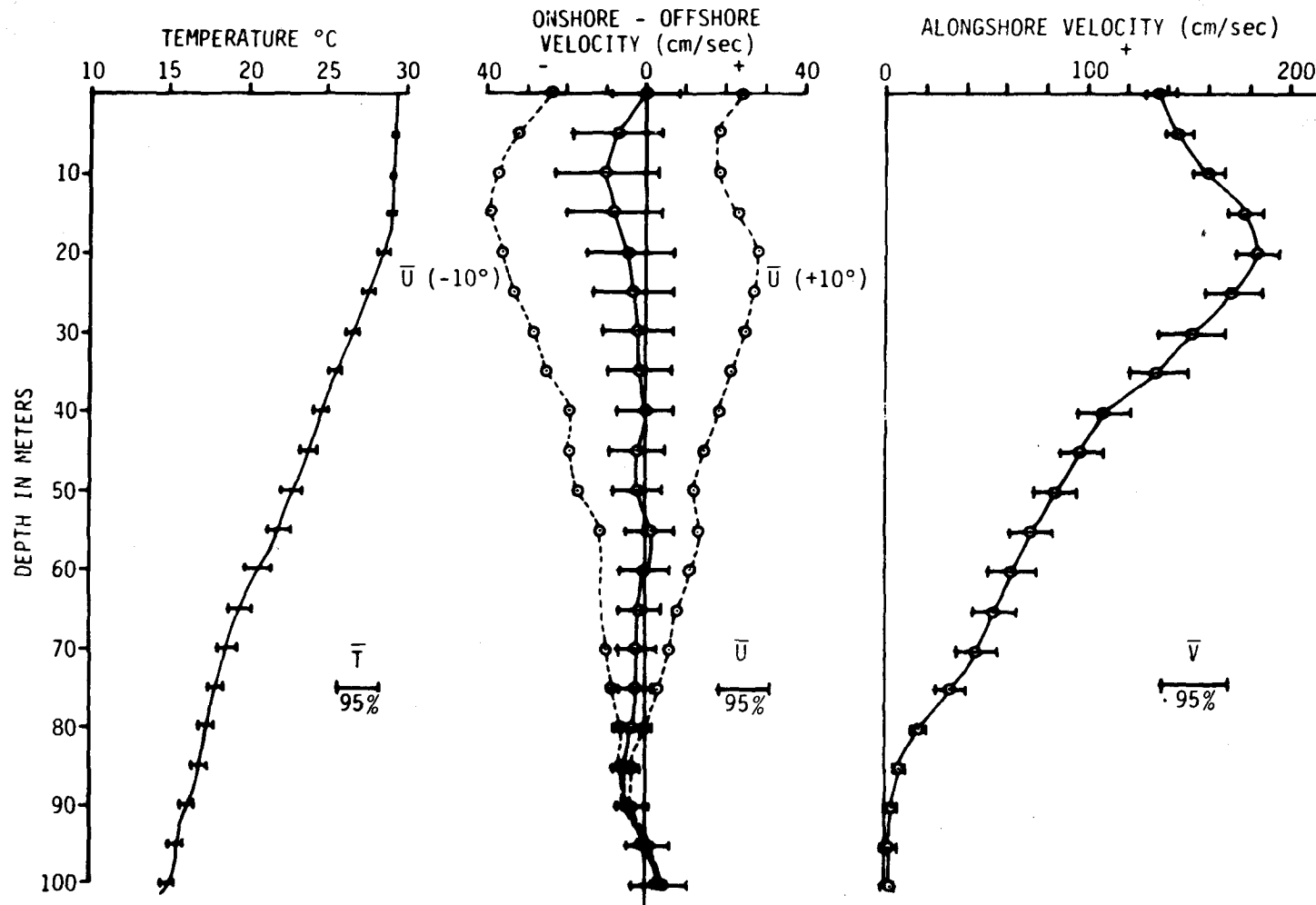


Figure 4.1. Mean profiles of temperature (\bar{T}), onshore (-) - offshore (+) velocity (\bar{U}) and alongshore velocity (\bar{V}) from 50 hour anchor station (36 hours for temperature). Coordinate system has been rotated 10° counter-clockwise from true north. $\bar{U} (+10^\circ)$ and $\bar{U} (-10^\circ)$ are average profiles for a further $\pm 10^\circ$ coordinate rotation. Horizontal bars indicate the 95% confidence limits for the estimate of the mean.

The confidence limits are indicated by the brackets in Figure 4.1. Also included in Figure 4.1 are profiles of \bar{u} for $\mp 10^\circ$ coordinate rotation.

The mean temperature profile was nearly isothermal (29°C) from the surface to the top of the thermocline at a depth of about 17 m. The temperature gradient was nearly uniform ($\frac{dT}{dz} \approx 0.18^\circ\text{C/m}$) from 17 m to a depth of 55 m. Between 55 m and 63 m the gradient increased to about 0.25°C/m . Below 63 m the gradient decreased to a value of about 0.20°C/m .

The mean profile for the onshore-offshore velocity (\bar{u}) indicated onshore (negative values) flow at all depths except between 53 and 60 m and 95 to 100 m (Fig. 4.1). The maximum onshore flow (-10 cm/sec) occurred at a depth of 10 m, with another local maximum of -5 cm/sec at about 85 m. The mean \bar{u} profile is also shown for a $\mp 10^\circ$ [$\bar{u} (-10^\circ)$, $\bar{u} (+10^\circ)$] coordinate rotation. Although the profile shapes were similar, the directional sense of the velocity vector changed sign. This demonstrates the sensitivity of the \bar{u} profile to coordinate rotation primarily due to the large values of the alongshore velocity component (\bar{v}). Since the \bar{u} profile coordinate system was rotated 10° counterclockwise, the $\bar{u} (-10^\circ)$ profile represents the true east-west velocity component. This profile showed westward flow (negative values) at all depths except near the bottom (95-100 m).

The main feature of the mean alongshore velocity (\bar{v}) profile (Fig. 4.1) was a subsurface maximum of 184 cm/sec at a depth of 20 m, near the top of the thermocline in the mean temperature profile. Similar subsurface maxima in the \bar{v} component of the Florida Current off Miami were demonstrated by D'Ángelo (1975). He found that the subsurface jet feature

occurred at irregular but frequent intervals, with formation and decay typically on a time scale between one-half and one day. Düing speculated that the feature may be a manifestation of the "shingle structure" described by Fuglister (1951 b) and also by von Arx, et al. (1955). He also suggested the possibility that spatially unresolved eddies were responsible for such vertical structure in the horizontal velocity. The time scale suggests that internal tides and near-inertial motions may be important.

The mean value of \bar{v} at the surface was 136 cm/sec. Below the subsurface jet, the velocity decreased rapidly to a depth of 40 m. The velocity shear in this layer ($\frac{d\bar{v}}{dz}$) was $3.75 \times 10^{-2} \text{ sec}^{-1}$. The velocity decreased nearly linearly between 40 and 70 m with a mean shear $\frac{d\bar{v}}{dz} = 2.1 \times 10^{-2} \text{ sec}^{-1}$, followed by another rapid decrease to a value of 8 cm/sec at 85 m. There was no evidence of southward flow near the bottom in the mean profile such as that found in deeper water off Miami by Düing (1975). Weak southward flow along the bottom existed near the beginning and end of the anchor station (Chap. 4.3).

The vertically intergrated transports were calculated for the mean \bar{u} and \bar{v} profiles in the original geographic coordinate system. The coordinate rotation required to provide zero net onshore-offshore transport was 11.2° counterclockwise. This is close to the assumed 10° isobath orientation and suggests that, at least over the 50 hour anchor station, the net transport was nearly parallel to the local bathymetry. In fact, the 95% confidence limits for \bar{u} (Fig. 4.1) indicate that the mean onshore-offshore flow was not significantly different from zero at all depths in the system rotated to alignment with the local isobath.

4.3 Temporal Variations of Velocity and Temperature

Contours of u and v current components at the anchor station were examined in the time-depth plane (Fig. 4.2 to 4.3). For the first fourteen hours of the anchor station, the u component was offshore at all depths except for a zone of onshore flow in the upper 20 m at profile five (Fig. 4.2). The offshore flow decreased rather uniformly with depth until onshore flow began along the bottom at profile eleven. By profile fifteen (21 hours after the record started), the flow was onshore throughout the water column and increased to a relative maximum at all depths eighteen hours later (profile twenty-seven). The onshore velocity decreased rapidly after profile twenty-seven, with some offshore flow above 15 m, then increased slightly again at the end of the anchor station. Transient subsurface jets occurred above 50 m throughout the record. Thus, although the onshore-offshore flow field had a basic baroclinic signature, the primary temporal variation was suggestive of a barotropic fluctuation with an apparent half-period of at least 36 to 40 hours. The oscillatory subsurface jet was strongly suggestive of near-inertial motion in the upper 30 to 50 m.

The subsurface maximum in the mean alongshore velocity (\bar{v}) profile (Fig. 4.1) was dominant in the time-depth representation of the v component (Fig. 4.3). The maximum value of over 260 cm/sec occurred at profile one at a depth of 20 m. Associated with the decrease of the offshore flow (Fig. 4.2) was a decay and vertical spreading of the strength of the v component jet. The influence of the vertical propagation of horizontal momentum continued through profile fifteen. Shortly after the onset of onshore flow, the v component reached a relative minimum above about 55 m and a relative maximum below that depth. As onshore

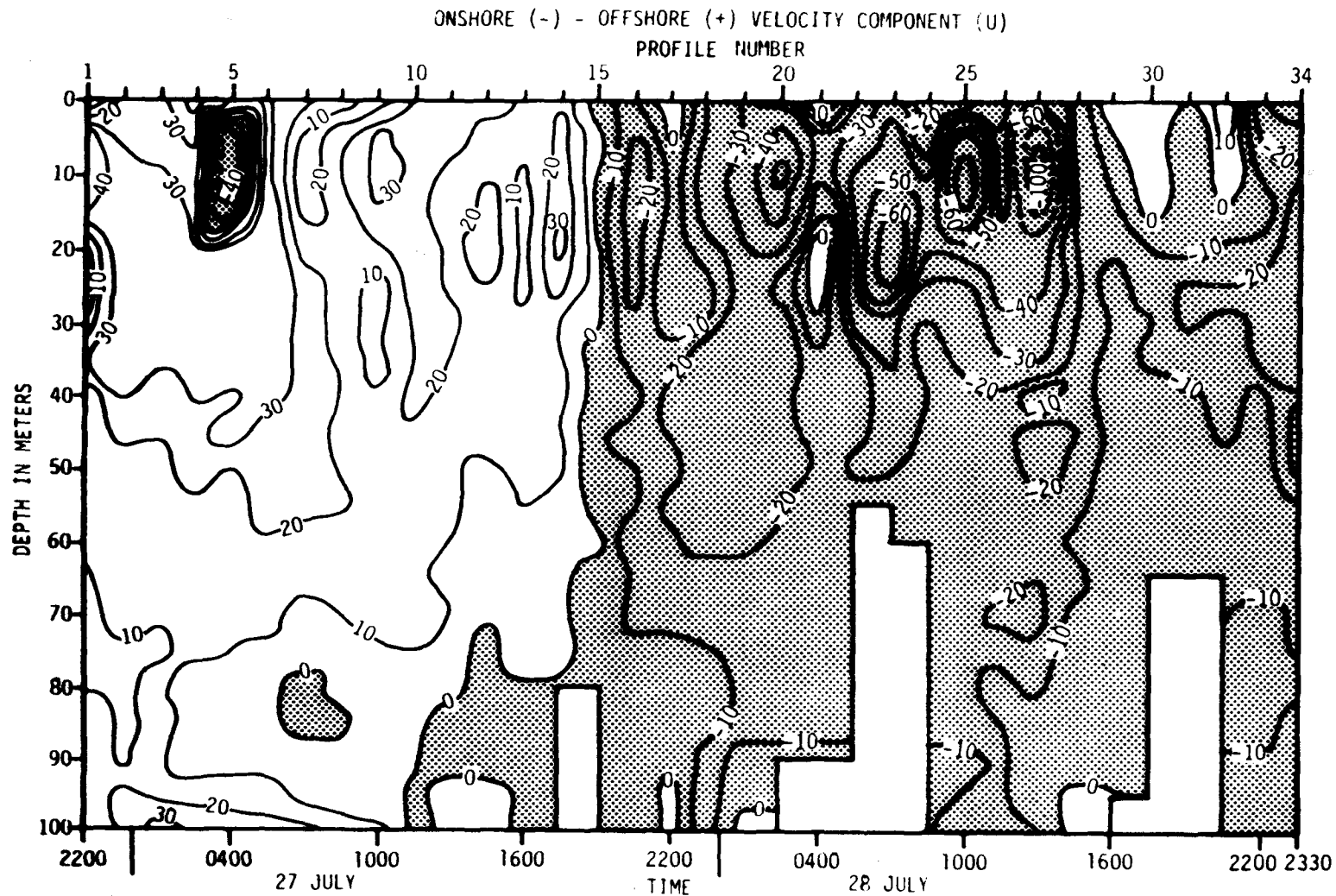


Figure 4.2. Time-depth contours of the onshore (-) - offshore (+) component (u) of velocity for the 50 hour anchor station. The standard contour interval is 10 cm/sec with departures indicated by dashed contours. Negative values (onshore flow) are shaded. Blank areas are gaps in the data due to the profiling current meter's failure to reach the bottom.

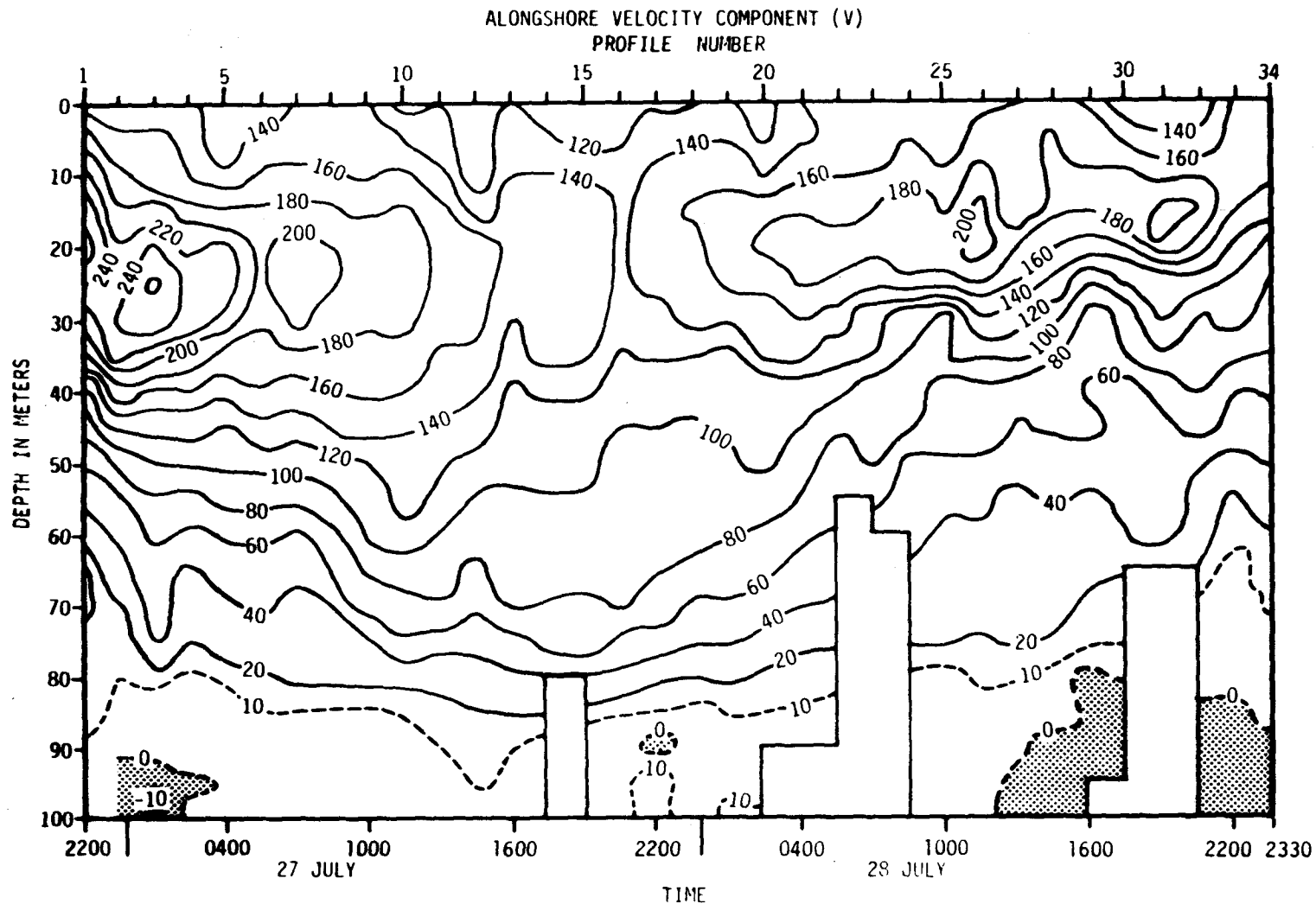


Figure 4.3. Time-depth contours of the alongshore component (v) of velocity for the 50 hour anchor station. The standard contour interval is 20 cm/sec with departures indicated by dashed contours. Negative values (south-southeastward flow) are shaded. Blank areas are gaps in the data due to the profiling current meter's failure to reach the bottom.

flow increased, the alongshore subsurface jet re-intensified, increasing from a minimum value of about 135 cm/sec at profile sixteen to over 200 cm/sec at profiles twenty-six, thirty-one, and thirty-two. Below the intensifying jet, from about 25 m to the bottom, the velocity generally continued to decrease to the end of the record. In contrast to the apparent barotropic nature of the onshore-offshore flow, the alongshore flow exhibited a progressive downward transfer of horizontal momentum coincident with a weakening of the subsurface maximum and the change from offshore to onshore flow. This was followed by progressive re-establishment of the subsurface jet concurrently with the increase of onshore flow. The nature of the alongshore flow variation was decidedly baroclinic but did correspond to the wave-like nature of the u component with approximately the same apparent half-period of 36 to 40 hours. The formation and decay rate of the subsurface jet was apparently on a slightly longer time scale than the one-half to one day rate observed off Miami by Dúing (1975). The oscillatory nature of the subsurface jet itself was suggestive of near-inertial motion in the upper 30 to 50 m. A weak southward (<10 cm/sec) near-bottom flow occurred near the beginning and end of the record.

The XBT Transect 3 was traversed just prior to the 50-hour anchor station (Fig. 4.4). The solid vertical line indicates the approximate anchor station location. This is the same XBT section as in Figure 2.7, and it is believed to represent thermal conditions at or near the time of maximum onshore excursion of the Florida Current. The strong upward bowing of the isotherms near the shelfbreak (Station 56) indicated possible upwelling. This feature was not evident during times when the Florida Current receded offshore (Fig. 2.6).

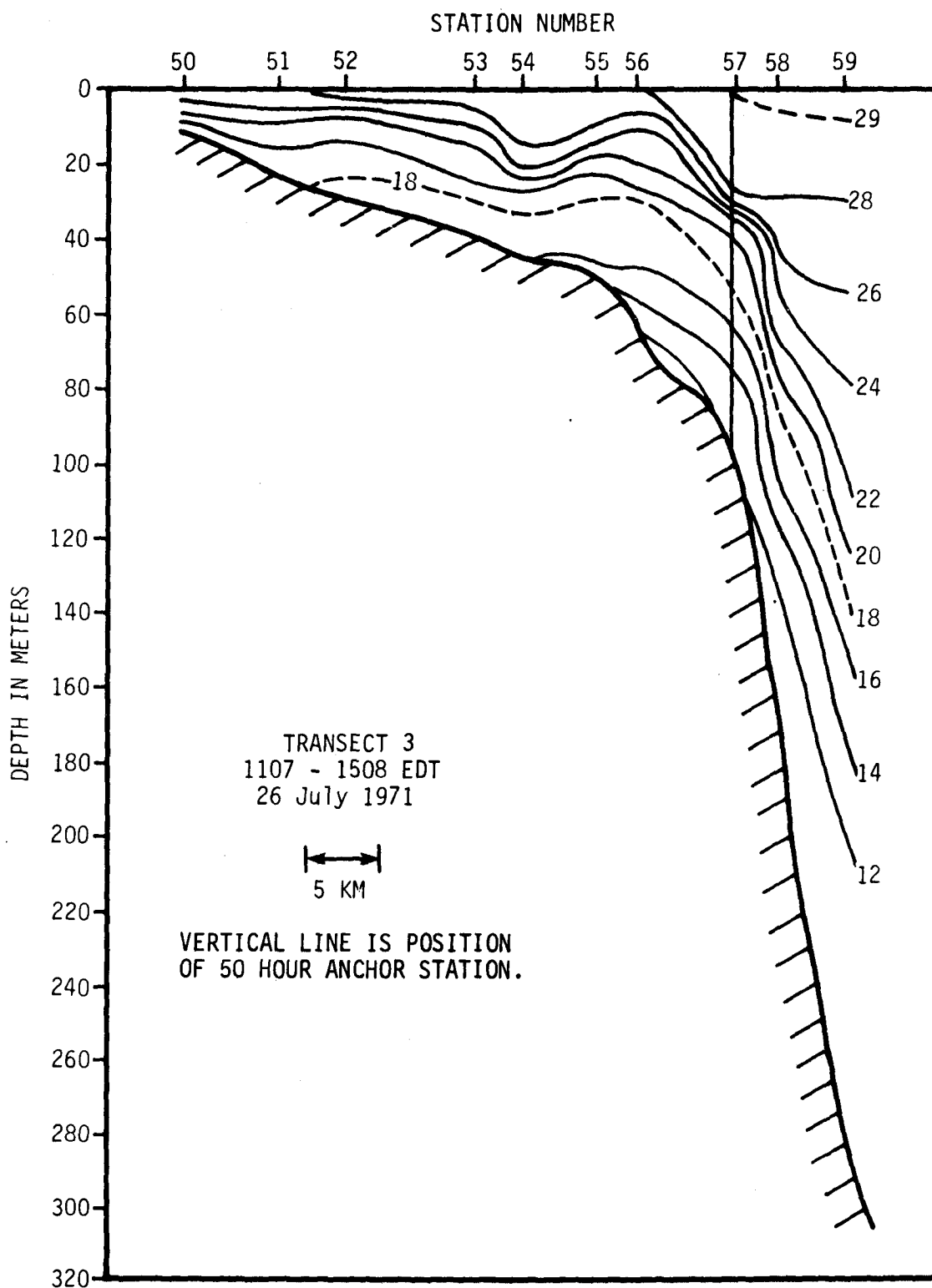


Figure 4.4. Temperature section along Transect 3 run between 1107 EDT and 1508 EDT, 26 July 1971. Vertical line at the shelfbreak indicates location of anchor station.

The time-depth variation of the abbreviated anchor station temperature record is shown in Figure 4.5. The last XBT station (59 in Fig. 4.4) was completed seven hours prior to the first anchor station profile. Since the observed u component flow was strongly positive in the early portion of the anchor station (Fig. 4.2), it is assumed that the flow had been offshore for some or all the seven hour sampling hiatus. As offshore flow continued, the overall thermal field was advected offshore, and accompanied by a relaxation of the bowed isotherms. Thus, the temperature increased rapidly at all depths, the effect manifested first along the bottom and then to progressively shallower depths. The general trend toward increasing temperature continued until the beginning of the onshore flow (profile 15), when the temperature trend reversed. As the onshore flow increased, presumably accompanied by upward vertical motion at the shelfbreak, the temperature decreased throughout the water column. The gradual deepening (shoaling) of the isotherms with decreasing (increasing) alongshore velocity (Fig. 4.3) suggests an approximate geostrophic balance in the alongshore flow variation. Although the XBT recorder failed after 36 hours, the wave-like nature of the velocity field was also apparent in the temperature field.

To estimate the validity of the geostrophic relationship for the mean alongshore velocity, the geostrophic velocity was calculated between XBT stations 57 and 59 (Fig. 4.4). The temperature-salinity relationships for the western portion of the Florida Current given by Parr (1937) were approximated (Table 4.1) for the calculation of specific volume anomalies. The estimated geostrophic velocity profile (V_g) was compared to that of the mean alongshore velocity (\bar{v}) from the 50-hour anchor station (Fig. 4.6). From 30 m to 90 m, the calculated geostrophic

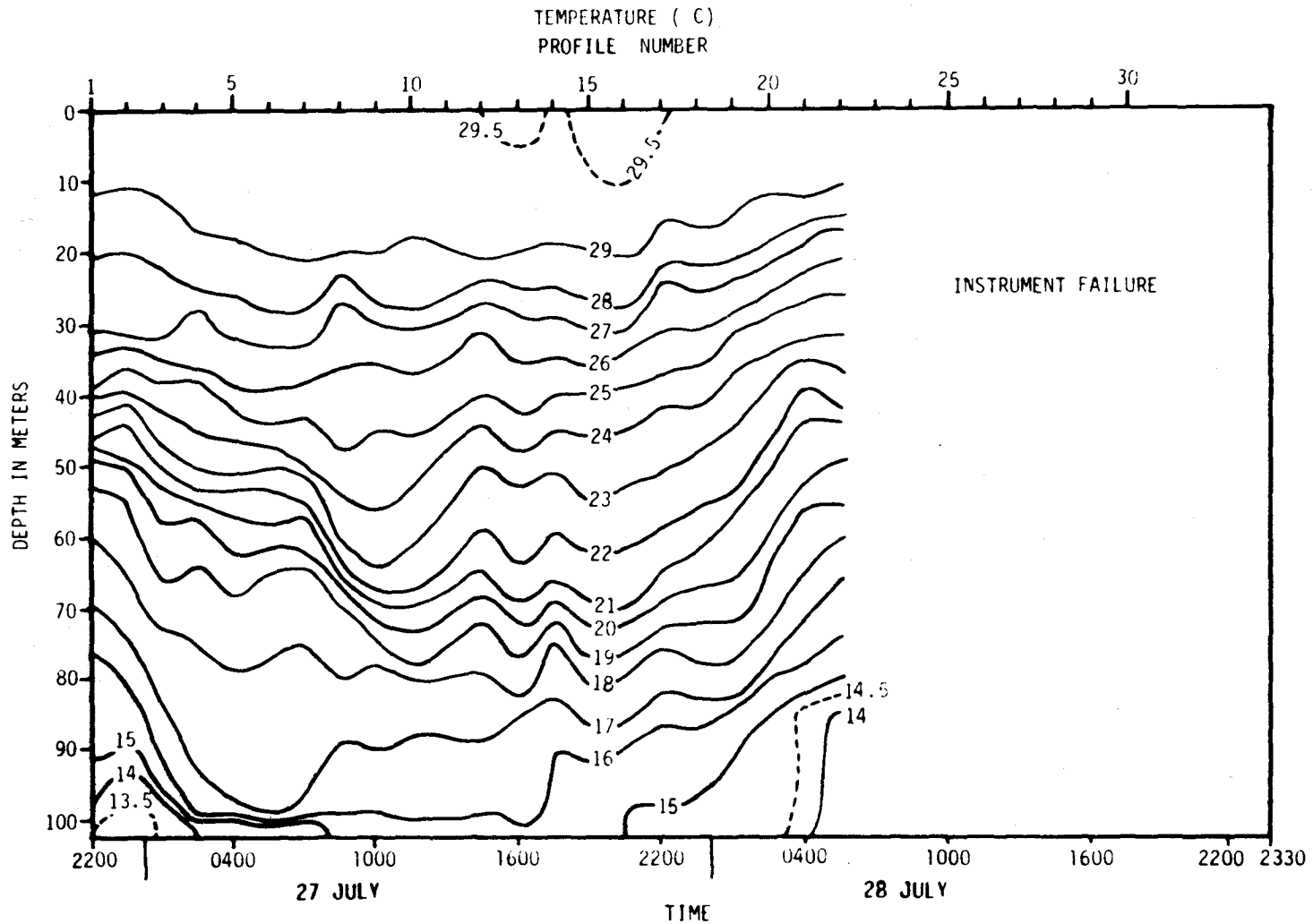


Figure 4.5. Time-depth contours of temperature for anchor station. The XBT recorder failed after 36 hours. The standard contour interval is 1.0°C with departures indicated by dashed contours.

TABLE 4.1. Approximated temperature-salinity relationship for geostrophic velocity computations. Values are based on results given by Parr (1937).

Temperature Range (°C)	Estimated Salinity (0/00)
26.0 - 30.0	36.00
23.0 - 25.9	36.30
18.0 - 22.9	36.50
16.0 - 17.9	36.30
14.0 - 15.9	36.00
12.0 - 13.9	35.80
10.0 - 11.9	35.50
<u>≤</u> 9.9	35.30

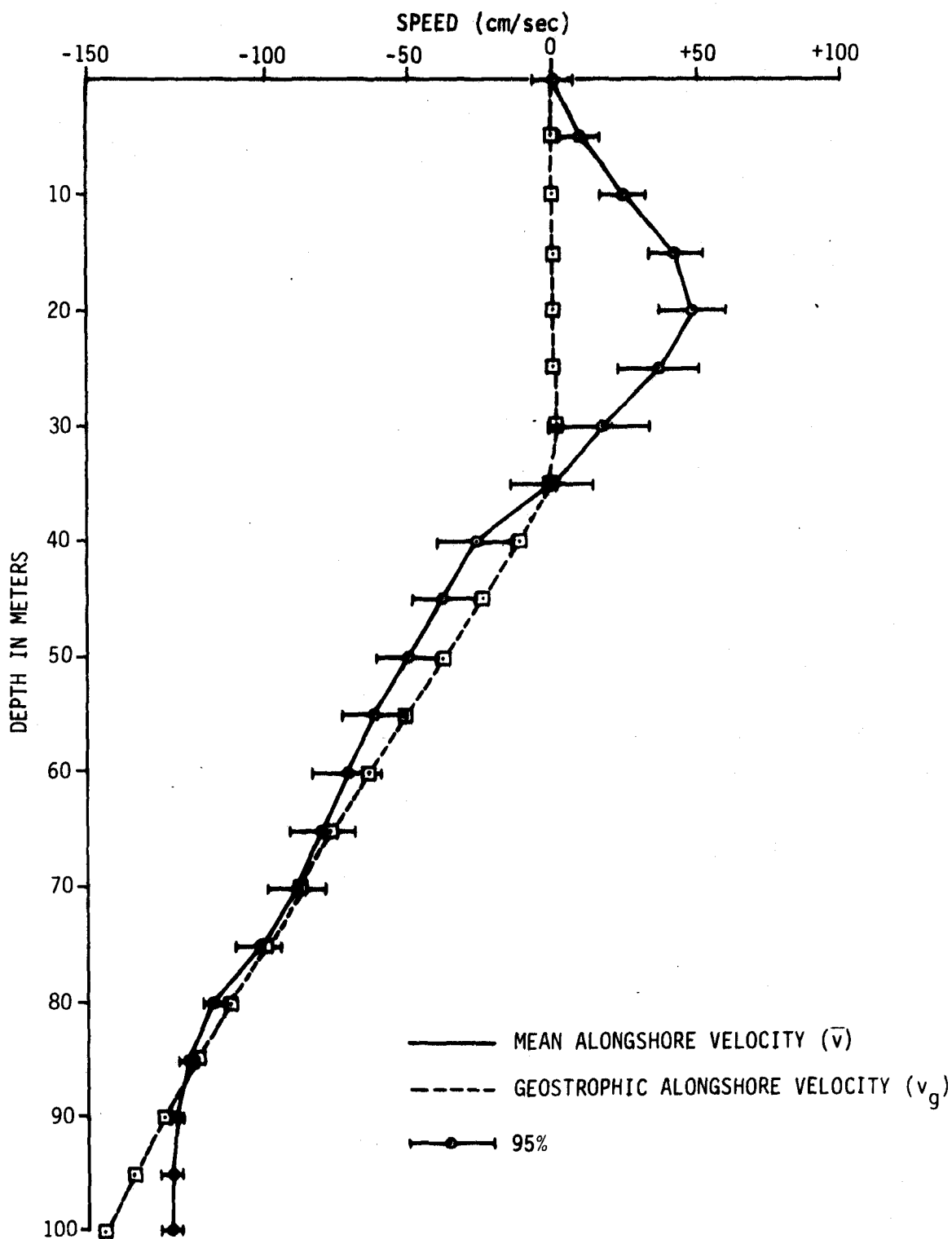


Figure 4.6. Comparison of calculated alongshore geostrophic velocity (dotted line) with measured mean profile from 50 hour anchor station (solid line). Geostrophic velocity calculated between XBT stations 57 and 59 (Fig. 4.4). Both profiles are referenced to zero surface velocity. Horizontal bars indicate the 95% confidence limits for the estimate of the measured mean.

velocity at each depth was within (or nearly so) the 95% confidence limits for the measured mean value. The departure of \bar{v} from geostrophy from 90 to 100 m was probably due to the bottom frictional effect. Above 30 m, the V_g profile had virtually no vertical shear and the measured subsurface jet was not evident. The oscillatory nature of the subsurface velocity maximum was suggestive of near-inertial (perhaps wind-induced) and longer period (i.e., 3- to 4-day) motions. The averaging operation would presumably have removed any inertial effects, but not those of the longer period motion. In addition, the XBT stations from which V_g was estimated were occupied about eight hours prior to the beginning of the anchor station. Hence, it is not surprising that the geostrophic relationship is not verified in the upper 30 m.

4.4 Temporal Variations of the Perturbation Velocity and Temperature

To more clearly show the perturbation structure of the velocity (u , v) and temperature (T) fields at the anchor station, the time-averaged vertical profiles for u , v , and T were removed and the residuals contoured in the time-depth domain (Figs. 4.7 to 4.9). The perturbation u component was nearly identical to that for the actual onshore-offshore flow (Fig. 4.2) since the mean velocity was not significantly different from zero at all depths. The primary feature was an oscillatory, basically barotropic flow (phase) with amplitude of 10 to 20 cm/s and an apparent half-period of at least 36 to 40 hours. Larger amplitude fluctuations (30 to 40 cm/s) occurred in the upper 30 to 50 m which were suggestive of baroclinic near-inertial motion (Fig. 4.7).

The time-depth variation of the perturbation alongshore velocity (Fig. 4.8) clearly demonstrates the strong baroclinic structure noted in

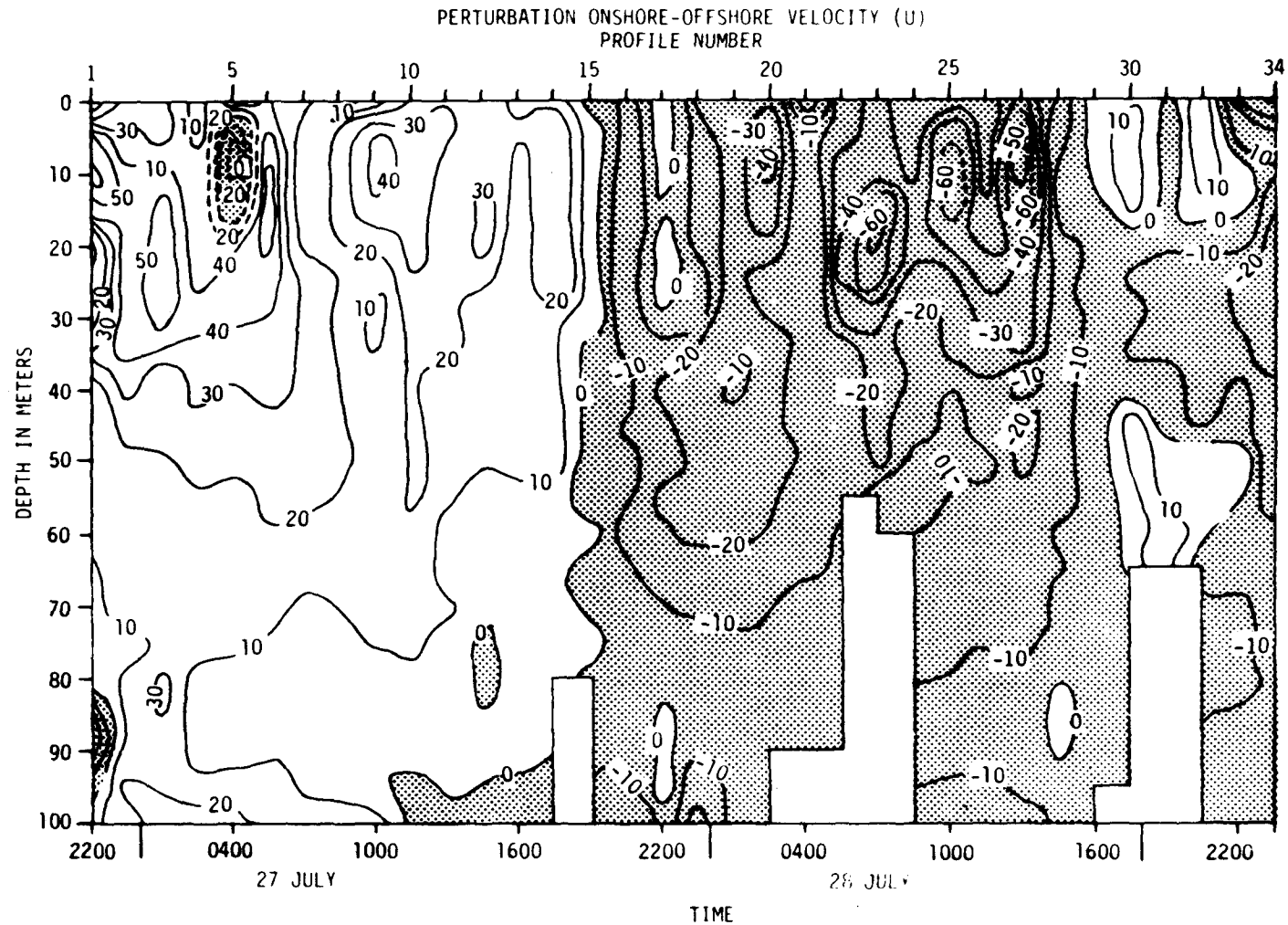


Figure 4.7. Time-depth contours of the perturbation onshore-offshore component (u) of velocity for the 50 hour anchor station. The standard contour interval is 10 cm/sec with departures indicated by dashed contours. Negative anomalies are shaded. Blank areas are gaps in the data due to the profiling current meter's failure to reach the bottom.

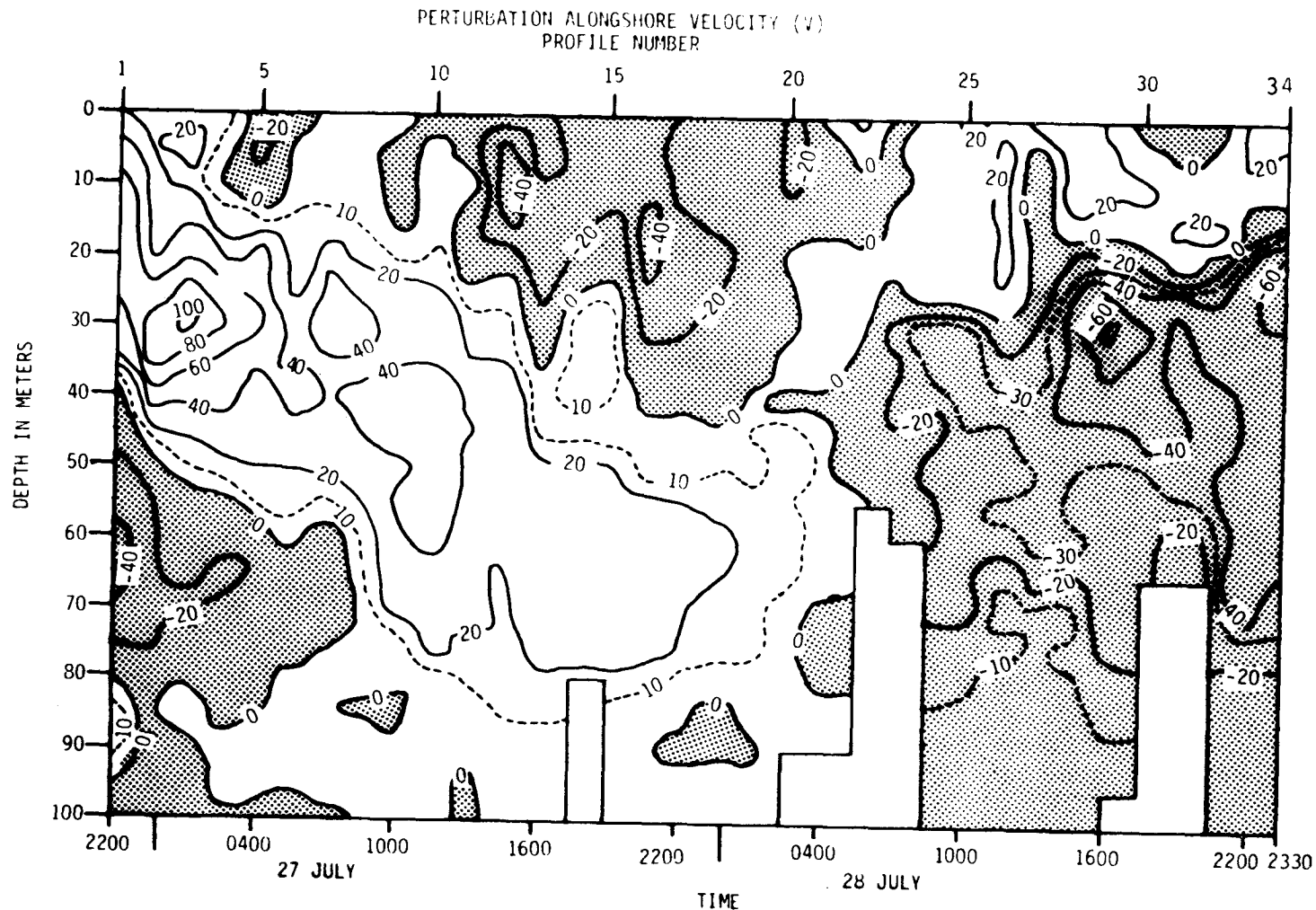


Figure 4.8. Time-depth contours of the perturbation alongshore (v) component of velocity for the 50 hour anchor station. The standard contour interval is 20 cm/sec with departures indicated by dashed contours. Negative anomalies are shaded. Blank areas are gaps in the data due to the profiling current meter's failure to reach the bottom.

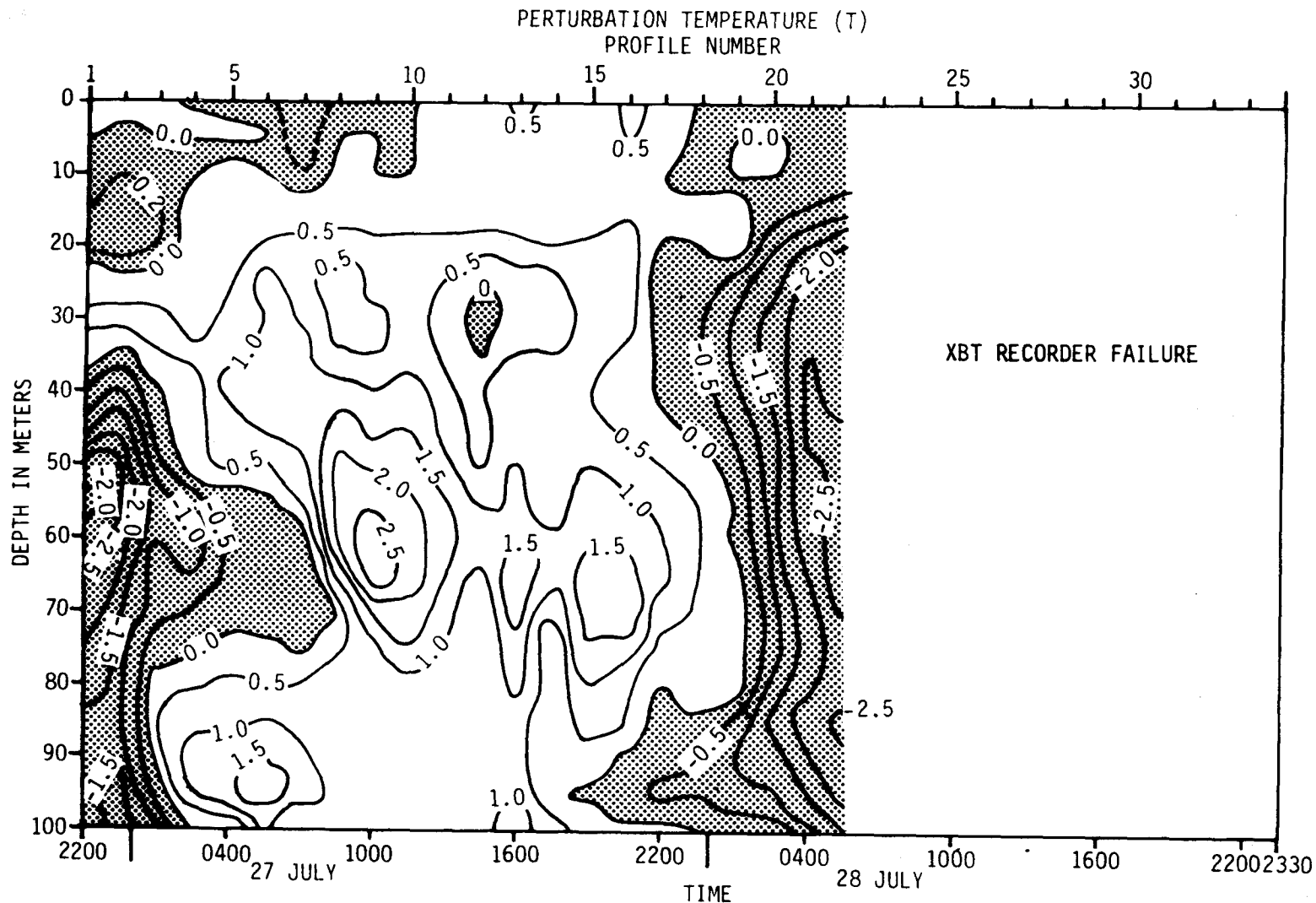


Figure 4.9. Time-depth contours of perturbation temperature for the anchor station. The XBT recorder failed after 36 hours. The standard contour interval is 0.5°C with departures indicated by dashed contours. Negative anomalies are shaded.

the absolute flow field (Fig. 4.3). Fluctuations on at least three fundamentally different time scales were evident:

1. Baroclinic near-inertial motion existed in the upper 30 to 50 m with amplitude of about 20 cm/s.
2. Oscillation occurred at an apparent half-period of at least 36 to 40 hours and a 180° phase difference between the upper and lower water column with the node at about 40 to 50 m. Amplitudes were on the order of 30 to 40 cm/s.
3. The time variation in the depth zone of maximum amplitude fluctuations (30 to 50 m) was suggestive of a longer period oscillation with a half-period of 45 to 50 hours or more.

The winds were steady northward and northwestward at about 2 to 4 m/s for the entire 50 hours.

The perturbation temperature field reflected the onshore-offshore advection of the horizontal temperature gradient structure shown in Figure 4.4 and discussed in Chapter 4.3. That is, during period of onshore flow, the isotherms were bowed upwards over the shelfbreak, indicating possible upwelling. Since the last XBT station was completed 7 hours prior to the first anchor station profile, it was assumed that the flow was directed offshore during the interim. The bowed isotherm effect then resulted in positive u anomalies to be associated initially with negative T anomalies then followed by positive T . The rapid change to positive T between 55 m and 80 m (region of maximum horizontal temperature gradient) was also associated with acceleration in the alongshore component (positive v) which is consistent with an adjustment for a

geostrophic balance. Negative u anomalies were associated with negative T throughout the water column, the effect manifested first along the bottom 20 m. This was presumably due to the apparent upwelling effect associated with onshore flow. In general, the perturbation T field was consistent with the influence of onshore-offshore advection of the observed temperature field, upwelling over the shelfbreak during onshore flow, relaxation of the effect during offshore flow, and an adjustment consistent with geostrophy for acceleration and deceleration of along-shore flow.

4.5 Stability Estimates

Gradient Richardson Numbers (Ri) were calculated from estimates of the Brunt - Väisälä frequency (N^2) using the observed temperature profiles and the estimated temperature-salinity relationship given in Table 4.1, together with the observed velocity shear.

The mean profiles for static stability ($\overline{N^2}$), velocity shear (\overline{S}) and gradient Richardson Number (Ri) were computed as follows:

$$\overline{N^2} = - \frac{g}{\rho} \frac{\Delta \overline{\rho}}{\Delta Z}$$

$$\overline{S} = \left[\frac{\Delta \overline{U}^2}{\Delta Z} + \frac{\Delta \overline{V}^2}{\Delta Z} \right]^{1/2}$$

$$\overline{Ri} = \frac{\overline{N^2}}{\overline{S}^2}$$

where $\frac{\Delta \overline{\rho}}{\Delta Z}$ = mean vertical density gradient profile computed from mean temperature profile with assumed T-S relation.

g = acceleration of gravity

\bar{S} = mean vertical velocity shear profile

\bar{U} = mean U velocity component

\bar{V} = mean V velocity component.

The results for \bar{N}^2 , \bar{S} and \bar{Ri} are shown in Figure 4.10. The static stability increased uniformly from about $0.6 \times 10^{-4} \text{ sec}^{-2}$ to a maximum of $9.2 \times 10^{-4} \text{ sec}^{-2}$ between 35 m and 40 m. The minimum value ($0.25 \times 10^{-4} \text{ sec}^{-2}$) was recorded just above the bottom from 90 m to 95 m. The mean velocity shear increased from $2.5 \times 10^{-2} \text{ sec}^{-1}$ near the surface to a maximum of $5.2 \times 10^{-2} \text{ sec}^{-1}$ at the same depth as the maximum \bar{N}^2 (35 to 40 m). The minimum \bar{S} ($0.6 \times 10^{-2} \text{ sec}^{-1}$) was in the bottom 5 m. The relative minimum in the shear at 20 m to 25 m corresponded to the maximum of the subsurface jet in the mean alongshore velocity (Fig. 4.1).

The mean Richardson Number profile indicated that, throughout most of the water column, the mean flow was marginally stable ($0.25 \leq Ri \leq 1$). The strong vertical shear in the mixed layer (upper 15 m) produced a dynamically unstable situation. The zone of maximum shear (35 to 40 m) was imbedded in the thermocline which yielded a marginally stable flow ($Ri \approx 0.4$).

The time-depth variation of Ri is shown in Figure 4.11. The upper 15 m was unstable ($Ri \leq 0.25$) for nearly the entire 36 hour period. Brief periods of stable flow occurred near profiles 4, 13, and 22 which may indicate tidal influences. The 20 to 30 m zone of the subsurface jet at the beginning of the record (Fig. 4.3) was dynamically stable with a layer of unstable flow just below. As the jet weakened, the flow became stable throughout the middle portion of the water column (20 to 70 m). Maximum values for Ri were recorded when the alongshore and

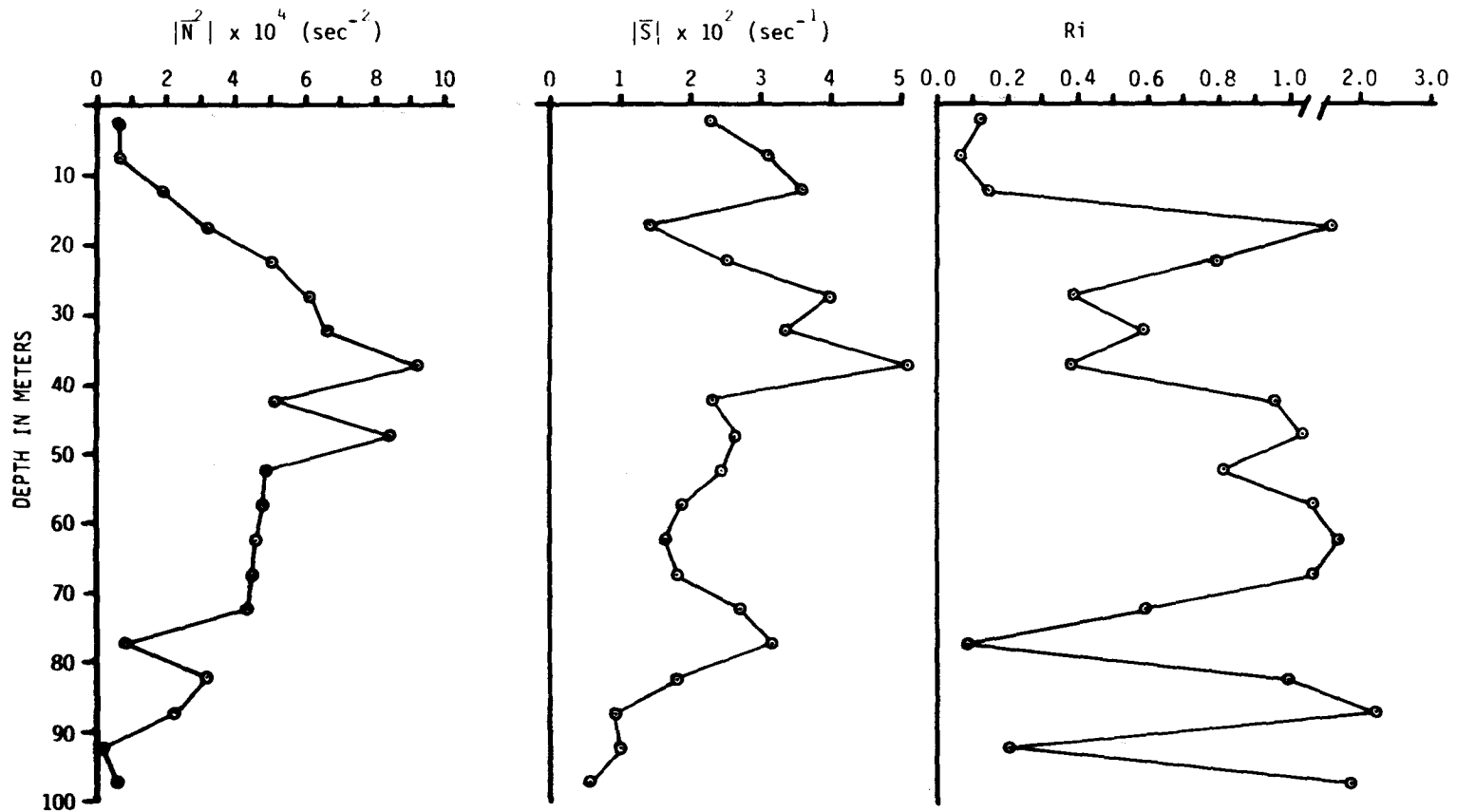


Figure 4.10. Mean profiles of static stability (\bar{N}^2), velocity shear (\bar{S}), and gradient Richardson Number (Ri) for the anchor station.

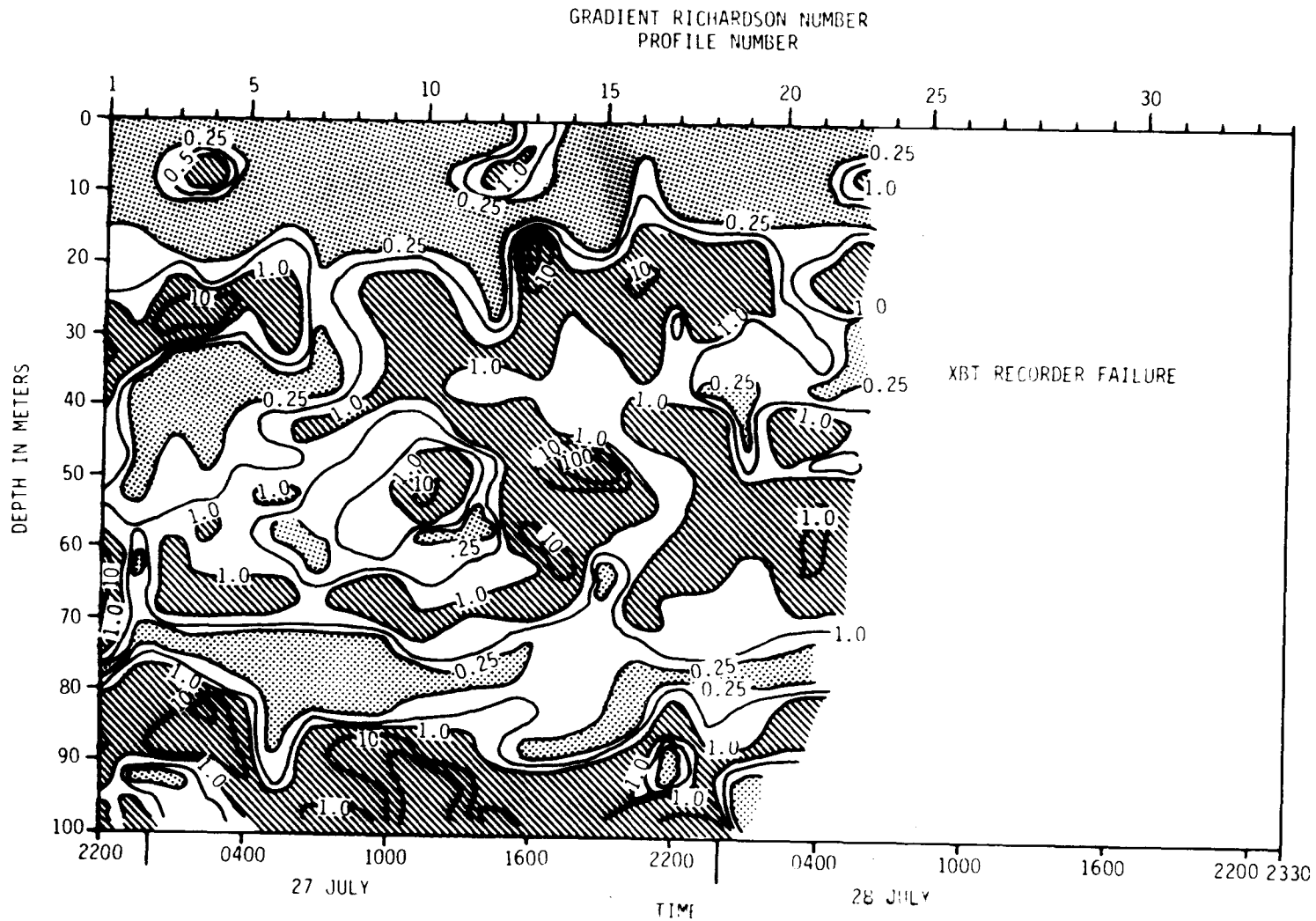


Figure 4.11. Time-depth contours of the gradient Richardson Number (R_i) for the anchor station. Contours are for $R_i = 0.25, 0.5, 1.0, 10.0$ and 100.0 . Areas where $R_i \leq 0.25$ are shaded and $R_i \geq 1.0$ striped.

onshore-offshore flow were at a minimum. A zone of consistently unstable conditions existed between 70 and 80 m throughout the anchor station. From 85 m to the bottom, the flow was generally stable, primarily due to the rapid decrease in shear in this layer.

4.6 Empirical Orthogonal Functions

The technique of empirical orthogonal functions (EOF), also known as principal components (Davis, 1973), was applied to the velocity profile data to examine the depth distribution of velocity variance. The technique computes the eigenvalues and eigenvectors of the variance - covariance matrix and orders them according to the amount of correlated variance. The EOF technique is especially useful for analysis of fields of several variables which are all believed to respond in some way to a single (or very few) major forcing function. For this reason, EOF has been applied successfully in meteorology (Lorenz, 1956; Kutzbach, 1967) and recently in oceanography (Kundu, et al., 1974; Brooks, 1975; Johnson, 1976).

Of the thirty-four current profiles, only twenty extended from the surface to 100 m. Fortunately they were spaced throughout the entire length of the 50-hour anchor station. The mean values for each component calculated from these twenty profiles fell within the 95% confidence intervals at every depth (Fig. 4.1). The lowering numbers used for the EOF analysis are 2 to 4, 6 to 7, 9 to 13, 16 to 19, 25 to 28, and 33 to 34. This provided a matrix of 21 variables (depths) and 20 observations, which yielded a maximum of 21 EOF's for both the u and v components.

Results of the calculations for each velocity component are shown in Table 4.2. Only the first five EOF's are listed since they account for 98% of the total variance for each component. The magnitude of the first three u and v EOF's versus depth are shown in Figure 4.12. The first EOF for u was largely uniform over depth (barotropic), and accounted for 87.2% of the total variance. The first EOF for v had a baroclinic structure with a peak at about 30 m, the region of strongest vertical shear just below the subsurface jet in the mean alongshore flow (Fig. 4.1). It accounted for 60.5% of the variance. The second and third EOF's for u had highly baroclinic structures but accounted for only a small amount of variance. The second EOF for v accounted for 28.8% of the variance and apparently reflected the phase difference and node location (35 to 40 m) between the upper and lower water column observed in the perturbation field (Fig. 4.8). The third EOF for v had an even more complex baroclinic structure but accounted for only about 4.2% of the variance. With 21 possible modes, white noise would be expected to yield about 5% variance per mode; hence, any mode with less than 5% variance is not likely to be significant.

The time variation of the first two EOF's for both velocity components was obtained by projecting the original u and v observations (means removed) onto the first two EOF's (Fig. 4.13). That is, the projections on EOF's I and II for each observation i are:

$$Y_{I,i} = \alpha_I^{(1)} X_i^{(1)} + \alpha_I^{(2)} X_i^{(2)} + \dots + \alpha_I^{(21)} X_i^{(21)} \quad i = 1, 20$$

$$Y_{II,i} = \alpha_{II}^{(1)} X_i^{(1)} + \alpha_{II}^{(2)} X_i^{(2)} + \dots + \alpha_{II}^{(21)} X_i^{(21)} \quad i = 1, 20$$

TABLE 4.2. Empirical orthogonal function variance.

EOF	<u>u Component</u>			<u>v Component</u>		
	Total Variance - 11,086 cm ² /sec ²			Total Variance - 15,800 cm ² /sec ²		
	Variance (cm ² /sec ²)	% Variance	Cumulative %	Variance (cm ² /sec ²)	% Variance	Cumulative %
1	9668	87.2	87.2	9557	60.5	60.5
2	677	6.1	93.3	4549	28.8	89.3
3	290	2.6	95.9	662	4.2	93.5
4	178	1.6	97.5	489	3.1	96.6
5	77	0.7	98.2	199	1.3	97.9

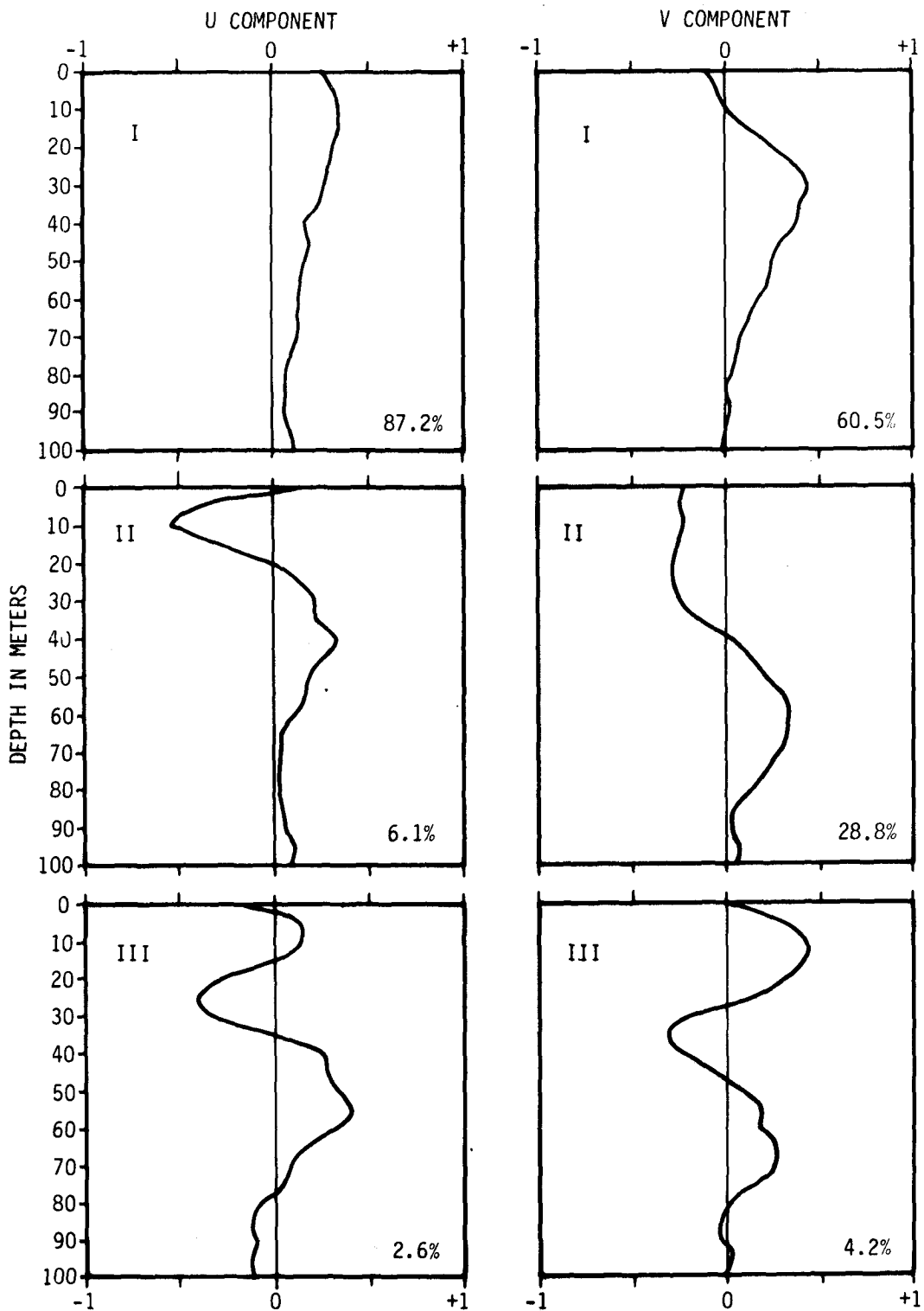


Figure 4.12. Empirical orthogonal functions (EOF) I, II, and III for the u and v velocity components. Percent of variance accounted for by each EOF is indicated.

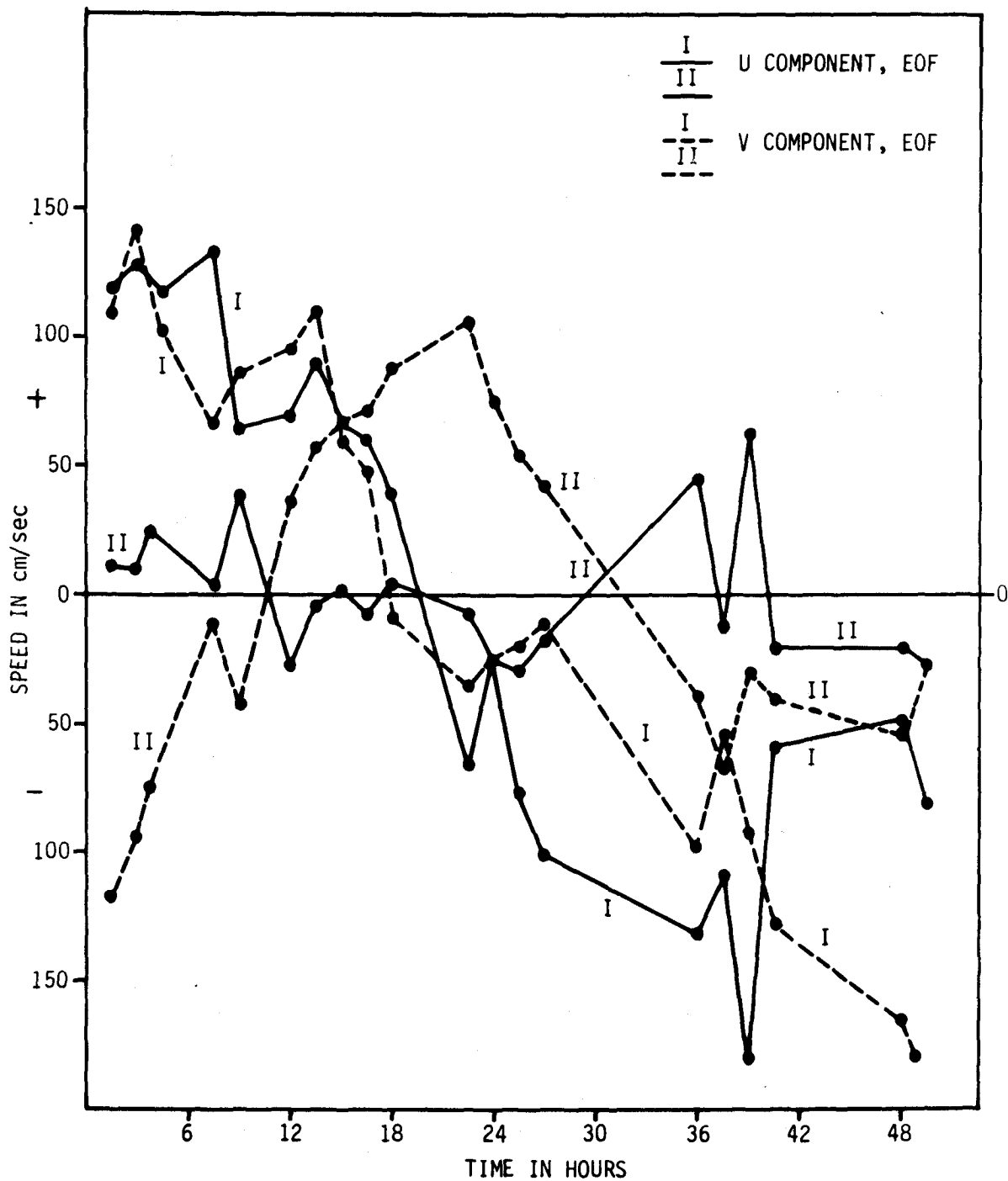


Figure 4.13. Time variation of first two empirical orthogonal functions (EOF-I, II) for the u and v velocity components.

where $Y_{I,i}$ $Y_{II,i}$ = projection of i^{th} original observation onto EOF's I and II.

$x_i^{(1)}, x_i^{(2)}, \dots, x_i^{(21)}$ = i^{th} observation of u and v (time mean removed) at each depth level (superscript)

$\alpha_I^{(1)} \dots \alpha_I^{(21)}; \alpha_{II}^{(1)} \dots \alpha_{II}^{(21)}$ = elements of eigenvectors I and II with superscript referring to depth level.

Because of this construction the velocity scales are larger than the original data but relative amplitude is preserved.

The temporal variation of the first function for u (Fig. 4.13) confirmed that the major portion of the variance (87.2%) had a wave-like structure with an apparent half-period of at least 36- to 40-hours. The first function for v (Fig. 4.13) exhibited a basically longer period variation suggestive of the half-period of at least 45- to 50-hours which was noted in the perturbation alongshore flow (Fig. 4.8). This effect was particularly noticeable in the 30- to 50-m depth zone. The EOF I for v had a peak at a depth of 30 m (Fig. 4.12) and was positive throughout the water column except for the upper 10 m. Fluctuation amplitudes of the first EOF's for u and v were of similar magnitude.

The second EOF for v had a wavelike structure and period similar to the first EOF for u but with an apparent phase difference of 90° . The vertical structure and time variation of EOF's I for u and II for v at the 3 to 4 day period were consistent with theoretical predictions offshore of the shelfbreak for a first mode topographic Rossby wave with

continuous density stratification and variable bottom topography (Wang and Mooers, 1976). They identified a stratification parameter $S = N_{\max} \cdot H_T / fL$, where N_{\max} is the maximum static stability, H_T and L are the maximum depth and width of the shelf, and f is the Coriolis parameter. For the anchor station, $S \approx 0.9$ which corresponds to intermediate density stratification. The anchor station location is at a distance offshore of $x/L \approx 0.8$ to 1.0 . In this region the following theoretically predicted results for the first mode topographic Rossby wave are consistent with the observed flow at the apparent 3 to 4 day period:

1. Although the predicted alongshore flow over the shelf is nearly depth independent, there is a node in the vertical structure over the slope region from $x/L \approx 0.5$ to 1.0 (Fig. 4(a); Wang and Mooers, 1976). The amplitudes above and below the node are of similar magnitude. This was the observed structure of EOF II for the v component (Fig. 4.12).
2. The horizontal velocity components should be in quadrature. Inshore of the cross-shelf position of the node for the alongshore velocity, v should lead u by 90° in the upper layer for clockwise rotation with counterclockwise rotation in the lower layer (below the node in vertical structure). This was the case for the observed flow at the 3 to 4 day period (Figs. 4.12 and 4.13).
3. The predicted onshore flow is relatively depth-independent, but with a slight decrease from the surface to the bottom (Fig. 11(a); Wang and Mooers, 1976). The observed EOF I for u had such a vertical structure (Fig. 4.12).

4. The amplitudes of u and v were observed to be of the same magnitude consistent with results predicted by the theory (Fig. 4.13).
5. The predicted vertical velocity for onshore flow is bottom-trapped over the shelfbreak (Fig. 11(b); Wang and Mooers, 1976). The upward bowing of the isotherms over the shelfbreak for the XBT transect shown in Figure 4.4 indicates that upwelling did occur during onshore flow.

The observations thus suggest that fluctuations at a 3-to 4-day period were consistent with theoretical predictions for a first mode topographic Rossby wave modified by the effects of density stratification and the local bottom topography. Although the presence of the Florida Current and its associated inclined frontal zone were not included in the model, the observations and theory are remarkably consistent.

5. SPECIFIC EVENTS

The results of the previous sections demonstrate that large negative temperature anomalies occur during the summer in the coastal waters near Cape Canaveral. With the use of two separate limited data sets, the nature of these cold water intrusions is examined in more detail in this chapter. The first deals with an apparent wave or eddy pattern in the bottom currents recorded during 28 May to 1 July 1970. The second is an analysis, using wind stress and temperature data, of one of the large temperature decreases noted during June to July 1971.

5.1 Temperature, Currents, and Winds - Summer, 1970

For the period from 28 May to 1 July 1970, bottom temperatures at BY1 and bottom currents at BY2 were recorded (Fig. 1.2). The current measurements were made at 10 minute intervals and averaged for hourly intervals. The record length was not long enough to allow low pass filtering as in the other time series discussed previously. Therefore, daily means were calculated for the bottom temperatures, onshore-offshore (USTR), and alongshore (VSTR) wind stress components. Semi-daily means were calculated for the onshore-offshore (u) and alongshore (v) current components. As before, the coordinate system for both the wind stress and current vectors was rotated 10° counter-clockwise from true north for alignment with the local bathymetry.

The calculated values for the bottom temperature (BY1), USTR, VSTR, and the u and v current components (BY2) are shown in Figure 5.1. Two large temperature decreases were observed. Between 3 June and 6 June,

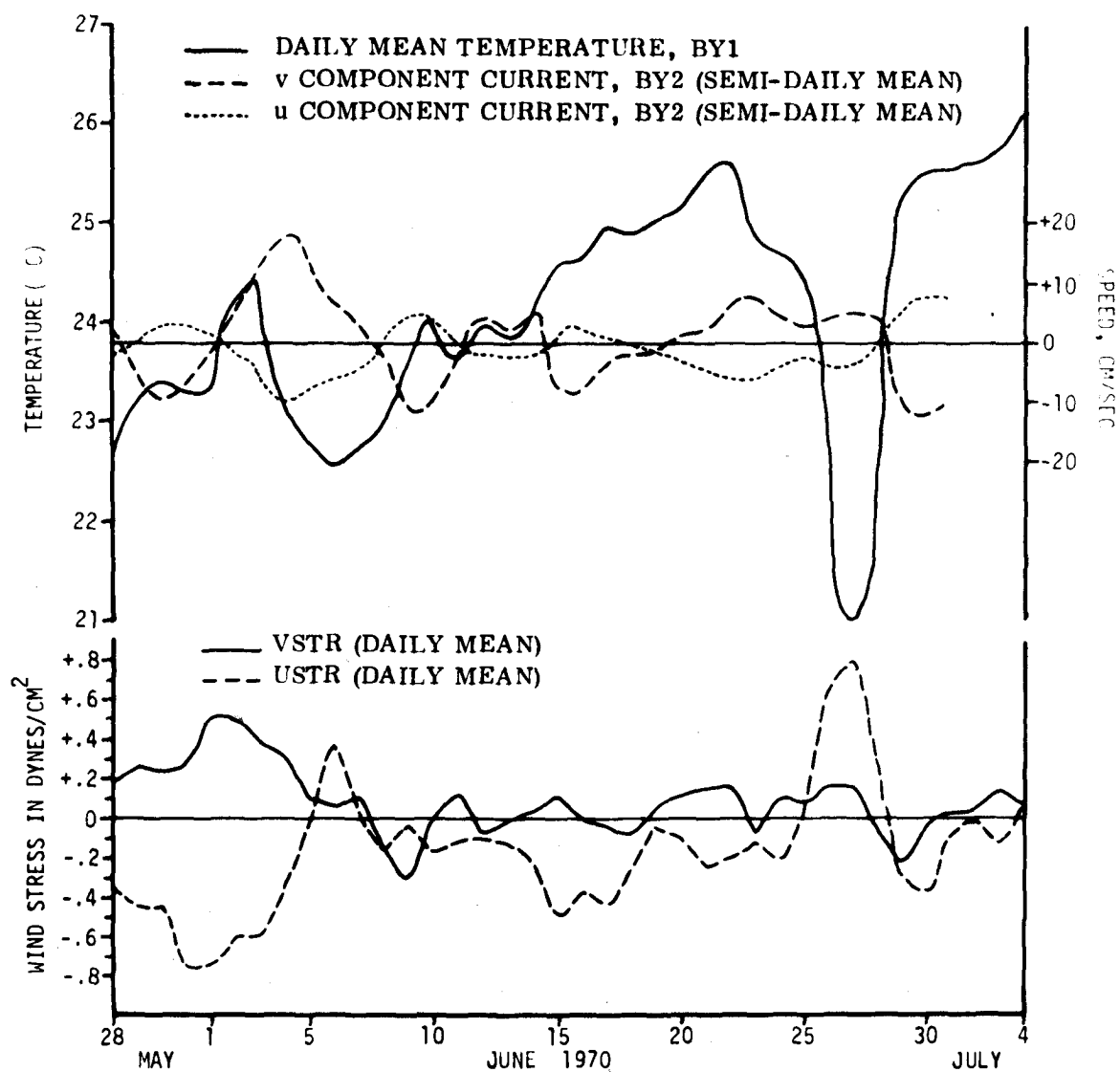


Figure 5.1. Daily mean temperature at BY1, onshore-offshore (USTR) and alongshore (VSTR) wind stress components, and semi-daily mean onshore-offshore (u) and alongshore (v) bottom current components at BY2 for the period of 28 May to 1 July 1970.

the temperature decreased about 20° followed by a rapid partial recovery by 9 June. The bottom temperature then rose gradually to a maximum of (26.6°C) on 22 June. It then decreased 40° within five days and recovered to the 22 June value in about two days. The current record indicated an alternating alongshore and onshore-offshore flow with a period of about a week to ten days. Onshore flow (negative u) was associated with both of the major temperature decreases. Accelerations of onshore flow were also associated with accelerations in the alongshore component. Visual correlation of the wind stress with the currents and temperature was not straightforward. A large increase (upwelling favorable) in USTR and VSTR was associated with the late June temperature anomaly. During the period of temperature rise from 6 June to 22 June, USTR was always negative (upwelling unfavorable) and VSTR was of small magnitude (generally $< 0.2 \text{ dynes cm}^{-2}$) and alternating sign.

Although both major temperature anomalies were associated with positive v and negative u current components (Fig. 5.1), the temperature began to rise about two days before a reversal to negative alongshore and offshore (positive) flow. The nature of the periodic current reversals can be seen with the aid of a progressive vector diagram (Fig. 5.2). The semi-daily means were used to construct the plot and whole days are labelled. The flow at the beginning of the record was northwestward with an abrupt reversal to southeastward on 28 May. Offshore and southward flow continued until 1 June followed by another reversal to the northwest. Between 3 and 4 June, the net flow since 28 May was essentially zero. The average onshore-offshore velocity for each half of the cycle was about 4 cm/sec while that for the v component was about 7 cm/sec. A similar oscillation (of shorter period) occurred twice in

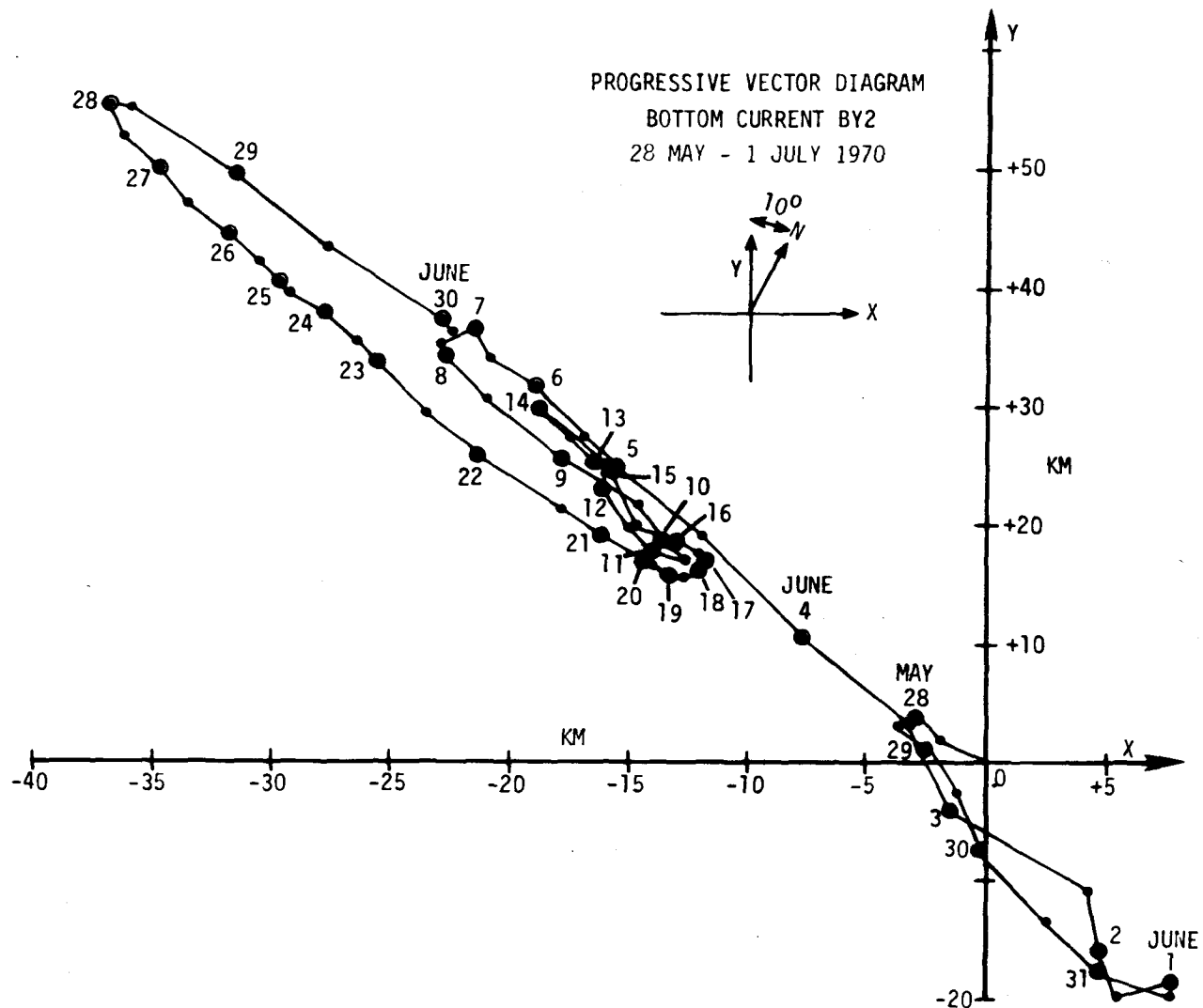


Figure 5.2. Progressive vector diagram for bottom current at BY2; 28 May to 1 July 1970. Each point represents semi-daily mean. Circled points are labeled with date. Horizontal axis scale is exaggerated by a factor of two relative to vertical axis.

the middle of the record with mean onshore-offshore and alongshore velocities of 3.2 and 6.0 cm/sec, respectively. The fluctuating flow was superimposed on an overall northwestward drift of about 1.6 km/day. There was no apparent consistency to the rotational sense of the current fluctuations.

A plot of the approximate displacement amplitudes for the onshore-offshore and alongshore flow (Fig. 5.3) reveals that, for nearly all the clearly defined bottom current oscillations, the actual reversals occurred within about twelve hours. The time between such reversals varied from about 3 to 10 days. Typical onshore-offshore and alongshore displacements for the longer time period were 20 and 40 km, respectively. For the shorter period they were typically 6 and 15 km. The bottom temperature at BY1 plotted against the onshore-offshore displacement amplitude at BY1 (Fig. 5.3) showed a strong visual correlation. For the most part, however, the temperature changes led the displacement by about one day. The exception was the case for the rapid temperature decrease beginning on 26 June which was preceded by about 6 days of consistently onshore-directed flow. The temperature began to recover, however, before the displacement reversal. The response differences may have resulted from the separation between the two buoy sites. The bottom temperature (BY1) buoy was about 13 km closer to shore than BY2 and at a slightly shallower water depth (19 m vs. 22 m). It would be expected that the responses to wind stress changes would appear first at the inshore buoy if Ekman divergence at the coast were the forcing function. The lack of a strong visual correspondence between upwelling favorable wind stress and bottom currents and temperature may be due to near-bottom influences. The onshore compensation flow for offshore flow

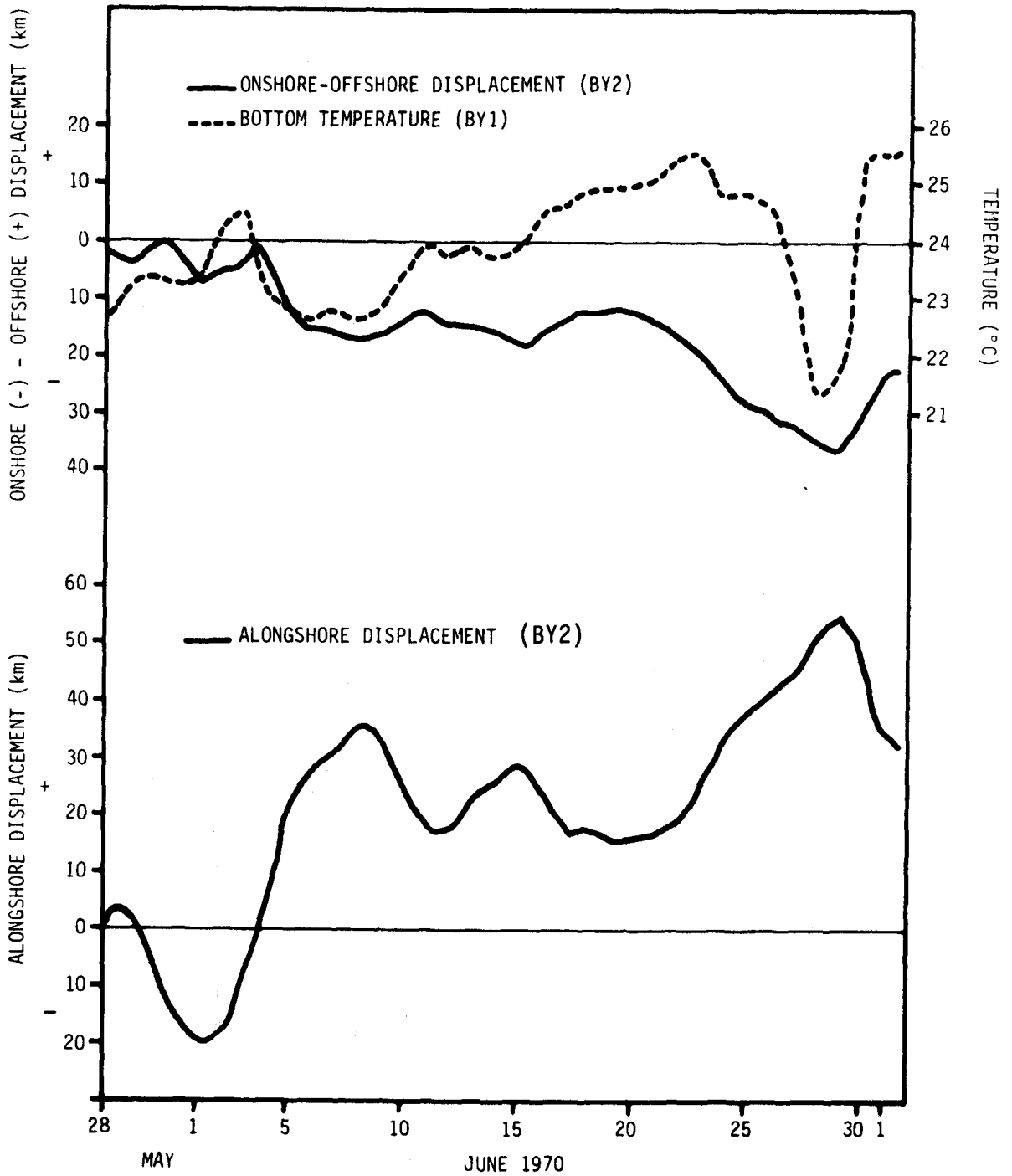


Figure 5.3. Approximate onshore-offshore and alongshore bottom current displacement amplitudes at BY2, and daily mean bottom temperature at BY1 for 28 May to 1 July 1970. Displacements are from semi-daily mean current components.

in the surface Ekman layer may not be evident near the bottom. Northward acceleration in the alongshore interior flow can drive onshore flow in the lower layer (e.g., Allen and Kundu, 1978). To the extent that fluctuations of the v component at BY2 represented fluctuations in the interior, the variation of the onshore-offshore flow at BY2 was consistent with such a balance (Fig. 5.1). The approximately 45° deflection of the flow to the left of the isobaths (Fig. 5.2) strongly suggests that the current meter was in the bottom Ekman layer.

5.2 An Apparent Upwelling Event - A Closer Look

The best documented example of an apparent upwelling event (large negative temperature anomaly) occurred during late July 1971. In addition to wind stress (USTR, VSTR) and surf temperature (SFT), bottom temperatures at four locations (BY1, BY2, CM1, and CM2) were recorded for 26 June to 23 July 1971 (see Fig. 1.2 or Fig. 5.5 for locations). There were also two XBT cruises; one on 28 to 29 June and the other from 23 to 26 July.

5.2.1 Time Variations

Since the time series for these records were too short to effectively filter in the manner described in Chapter 3, daily means were computed for all data sets and are shown in Figure 5.4. Records for the wind stress, surf temperature, and bottom temperature at BY1 and BY2 are continued past 23 July since data were available at those locations. The temperature records for SFT, BY1, BY2, and CM1 are visually well-correlated. The average overall correlation coefficient among the four records was +0.85 with zero lag (for daily means) and significant at the 99% level. The temperature at CM2 was visually somewhat different from

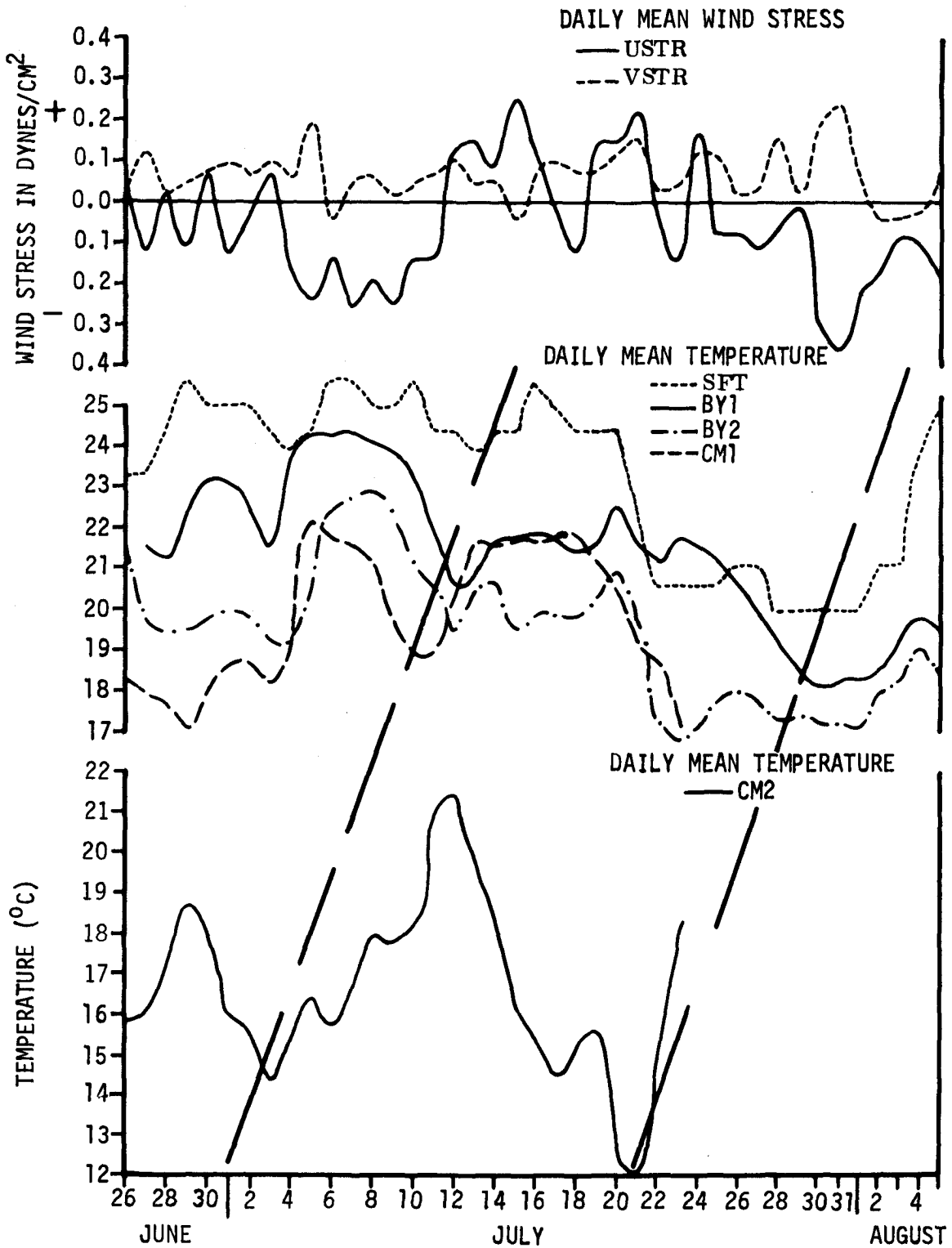


Figure 5.4. Daily mean values for USTR, VSTR, SFT, BY1, BY2, CM1 and CM2 for 26 June to 23 July 1971. Data for USTR, VSTR, SFT, BY1 and BY2 are extended to 5 August to show temperature depression. Dashed diagonal lines indicate assumed correspondence of temperature minima.

the other four. Its large scale fluctuation had an apparent fortnightly period with smaller amplitude, higher frequency fluctuations superimposed. There was an apparent relation between the temperature depressions at CM2 and those for the other four records as suggested by the dashed diagonal lines in Figure 5.4. The bottom depth at CM2 was about 62 m, while at CM1 it was about 20 m. The horizontal distance between CM1 and CM2 was about 24 km and the time difference between arrival of temperature minima at CM1 and CM2 was about 8 days (Fig. 5.4). For strictly two dimensional flow, the average onshore velocity would then be about 3.5 cm/sec which is close to the average onshore velocity measured at BY2 during June to July 1970 (Chapter 5.1) for the onshore portion of the 7-day cyclic flow.

There is no apparent visual correlation between the large temperature decreases at CM2 and the onshore-offshore (USTR) and alongshore (VSTR) wind stress. However, VSTR was generally positive (upwelling favorable) throughout the record. The major temperature depressions in the SFT, BY1, BY2, and CM1 records appear to be correlated with positive (upwelling favorable) offshore stress. This suggests that a major meandering of the Florida Current, perhaps initiated by the upwelling favorable alongshore stress, introduced cold water along the bottom onto the shelf area. Once the cold water had spread over the shelf, so long as the alongshore stress remained positive, the temperature records suggested a response to the onshore-offshore stress as typical wind-driven coastal upwelling. The link between upwelling favorable wind stresses and temperature was not dramatic. It is probable that the temperature is sensitive to relative phases of superimposed responses to many time scales of wind forcing. In addition, the temperature fluctuations de-

pend upon the vertical and horizontal gradients as well as the time dependent flow field. The gradients themselves may also be functions of time which leads to a variable dependence of temperature on currents and stress. This is to be expected particularly in the area of a major western boundary current.

5.2.2 Horizontal Variations

Mention was made in Chapter 2.2 of the lack of significant temperature depression at the surface during XBT surveys when cold water intruded along the bottom over the entire shelf area. A comparison of surface temperature measured during 23 to 25 July 1971 on R/V VENTURE Cruise 7102 (Fig. 5.5) with the bottom temperature for the same time period (Fig. 2.8), demonstrates this effect. Although there was a large pool of cold water over the shelf in the lower layer, the only significant surface effect occurred inshore and north of CM1 (Fig. 5.5), a distance 15 to 20 km from shore. The surface temperature in this zone was between 23.8°C and 26.0°C. In addition a large temperature depression existed in the surf temperature (SFT) record (Fig. 5.4). Theoretical (e.g. Allen, 1973) and experimental (e.g. Smith, 1974; Walin, 1972) considerations suggest that the major baroclinic effects in upwelling zones are confined to a narrow coastal band defined by the internal "Rossby radius of deformation." This value is given by $\delta_R = HN/f$ where H is a characteristic depth value, N is the Brunt-Váisálá frequency, and f is the Coriolis parameter. For the XBT sections, a characteristic depth for the shelf area was about 40 m. During 23 to 25 July, the approximate mean vertical temperature gradient ($\frac{dT}{dz}$) was about 0.30°/m. Considering a constant value of salinity of 36.0 o/oo, the value $N \approx 3 \times 10^{-2}$ rad/sec. With a value of 7×10^{-5} rad/sec for f, the value for the

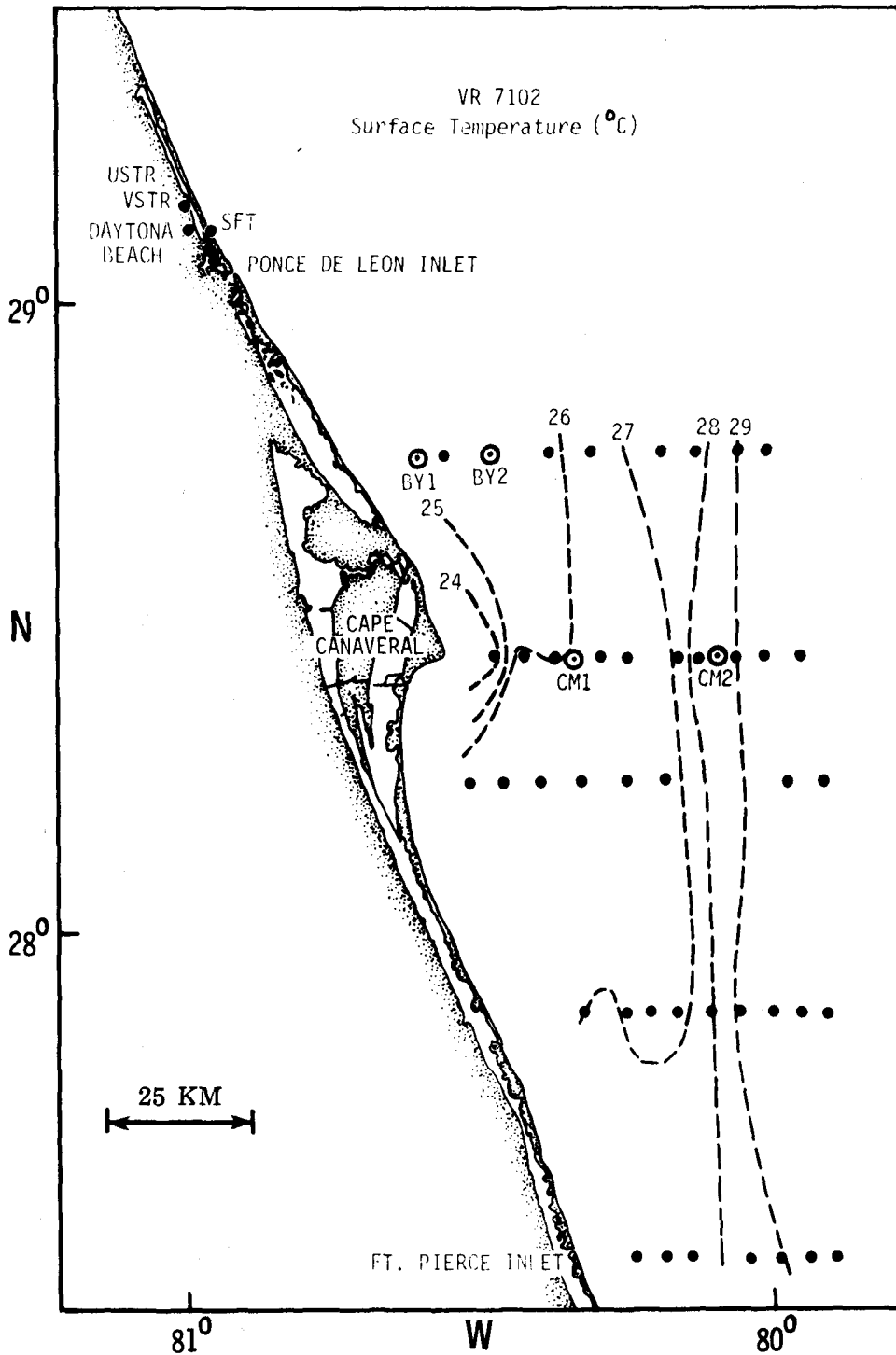


Figure 5.5. Surface temperature during XBT survey for 23 to 25 July 1971: R/V VENTURE Cruise 7102. Dots indicate station locations. Also indicated are locations of measurements for USTR, VSTR, SFT, BY1, BY2, CM1 and CM2.

Rossby deformation radius is thus $\delta_R \approx 17$ km, which is close to the observed distance where surface expression of the temperature depression occurred in the XBT field.

A model of upwelling which includes both bottom topography and continuous stratification (Wang and Mooers, 1976) predicts that barotropic continental shelf waves and baroclinic internal Kelvin waves may be coupled. The internal Kelvin waves possess a characteristic of offshore scale which is the Rossby deformation radius (δ_R) while the shelf waves have an offshore scale of the order of L , the width of the continental shelf ($L \approx 50$ km directly off Cape Canaveral). Several authors have pointed out that flow in an upwelling region may be strongly modified by flow perturbations generated outside the local region (Hurlbert and Thompson, 1973; Mooers and Allen, 1973; Gill and Clarke, 1974). Considering the results of this thesis, a process such as this appears to be logical for the coastal area near Cape Canaveral.

Meandering of the Florida Current not directly attributable to the local wind stress also will inject cold water into the bottom layers of the coastal zone. This meandering may be the result of large scale barotropic continental shelf waves, which may be generated by the winds further to the north. The effect of the cold water intrusion on the surface layer is then confined to a narrow coastal zone whose width corresponds approximately to the Rossby radius of deformation and is apparently associated with the Ekman divergence at the coast caused by the local wind stress. A lack of longer records for currents, and reliance entirely on surf and bottom temperature records precluded a comprehensive test of this hypothesis.

5.2.3 Effects of Cape Canaveral

The summer occurrences of negative coastal water temperature anomalies found by Taylor and Stewart (1959) were largely confined between Fernandina Beach and Canova Beach, Florida (see Fig. 1.1 for locations). The greatest anomalies, however, were confined to a zone of about 50 km on either side of Cape Canaveral, the only prominent Cape in the South Atlantic Bight south of the Carolinas. The depression of surface temperature evident in Figure 5.5 was generally confined to a narrow coastal zone north of Cape Canaveral.

Manifestations of intensified upwelling have been observed near capes and points along the California coast (e.g. Reid, et al., 1958; Hubbs, 1960). In particular, upwelling effects were found to be intensified south of the capes and suppressed to the north. Arthur (1965) subsequently showed that, near boundaries, it was necessary to include frequently neglected terms in the estimation of horizontal divergence. Specifically, he demonstrated that the terms involving the change of relative vorticity along a streamline as well as planetary vorticity effects could contribute significantly to upwelling south of capes (for southward flow) along the California coast. This would cause an asymmetry in the observed upwelling north and south of coastal projections.

It is reasonable to assume then that Cape Canaveral may have some local effect on coastal upwelling. Following Arthur (1965), one form of the vorticity equation may be written as:

$$(\zeta + f) \frac{\partial w}{\partial z} = \underbrace{\frac{D\zeta}{Dt}}_{(a)} + \underbrace{\beta v}_{(b)} - \underbrace{\left\{ \frac{\partial w}{\partial y} \frac{\partial u}{\partial z} - \frac{\partial w}{\partial x} \frac{\partial v}{\partial z} \right\}}_{(c)} - \underbrace{\left\{ \frac{\partial P}{\partial x} \frac{\partial \alpha}{\partial y} - \frac{\partial P}{\partial y} \frac{\partial \alpha}{\partial x} \right\}}_{(d)}$$

$1 \times 10^{-10} \text{ sec}^{-1}$; thus, the local rate of change of vorticity ($\frac{\partial \zeta}{\partial t}$) would have magnitude similar to advective changes for a time scale of about one day.

For a vertical velocity of $5 \times 10^{-4} \text{ cm/sec}$, term (c) has a magnitude of about $10^{-12} \text{ sec}^{-2}$ and is neglected compared to the planetary vorticity term (b). However, this term (c) represents the twisting of non-vertical vorticity into the vertical by horizontal gradients of vertical motion which may be significant under some circumstances. Term (d) is generally of the order of $10^{-13} \text{ sec}^{-2}$ and is also neglected.

Evaluation of terms (e) and (f) requires some knowledge of the eddy viscosity coefficients. Carter and Okubo (1965) used observations during summer of dye patches in the coastal waters off Cape Canaveral to estimate $A_v \approx 1.0 \text{ cm}^2/\text{sec}$ and $A_H \approx 10^3 \text{ cm}^2/\text{sec}$. With these estimates of A_v and A_H , the vertical and horizontal vorticity diffusion [terms (e) and (f)] are $4 \times 10^{-13} \text{ sec}^{-2}$ and $4 \times 10^{-16} \text{ sec}^{-2}$, respectively, and will be neglected. For coefficients more typically cited (Arthur, 1965) such as $A_v \approx 10 \text{ to } 10^2 \text{ cm}^2/\text{sec}$ and $A_H \approx 10^6 \text{ to } 10^8 \text{ cm}^2/\text{sec}$, the vorticity diffusion terms can become comparable to the planetary vorticity term and probably should not be neglected. Actually, the vertical vorticity term is the one which is usually assumed to be principally responsible for the offshore Ekman transport in the surface layer driven by the wind stress (Smith, 1968). For purposes of this discussion it will nevertheless be neglected since interest is primarily in how the presence of Cape Canaveral may augment or suppress upwelling. On the basis of the order of magnitude estimates, equation (1) may be approximated by,

$$f \frac{\partial w}{\partial z} = \frac{D\zeta}{Dt} + \beta v \quad (2)$$

$$\text{and } \frac{D\zeta}{Dt} = \frac{\partial \zeta}{\partial t} + u \frac{\partial \zeta}{\partial x} + v \frac{\partial \zeta}{\partial y}.$$

The vorticity may be written in natural coordinates (von Arx, 1962) as:

$$\zeta = \frac{c}{R} - \frac{\partial c}{\partial n} \quad (3)$$

where c is the speed, R is the radius of curvature of the streamline, and $\frac{\partial c}{\partial n}$ is the velocity gradient normal to the streamline. A tendency for counterclockwise rotation is positive by convention.

Very little data are available near Cape Canaveral suitable for evaluation of the validity of equation (2); however, estimates may be obtained from hydrographic surveys and drifter studies in the region during August 1962 made by Bumpus (1964). An estimate of 50 km for a streamline radius of curvature (R) was made from the horizontal distribution of σ_t at 10 m shown in Figure 6 in Bumpus (1964). Drifters released offshore from Cape Canaveral had velocities approaching one knot; thus, the assumed typical horizontal velocity of 50 cm/sec is probably reasonable.

Idealized streamlines and the signs of $\frac{D\zeta}{Dt}$ and βv for both northward and southward flow around Cape Canaveral are shown in Figure 5.6. For southward flow, both terms are negative north of the cape (Fig. 5.6 a) and, according to equation (2), contribute to positive (upward) vertical velocity (w). South of the cape, the terms are of opposite sign and the contribution of the combined terms depend on their relative magnitude. For northward flow (Fig. 5.6 b), $\frac{D\zeta}{Dt}$ is negative north of the cape and

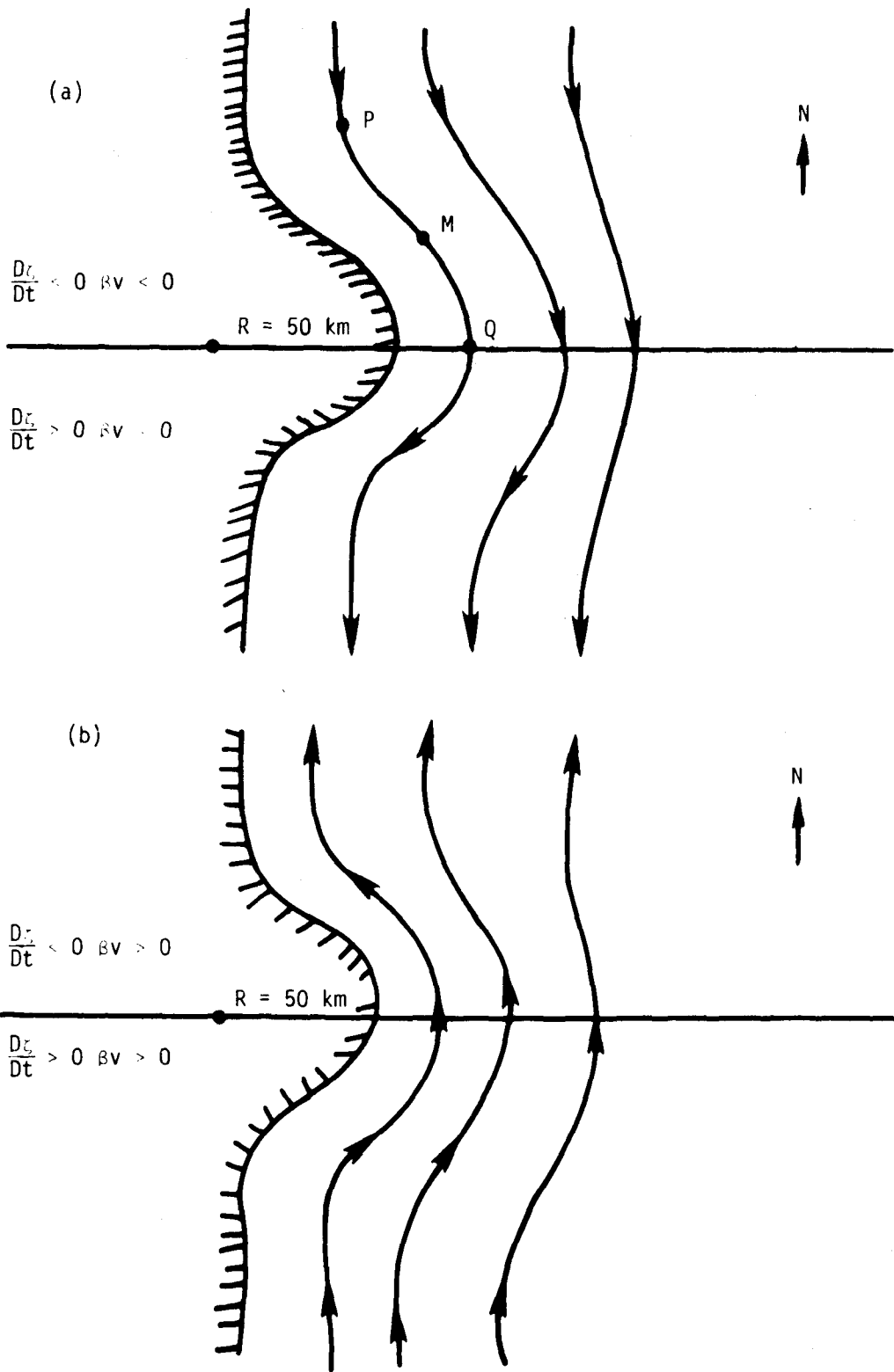


Figure 5.6. Streamlines for idealized flow around Cape Canaveral with signs of terms in equation (2): (a) southward flow (b) northward flow. Points P, Q, and M are referred to in text.

will be upwelling favorable, while βv is of opposite sign. The combined result again depends on their relative absolute values. South of the cape, both terms contribute toward convergence and downwelling.

An estimate of the vertical velocity can be made from equations (2) and (3). Consider a fluid particle moving from point P to point Q in Figure 5.6 (a). With $c = 50$ cm/sec, $R_Q = 50$ km, and $R_P = \infty$, the vorticities at Q and P from equation (3) are,

$$\zeta_Q = -1.0 \times 10^{-5} \text{ sec}^{-1}$$

$$\zeta_P = 0$$

where the normal velocity gradient is assumed for simplicity to be a positive constant, which can be taken as zero. The fluid particle would move from P to Q (50 km) in about 10^5 sec, thus, at point M,

$$\left(\frac{D\zeta}{Dt}\right)_M \approx -1.0 \times 10^{-10} \text{ sec}^{-2}$$

Evaluating the right hand side of equation (2) at the point M for $\beta v = -1.0 \times 10^{-11} \text{ sec}^{-2}$ gives,

$$\left(\frac{D\zeta}{Dt}\right)_M + (\beta v)_M = -1.1 \times 10^{-10} \text{ sec}^{-2}$$

Thus,

$$\left(f \frac{\partial w}{\partial z}\right)_M = -1.1 \times 10^{-10}$$

or

$$w|_z = -50 = 5.5 \times 10^{-3} \text{ cm/sec.}$$

This vertical velocity is well within the range typical of classical wind-driven upwelling (Smith, 1968). For the assumed values of c and R , $\left|\frac{D\zeta}{Dt}\right|$ is an order of magnitude greater than $|\beta v|$. Thus, for both north-

ward and southward flow around Cape Canaveral, intensified upwelling would be expected north of the cape while downwelling would occur to the south.

From these results, it is reasonable to assume that the effects of Cape Canaveral on observed upwelling probably are significant. Both northward and southward flow contribute to divergence north of the cape, and convergence to the south. This is consistent with the observed horizontal sea surface temperature field found in late July (Fig. 5.5) where the surface temperature depression was confined generally to a narrow coastal zone north of Cape Canaveral. Effects of the coastline irregularity are not confined to the modification of local wind-driven upwelling. Evidence in this thesis suggests that some of the observed temperature and current fluctuations were likely due to propagating disturbances such as continental shelf waves (or Kelvin waves) generated by winds to the north of Cape Canaveral. The effects of alongshore variations of the coastline and bottom topography on continental shelf waves has been discussed by Allen (1976). One of the cases considered was that of an impulsively applied constant wind stress forcing. For an upwelling favorable wind stress, he found that the steady onshore-offshore velocities set up by the perturbation flow were such that the basic onshore flow driven by the wind stress was increased over a ridge in the bottom topography (assumed equivalent to a coastal cape). This suggests still another process by which the presence of Cape Canaveral may produce an intensification of coastal upwelling.

6. SUMMARY AND CONCLUSIONS

During 1970 and 1971, measurements of temperature, currents and wind stress were made at various locations off the central eastern coast of Florida. A summary of an analysis of these measurements is presented below. The summary is organized to address the thesis objectives as outlined in Chapter 1.3.

1. Results of XBT surveys along standard transect lines indicated a pronounced seasonal difference in the horizontal and vertical thermal structure of the coastal waters near Cape Canaveral. Temperature sections were averaged to portray four major seasonal conditions: winter-spring, summer, fall, and winter. Mean vertical temperature gradients typical for summer conditions were about $0.30^{\circ}/\text{m}$ while for winter the conditions were nearly zero. Bottom temperatures during the summer period were as cold or colder than those measured during mid-winter (15 to 18°C). The horizontal temperature gradient at 100 m depth near the shelfbreak during summer was $\frac{\Delta T}{\Delta X} \approx \frac{7.5^{\circ}\text{C}}{8 \text{ km}}$ compared to $1.0^{\circ}\text{C}/8 \text{ km}$ during December. This difference was attributed to a greater strength and onshore movement of the Florida Current during summer months. Results of two XBT transects orthogonal to the coast about 60 hours apart demonstrated that large pools of cold bottom water remained over the mid-shelf area as a net result of onshore penetration and subsequent retreat of the Florida Current. The alongshore, cross-shelf, and vertical extents of these lenses were about 80 km , 10 km , and 5 m , respectively. The total

volume of about $2 \times 10^9 \text{ m}^3$ was formed and removed on an apparent time scale of 2 to 3 days.

2. Bottom temperatures at four sites as well as surf temperature records all indicated large negative temperature anomalies during summer months. Many of these anomalies were associated with upwelling favorable wind stress components; i.e. positive in the alongshore direction to the north-northwest and positive in the offshore direction. Overall correlation coefficients among the bottom temperatures and surf temperature for short (48 day) records during the summer averaged about +0.85 and the correlation with the offshore wind stress averaged about -0.66. Both were significant at the 99% level. The negative correlation reflected decreasing temperatures associated with offshore (positive) wind stress. The correlation between the temperatures and the alongshore stress was also negative but of lower value (average = -0.41). For longer records and during winter periods the strong correlation between wind stress and temperature was not apparent.

Spectrum analyses were performed for two seasonally different (winter/summer), overlapping records of two-day, low-pass filtered bottom temperature, surf temperature, and wind stress. For winter conditions, the bottom and surf temperatures were found to be significantly coherent with the alongshore wind stress at a period of about 11.5 days. The temperature records were also found to be significantly coherent with both wind stress components at periods of 5.8 and 3.5 to 3.8 days. Significant coherence also was found between the surf temperature and both wind stress components at periods of

4.6 and 2.1 days. The phase relations between surf temperature and alongshore stress at 23 days, bottom temperature and alongshore stress at 11.5 days, and bottom temperature and both wind stress components at 3.8 days were found to be consistent with those expected from typical wind-driven coastal upwelling. That is, the temperatures should be in phase with the offshore stress and lag the alongshore stress by 90° .

The frequency domain relationships between the temperature and wind stress were quite different for the summer records. The surf temperature was found to be coherent with the alongshore stress only at periods of 2.1 and 11.5 days. The bottom temperature was coherent with the offshore stress only in the 2- to 3-day band and essentially in phase with the stress. The 11.5 day period was a persistent feature for both winter and summer. This result is consistent with Düing, et al. (1977) who found that the seasonal changes in atmospheric variables did not affect the v-component Florida Current amplitudes in 10- to 13-day period band. Oscillations at those periods were interpreted as continental shelf waves which are generated by well-defined atmospheric forcing events, regardless of season.

3. A 50-hour current and temperature profiling anchor station was established near the shelfbreak (102 m depth) during late July 1971. The mean alongshore flow component at the surface was about 136 cm/sec and increased to a subsurface maximum of 184 cm/sec at a depth of 20 m, very near the top of the thermocline computed for the mean temperature profile. Maximum vertical shear for the mean alongshore

flow was $-3.75 \times 10^{-2} \text{ sec}^{-1}$, measured just below the subsurface flow maximum. The coordinate rotation required for zero net onshore-offshore transport indicated that the mean flow was nearly aligned with the local bathymetry. The time variation of the velocity over the 50 hours revealed a wave-like character for both components.

Decreasing alongshore flow in the upper 55 m (increasing below that depth), and decay of the subsurface jet coincided with a decreasing offshore flow and a switch to onshore flow at all depths. The half-period for the apparent wave was about 36- to 40-hours, which was consistent with the time series evidence for organized motion at periods of 3- to 4-days. The time variation of the vertical temperature profiles was consistent with onshore advection of colder water accompanied by upward bowing of the isotherms of the shelfbreak evident in XBT sections. Relaxation of the bowed isotherms and increasing temperature throughout the water column was associated with offshore flow. The gradual deepening (shoaling) of the isotherms with decreasing (increasing) alongshore velocity was consistent with geostrophic adjustment in the alongshore flow. Comparison of geostrophic shear calculated from XBT stations (with the aid of a historical .T-S relation) and the shear in the measured mean alongshore velocity revealed excellent agreement from 30- to 90-m depth. Below 90 m frictional effects were evident. The measured subsurface jet in the upper layer was not reproduced in the geostrophic shear; hence, the surface layer flow is assumed to be ageostrophic probably due to frictional effects.

The perturbation velocity and temperatures (time-averaged vertical profiles removed) suggested at least three time scales of motion:

- (1) baroclinic near-inertial (~ 26 hrs) motion in the upper 30- to 50-m with amplitudes of 20- to 40-cm/sec for both velocity components;
- (2) 3- to 4-day period motion uniform with depth for the onshore-offshore flow and a 180° phase difference between the upper and lower water column (node at about 40- to 50-m) for the alongshore component; and
- (3) longer period motion evident in the alongshore flow with an apparent period of at least 4- to 5-days.

Estimates of mean dynamic stability (Richardson Number) suggested that, throughout most of the water column, the flow was marginally stable ($0.25 \leq Ri \leq 1$). The strong vertical shear in the upper mixed layer (15 m) produced a dynamically unstable layer ($Ri < 0.25$). This layer generally remained unstable throughout the entire 50-hour anchor station. Maximum values for Ri were recorded when both alongshore and onshore-offshore flow were at a minimum.

Results of an empirical orthogonal function analysis of the velocity components revealed that the onshore-offshore flow was very nearly barotropic for the first EOF which accounted for 87.2% of the total variance. The first EOF for the alongshore component was strongly depth dependent and accounted for 60.5% of the variance. The second EOF for the v component reflected a phase difference between the upper and lower layers and accounted for 28.8% of the total variance.

The time variations of the first EOF's for u and v confirmed the 3- to 4-day, and 4- to 5- (at least) day fluctuations, respectively, which were evident in the perturbation time-depth contours. The second EOF for v had a wavelike character similar to the first EOF for u but with an apparent phase difference of 90° . The vertical structure of these two EOF's suggested clockwise rotation above 35 m to 40 m and counterclockwise rotation below that depth at the 3 to 4-day period, in agreement with a theoretically calculated first mode topographic Rossby wave (Wang and Mooers, 1976).

4. Simultaneous short-term measurements of bottom current and temperatures were made at two buoy sites during June to July 1970. An alternating northwestward and southeastward flow had apparent periodicities of about 3- to 10-days. Onshore flow was generally associated with decreasing temperature and upwelling favorable (positive) wind stress components. Typical onshore-offshore and along-shore velocities were 3 to 4 cm/sec and 6 to 7 cm/sec, respectively. Positive (negative) accelerations in the alongshore flow were concurrent with onshore (offshore) accelerations suggesting that the interior alongshore flow was driving the onshore-offshore flow in the near-bottom zone, consistent with bottom Ekman layer dynamics.

A large temperature decrease was recorded at four bottom-mounted instruments as well as at the surf temperature location during late July 1971. From an XBT survey, coastal upwelling surfaced only in a very narrow (less than 15 to 18 km wide) coastal band north of Cape Canaveral. This width scale was shown to correspond roughly to the calculated "Rossby radius of deformation." The Rossby deformation

radius has been shown to be the basic baroclinic length scale associated with coastal upwelling areas (Mooers and Allen, 1973). A vorticity analysis suggested that the presence of Cape Canaveral can modify upwelling due to induced change in vorticity along a streamline in flow around the cape. For the scale magnitudes considered, upwelling was found to be enhanced north of the cape for both northward and southward flow. This result is consistent with the pattern noted in the surface temperature field.

5. The results believed significant to the distribution and abundance of the calico scallop resource were the following:
 - (1) The alternating bottom-current found during June to July 1970, if typical, provides a mechanism for localizing the scallops. Calico scallop larvae were found in the laboratory to be planktonic for about 16 days. Minimum and maximum displacements for a 16 day period were found to be 7 and 40 km, respectively, well within the known commercial scallop fishery grounds.
 - (2) The observed elongated, elliptical scallop beds are consistent with the patterns found by Carter and Okubo (1965) for diffusion in a horizontally and vertically sheared flow.
 - (3) Scallops were found to spawn spontaneously in the laboratory when the water was raised from 20 to 25°C. For a nearly year-long bottom temperature record, the temperature exceeded 25°C for only 9% of the time and it exceeded 20°C 56% of the time. Temperatures $\leq 15^\circ\text{C}$ are believed to be lethal to the calico scallop. XBT surveys during summer revealed bottom tempera-

tures $\leq 15^{\circ}\text{C}$ at depths as shallow as 40 m, well within the scallop's 20- to 60-m depth range.

Certain general recommendations may be made on horizontal and vertical instrument spacing for future work in this area. The frequency domain results were based primarily on bottom temperature records. The variation in bottom temperature is dependent on an established bottom temperature gradient (not always large) and horizontal motion along the bottom. The temperature gradient is time dependent and varies both cross-shelf and alongshore. This results in variable effects on temperature due to advection. In addition, the bottom mounted instruments were probably located in the bottom friction layer.

Nevertheless, certain general recommendations may be made regarding future observations. The vertical structure of the empirical orthogonal functions for the velocity at the shelfbreak suggest that two current meters, one at about 20 m and the second at about 70 m would be sufficient to resolve about 90% of the variance in both the onshore-offshore and alongshore flow. The time variation of the EOF's suggests that, for low frequency motion (period greater than 2 days), a sampling interval of about 2 hours would suffice.

Current meter arrays in the cross-shelf direction should be placed to resolve the theoretically predicted model structure for coastal-trapped waves. For example, Wang and Mooers (1976) showed that the first mode for the alongshore velocity of a coastal-trapped wave has a node at an offshore distance of about $0.8L$ where L is the shelf width, or about 40 km off Cape Canaveral. In addition, at least one current

meter array should be located well within the Rossby deformation radius which was estimated to be about 17 km in the summer. Record durations of at least six months would be required to resolve the longer period fluctuations (20- to 30-days) noted in some of the temperature spectra.

The horizontal and vertical temperature field and its temporal variation on the 3- to 4-day time scale could be well described by rapid, repetitive XBT surveys (perhaps one per day) over a two week period. The effects of Cape Canaveral on upwelling intensification and/or suppression as well as the structure within the deformation radius could be adequately described by such measurements. The sea surface temperature can now be monitored by satellite with a ground resolution of about 800 m (HCMP satellite). Satellite measurements would provide an inexpensive way to monitor upwelling and construct time series of the horizontal sea-surface temperature field, cloud cover permitting. Finally, salinity measurements should be included in any measurement program to adequately resolve the problems associated with stability, geostrophy, and water masses and their sources. A recommended program for the study of hydrographic structure and synoptic events in the South-Atlantic Bight was proposed which would meet these requirements (Witte, et al., 1977).

APPENDIX A

SPECTRUM ANALYSIS OF SELECTED WIND STRESS AND TEMPERATURE RECORDS

A.1 Data Analyzed

Initial analysis of the frequency content of the low-pass filtered wind stress and temperature records concentrated on four data sets:

1. Buoy 1 bottom temperature (BY1) and u and v component of wind stress (USTR, VSTR) for the period 1 April to 11 July 1970.
2. Buoy 2 (BY2) bottom temperature, buoy 1 (BY1) bottom temperature, and u and v components of stress (USTR, VSTR) for 16 November 1970 to 18 January 1971.
3. Same variables as (2), plus surf temperature (SFT) for period of 21 March to 18 May 1971.
4. Same variables as (3) for 1 July to 18 August 1971.

The records for (2), (3), and (4) above were the only ones for which bottom temperatures were recorded at both buoy sites.

The time series were treated in the manner described in Chapter 3. Each of the four data sets are discussed separately.

A.2 April to July 1970

The low-pass filtered u and v wind stress components (USTR, VSTR) and the bottom temperature at BY1 for 1 April to 11 July 1970 are shown in Figure A.1. Sample interval was 8 hours and the record length was 303 points (101 days). While the BY1 temperature exhibited some high frequency fluctuation (order of several days), the record was clearly

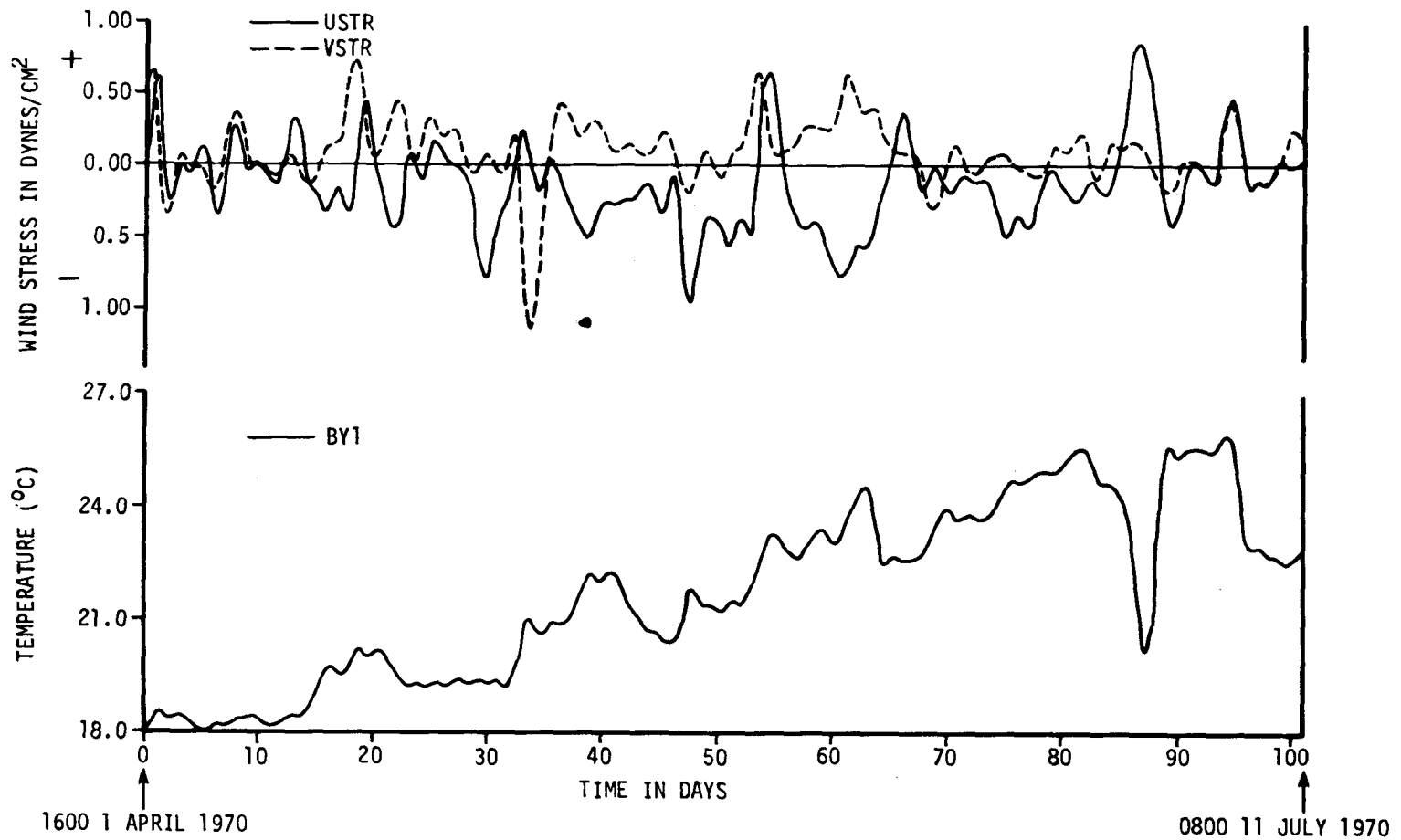


Figure A.1. Low-passed u and v wind stress components (USTR, VSTR) and bottom temperature (BY1) for 1 April to 11 July 1970.

dominated by an apparent 20 to 30 day periodicity with peak to trough amplitudes of about 2C° superimposed on an overall warming trend. The wind data exhibited much more high frequency information content with no readily apparent direct relationship to the temperature. The large temperature decrease near day 87 was discussed in Chapter 5.

First order statistics for each series as well as the overall correlation coefficients between records are presented in Table A.1. Correlation coefficients were computed for the data sets after detrending and lag adjustment correction for maximum absolute value of the cross correlation function. The time delay associated with the adjustment is also indicated in Table A.1. The low correlation coefficient values reflect the lack of visual correlation between wind and temperature. The negative value for USTR vs. BY1 indicates that decreasing temperature was associated with offshore wind stress. The USTR led the temperature by 4.3 days. The coefficient for VSTR vs. BY1 was positive indicating that positive alongshore stress was associated with increasing temperature.

The normalized autospectra for detrended USTR, VSTR, and BY1 were computed with 54 lags (M), an effective computational bandwidth (BW_e) of 0.035 cycles per day (cpd), and 14.0 degrees of freedom (DOF) (Fig. A.2). The spectrum for BY1 was essentially "red" with 98% of the variance accounted for at periods greater than about 50 days. The spectrum for USTR had a distinct peak at a period (T) of one week. The VSTR spectrum had a broad peak extending over periods between 18 and 36 days, and another at about 4.5 days.

TABLE A.1. Statistics for low-passed u and v wind stress components (USTR, VSTR) and bottom temperature at BY1 for 1 April to 11 July 1970. Record length = 303 points. $\Delta t = 8$ hours.

Data Set		Maximum	Minimum	Mean	Standard Deviation
USTR (dynes/cm ²)		0.84	-0.98	-0.15	0.30
VSTR (dynes/cm ²)		0.72	-1.19	0.09	0.23
BY1 (°C)		26.1	17.9	21.8	2.4
1	2	Correlation Coefficient		Time Lag in Days (+ indicates column 1 leads column 2)	
USTR vs	BY1	- .34 *		+4.3	
VSTR vs	BY1	+ .22		-2.3	

*SIGNIFICANT AT 95% LEVEL

AUTO SPECTRA, 1 APRIL TO 11 JULY 1970

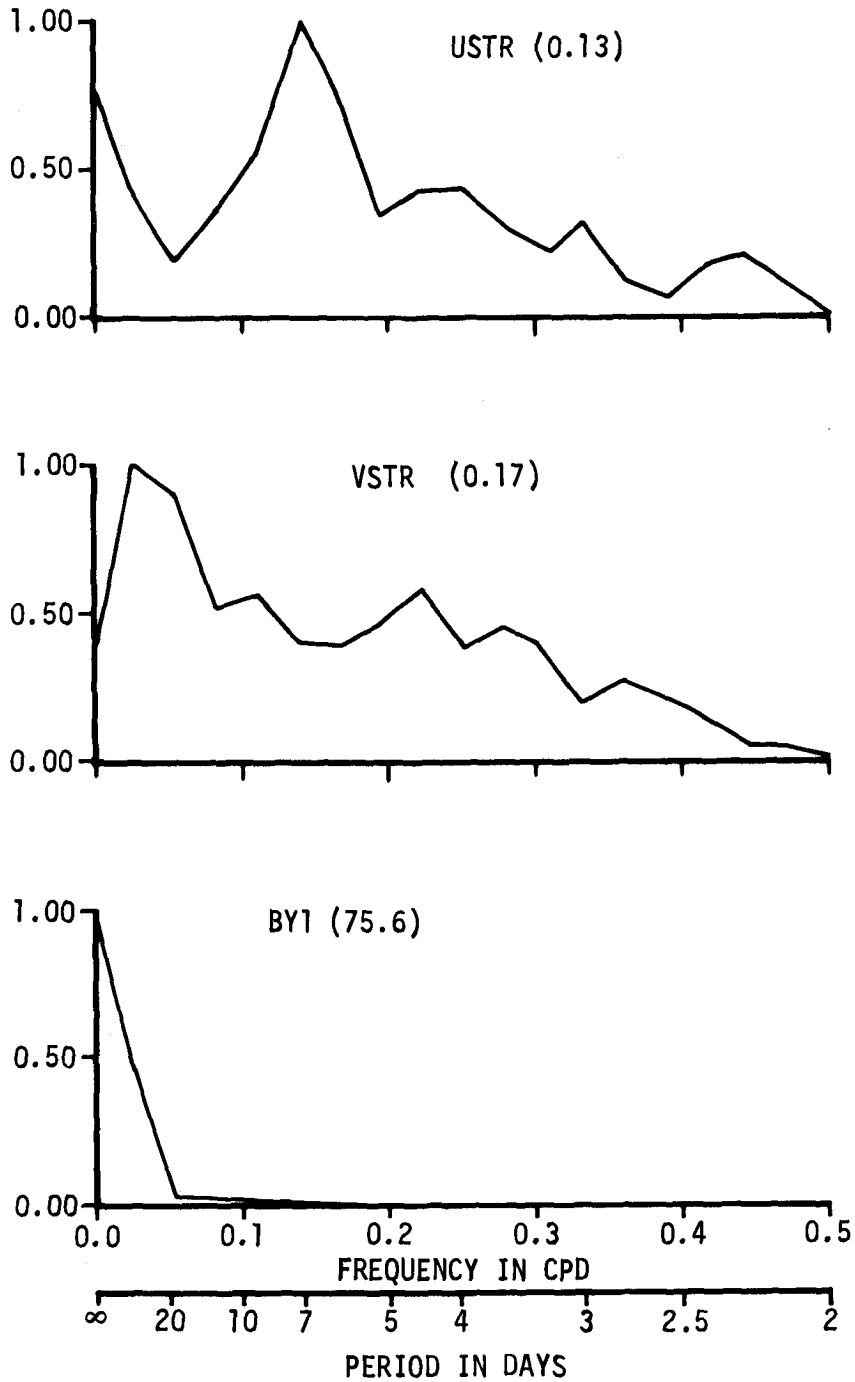


Figure A.2. Autospectra for USTR, VSTR, and BY1; 1 April to 11 July 1970, Normalization factors are given in parentheses. $N = 303$, $\Delta t = 8$ hours, $M = 54$, $BW_e = 0.035$ cpd, $DOF = 14.0$.

The coherence squared and phase for BY1 vs. USTR and VSTR are shown in Figure A.3. The coherence squared (coherence) is considered significant if it is greater than or equal to the 95% confidence level. For BY2 vs. USTR, coherence was significant in the extreme low frequency end of the spectrum ($T > 36$ days). The record length was, thus, not sufficient to resolve these low frequency motions. The temperature and both stress components were coherent at a period centered at about 2.4 days. The temperature lagged the wind by about 90° in phase. The phase sense is correct for the alongshore stress to indicate coastal Ekman divergence; however, the energy content of the BY2 record was very low at those frequencies.

A.3 November 1970 to January 1971

The low-passed u and v wind stress components (USTR, VSTR) and BY2, BY1 bottom temperatures from 16 November 1970 to 18 January 1971 are shown in Figure A.4. Sample interval was 8 hours and record length was 189 points (63 days). The temperature records contained a somewhat higher frequency content than that shown in Fig. A.1, but were similarly dominated by 20 to 30 day oscillations. The temperature fluctuations at BY1 and BY2 are visually quite coherent and nearly in phase for the last half of the record. There is no strong visual correlation between the temperature and either component of the wind stress, however.

First order statistics for each data set as well as overall correlation coefficients are shown in Table A.2. The mean temperature (18.8°C) was higher at the offshore buoy (BY2) than at BY1 (18.2°C). The mean wind stress was southeastward, consistent with winter conditions, but of low magnitude. The temperatures at BY1 and BY2 were

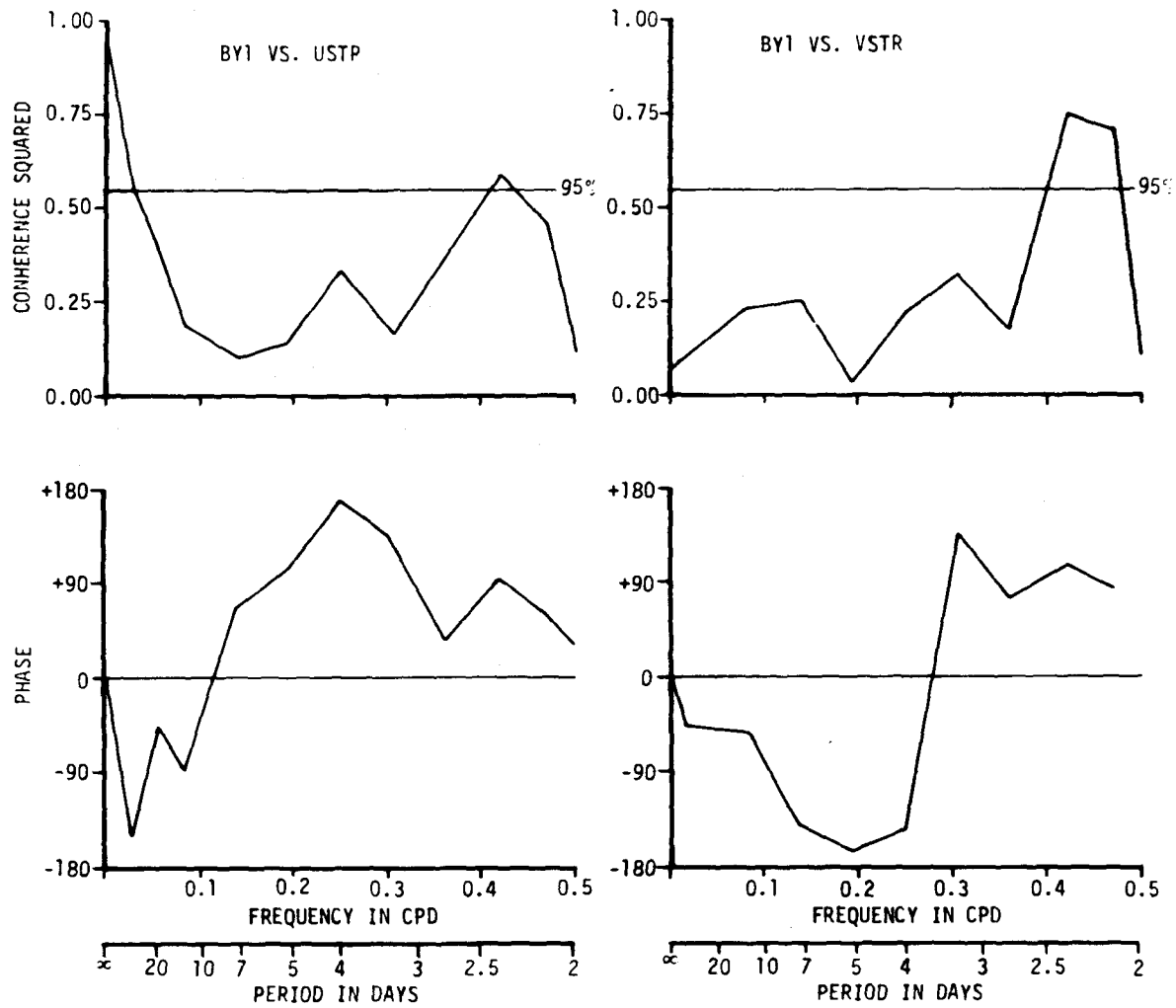


Figure A.3. Coherence squared and phase for BY1 vs. USTR and VSTR; 1 April to 11 July 1970. $N = 303$, $\Delta t = 8$ hours, $M = 54$, $BW_e = 0.035$ cpd, $DOF = 14.0$.

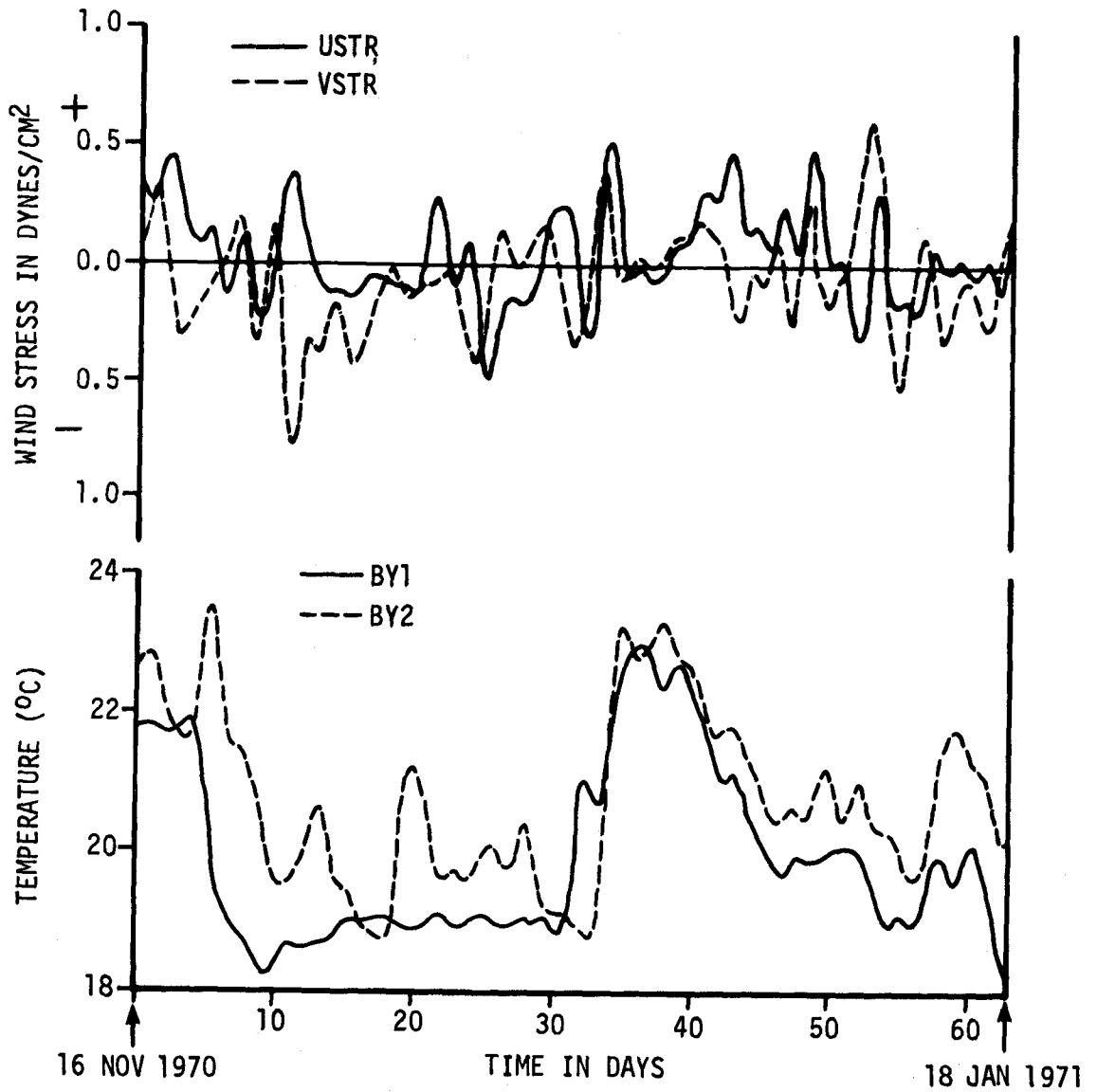


Figure A.4. Low-passed u and v wind stress components (USTR, VSTR), and bottom temperatures at BY1 and BY2 for 16 November 1970 to 18 January 1971.

TABLE A.2. Statistics for low-passed u and v wind stress components (USTR, VSTR) and bottom temperatures at BY1, BY2 for 16 November 1970 to 18 January 1971. Record length = 189 points. $\Delta t = 8$ hours.

Data Set		Maximum	Minimum	Mean	Standard Deviation
USTR (dynes/cm ²)		0.55	-0.49	0.05	0.20
VSTR (dynes/cm ²)		0.62	-0.78	-0.07	0.22
BY1 (°C)		23.0	18.2	19.9	1.3
BY2 (°C)		23.5	18.8	20.8	1.2
1	2	Correlation Coefficient		Time Lag in Days (+ indicates Column 1 leads Column 2)	
USTR vs.	BY1	+.37*		+1.3	
	BY2	+.35*		+1.3	
VSTR vs.	BY1	+.42**		-1.3	
	BY2	+.39*		+1.3	
BY1 vs.	BY2	+.81**		+1.6	

*SIGNIFICANT AT 95% LEVEL

**SIGNIFICANT AT 99% LEVEL.

slightly better correlated with the alongshore stress component (VSTR) than with the onshore-offshore component (USTR); however, the magnitudes of the correlation coefficients were small. The sign of the correlation coefficients were all positive which reflects rising temperatures with positive values of u and v wind stress. The correlation between BY1 and BY2, however, was high, with a coefficient of +0.81 at a lag of 1.6 days.

The normalized autospectra computed for all four detrended time series are shown in Figure A.5. The equivalent computational bandwidth BW_e was 0.057 cpd, with 33 lags and approximately 14.3 degrees of freedom (DOF). The spectra for BY1 and BY2 were essentially totally "red." The low frequency content completely dominated the record. About 98% of the variance in BY1 and 91% in BY2 were at frequencies below 0.045 cpd ($T = 22$ days). The spectrum for the USTR had a predominant peak at a period of 11 days. The v component had two small peaks at about 3.7 and 7.3 days (the latter peak may be the second harmonic of the first).

The phase and coherence squared for the temperature at BY1 and BY2 vs. USTR and VSTR, and for BY2 vs. BY1, are shown in Figure A.6. BY1 was significantly coherent with the stress only at very low frequency ($T > 22$ days). BY2 was significantly coherent with VSTR at a period of 22 days and very nearly so with both USTR and VSTR at 3.1 days. The phase at the latter period indicated that the temperature led VSTR by about 2.7 days and lagged USTR by about 2 days. For BY2 vs. BY1, significant coherence occurred at periods longer than 7.3 days with a peak at $T = 22$ days. Throughout this frequency band the phase sense was such that BY1 led BY2.

AUTOSPECTRA, 16 NOVEMBER 1970 TO 18 JANUARY 1971

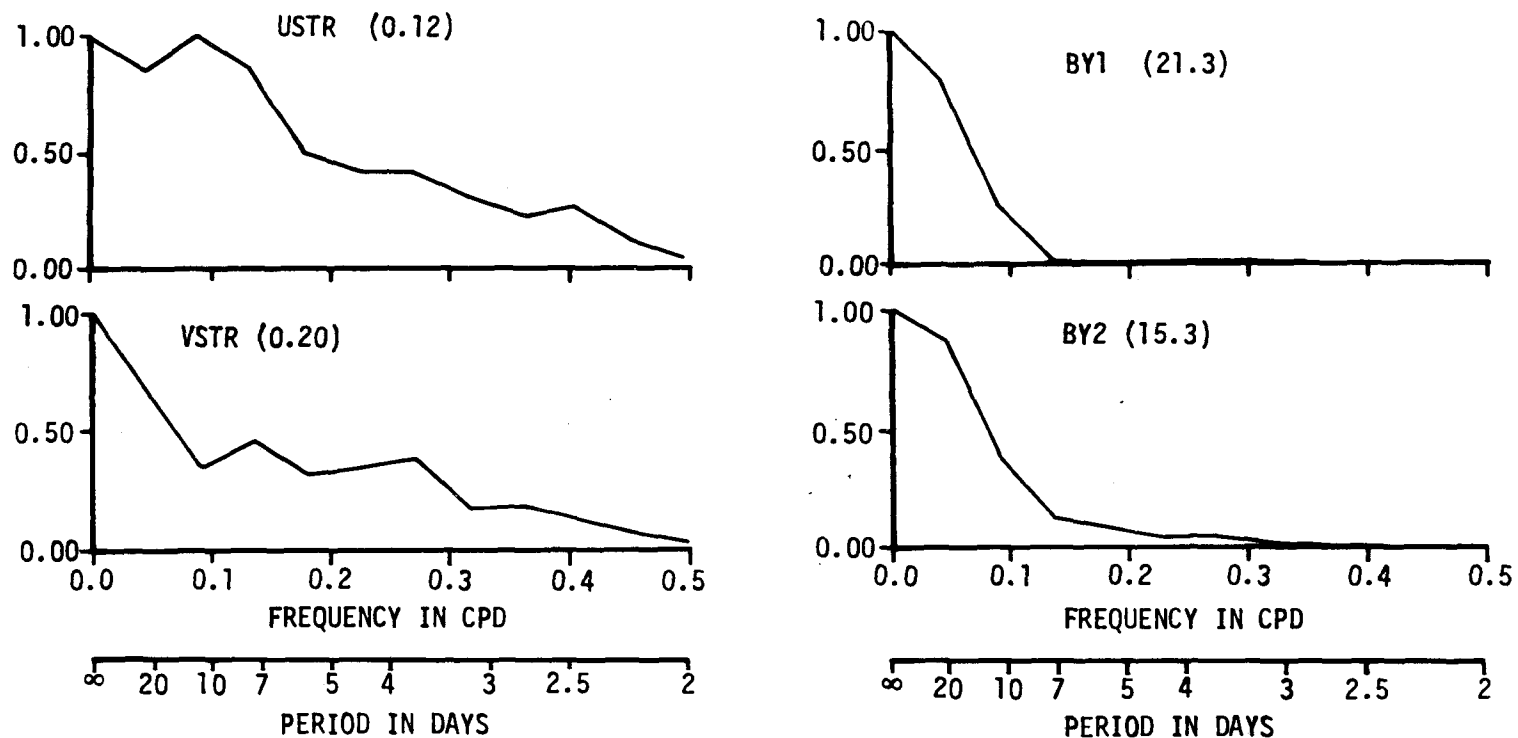


Figure A.5. Autospectra for USTR, VSTR, BY1 and BY2; 16 November 1970 to 18 January 1971. Normalization factors are given in parentheses. $N = 189$, $\Delta t = 8$ hours, $M = 33$, $BW_e = 0.057$ cpd, $DOF = 14.3$.

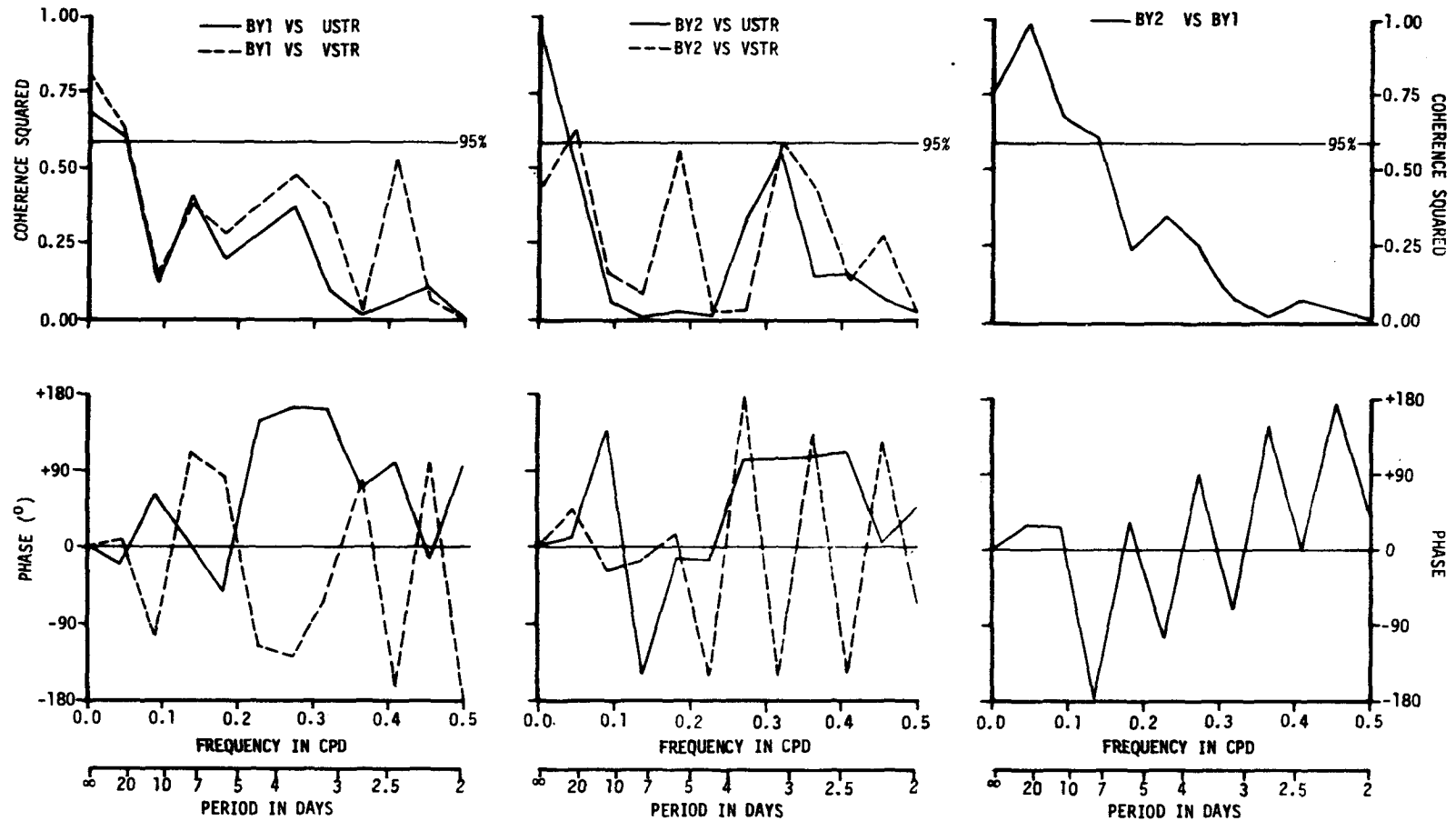


Figure A.6. Coherence squared and phase for BY1 and BY2 vs. USTR and VSTR, and BY2 vs. BY1; 16 November 1970 to 18 January 1971. $N = 189$, $\Delta t = 8$ hours, $M = 33$, $BW_e = 0.057$ cpd, $DOF = 14.3$.

As in the results of A.2, the long period fluctuations dominated the bottom temperature records and generally tended to confuse the analysis. The indication was that either the record length was too short to resolve the low frequency fluctuations or that these fluctuations were essentially aperiodic or episodic.

A.4 March to May 1971

The low-passed u and v stress components (USTR, VSTR) surf temperature at Daytona Beach (SFT), and bottom temperature at BY1 and BY2, for 21 March to 18 May 1971 are shown in Figure A.7. Sample interval was again 8 hours and the record length was 174 points (58 days). This data set represented the transition period from winter to summer conditions. The BY1 and BY2 temperatures are strongly correlated visually and nearly in phase, especially during the latter portion of the record. The surf temperature reflected the overall warming trend in the transition from winter to summer. The negative temperature anomalies in SFT, BY1, and BY2 exhibit some visual correlation to upwelling favorable wind stress (i.e. USTR and VSTR both positive), especially between days 30 to 40 and after day 53.

The statistics for each time series as well as the cross-correlation coefficients are shown in Table A.3. The mean bottom temperatures at BY2 and BY1 were identical (19.6°C) although the offshore buoy recorded the coldest temperature of the two (16.9°C). The mean surf temperature (19.1°C) was slightly colder than either bottom temperature mean but also had the warmest and coldest readings of the three temperature series. The mean wind stress was nearly zero for this time period. The correlation coefficients between the wind stress and the tempera-

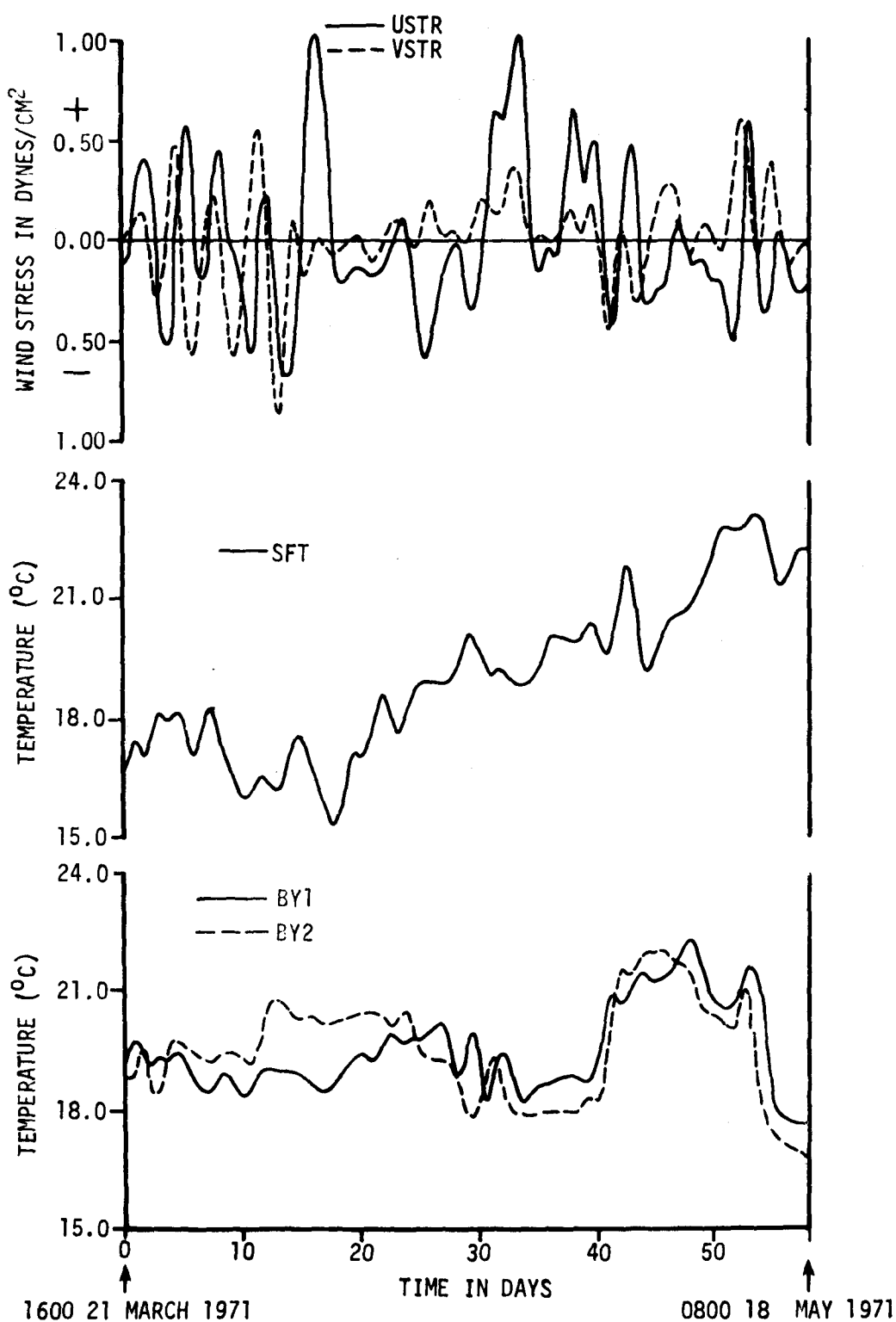


Figure A.7. Low-passed u and v wind stress components (USTR, VSTR), surf temperature (SFT), and bottom temperature at BY1 and BY2 for 21 March to 18 May 1971.

TABLE A.3. Statistics for low-passed u and v wind stress components (USTR, VSTR), surf temperature at Daytona Beach (SFT), and bottom temperatures at BY1 and BY2 for 21 March to 18 May 1971. Record Length = 174. $\Delta t = 8$ hours.

Data Set		Maximum	Minimum	Mean	Standard Deviation
USTR (dynes/cm ²)		1.04	-0.67	0.02	0.37
VSTR (dynes/cm ²)		0.61	-0.91	0.01	0.24
SFT (°C)		23.2	15.3	19.1	2.0
BY1 (°C)		22.3	17.7	19.6	1.1
BY2 (°C)		22.1	16.9	19.6	1.3
1	2	Correlation Coefficients		Time lag in Days (+ indicates Column 1 leads Column 2)	
USTR vs.	SFT	+.22		-2.0	
	BY1	-.23		+0.6	
	BY2	-.25		-2.3	
VSTR vs.	SFT	+.31		0.0	
	BY1	+.31		+3.3	
	BY2	-.35		-1.3	
SFT vs.	BY1	+.67**		0.0	
	BY2	-.50*		-1.0	
BY1 vs.	BY2	-.51*		+3.0	

*SIGNIFICANT AT 95% LEVEL.

**SIGNIFICANT AT 99% LEVEL.

tures were low in all cases. The SFT was positively correlated (0.67) with the BY1 temperature and negatively correlated (-0.50) with BY2. The overall correlation between BY1 and BY2 was relatively low and negative (-0.51); however, they were obviously positively correlated during the latter portion of the record (Fig. A.7). This indicates that some caution should be used when interpreting the overall coefficients, especially in terms of strictly two-dimensional onshore-offshore flow. These results suggest that alongshore advection may also have a significant influence on the temperature.

The autospectra for all five detrended series are shown in Figure A.8. Unstable estimates of the SFT spectrum dictated a maximum lag of only 7 days ($M = 21$), resulting in a BW_e of .089 cpd with 20.7 DOF. The SFT, BY1 and BY2 spectra were again essentially "red." Over 90% of the variance in each was accounted for at periods greater than 14 days. The USTR and VSTR spectra both had a peak at a period of about 3.5 days.

The coherence squared and phase for SFT and BY1 vs. USTR and VSTR are shown in Figure A.9. The surf temperature was coherent with both USTR and VSTR at the 3.5 day period, but with negative phase indicating the temperature led the stress. The temperature at BY1 was coherent with both stress components at periods of about 7 days. The phase was positive near 90° for both components which indicates the stress led the temperature by about 1.3 days. The same plots for BY2 vs. USTR and VSTR, SFT vs. BY2 and BY1, and BY2 vs. BY1 are shown in Figure A.10. BY2 was coherent with USTR at a period of about 3.5 days and very nearly in phase. The BY2 temperature was also coherent with VSTR at a period of about 4.7 days with the stress leading the temperature by about 1.6

AUTOSPECTRA, 21 MARCH TO 18 MAY 1971

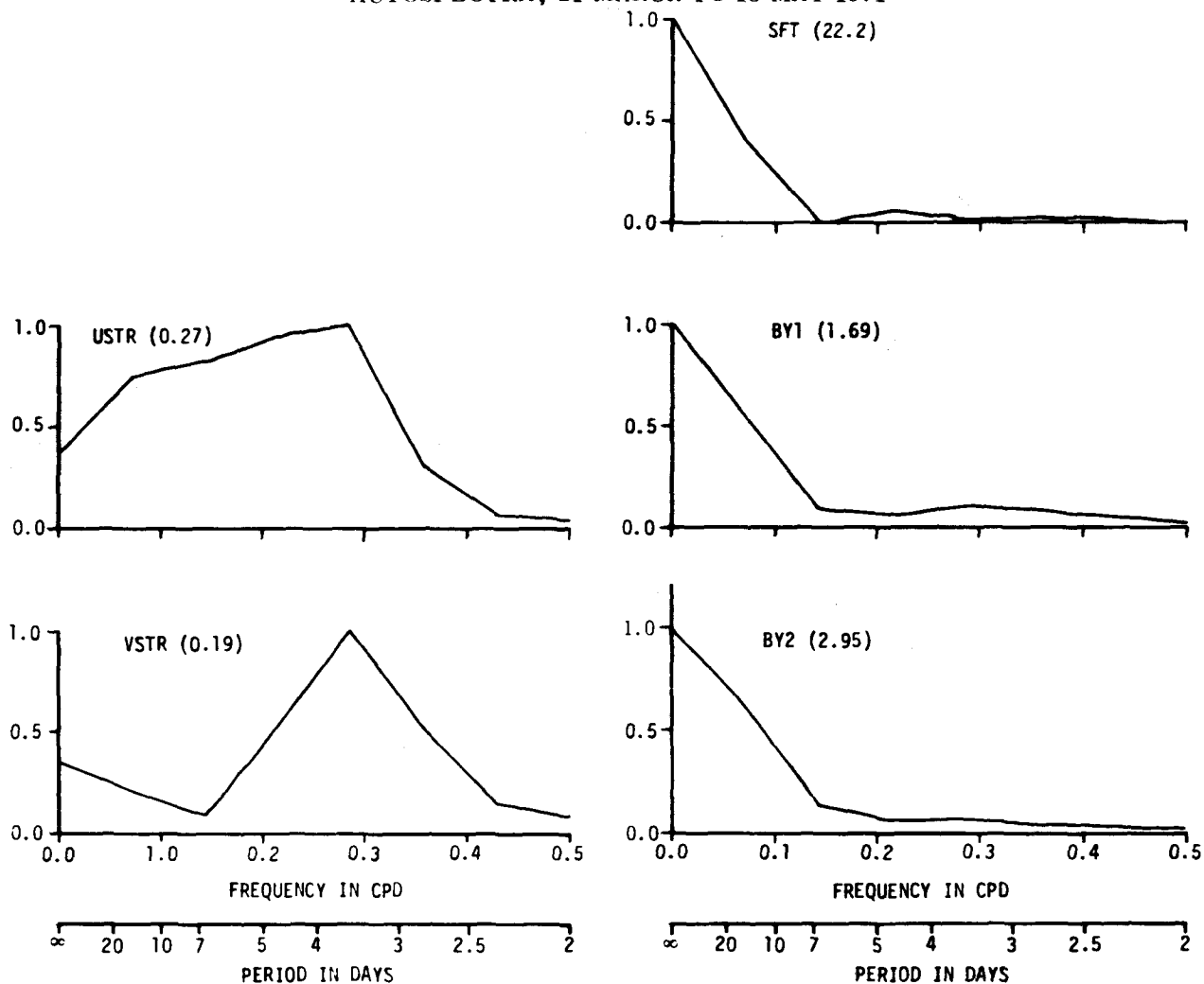


Figure A.8. Autospectra for USTR, VSTR, SFT, BY1 and BY2; 21 March to 18 May 1971. Normalization factors are given in parentheses. $N = 174$, $\Delta t = 8$ hours, $M = 21$, $BW_e = 0.089$ cpd, $DOF = 20.7$.

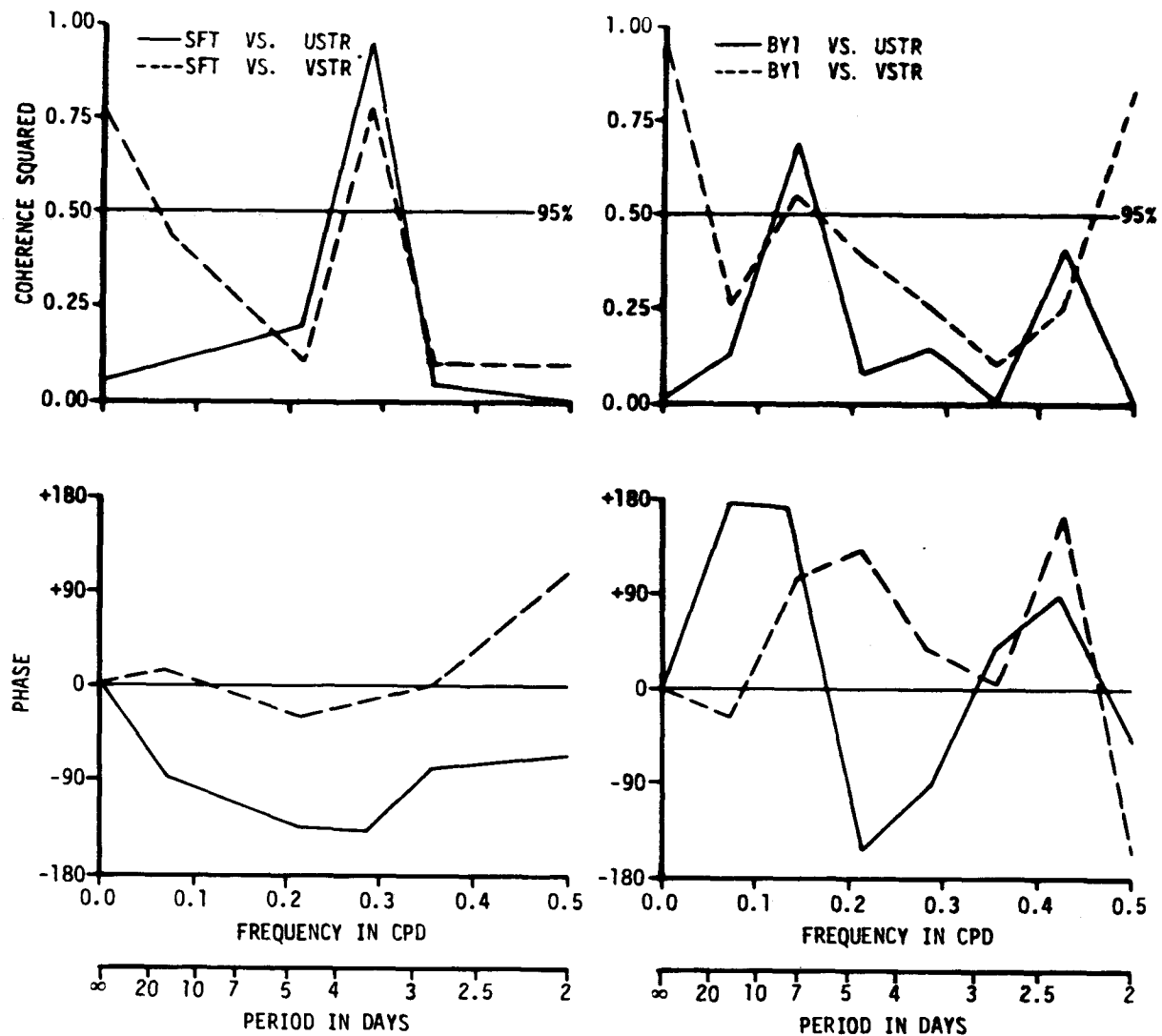


Figure A.9. Coherence squared and phase for SFT and BY1 vs. USTR and VSTR; 21 March to 18 May 1971. $N = 174$, $\Delta t = 8$ hours, $M = 21$, $BW_e = 0.089$ cpd, $DOF = 20.7$.

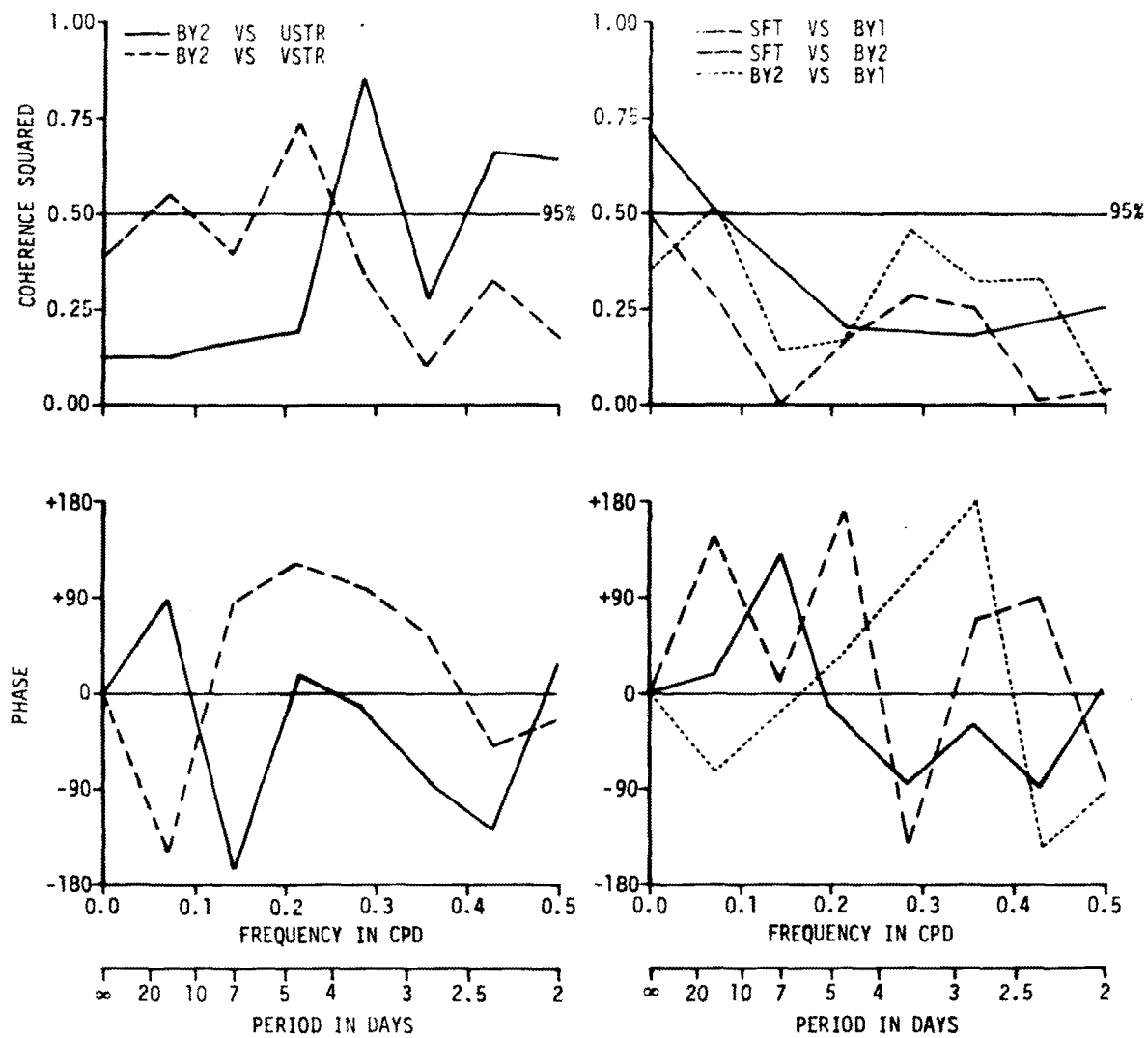


Figure A.10. Coherence squared and phase for BY2 vs. USTR and VSTR, SFT vs. BY1 and BY2, and BY2 vs. BY1; 21 March to 18 May 1971. $N = 174$, $\Delta t = 8$ hours, $M = 21$, $BW_e = 0.089$ cpd, $DOF = 20.7$.

days. A coherent peak for BY2 vs. the VSTR also existed at $T = 14$ days. In addition, the temperature at BY2 showed some significant coherence with USTR for the period range of 2.0 to 2.5 days. The phase in this range was generally negative, however, indicating the temperature was leading the wind. The temperatures at BY2 and BY1 were coherent only at the 14 day period with the phase indicating that BY2 led BY1 by about 3 days. There was no significant coherence between SFT and BY2 and between SFT and BY1 for frequencies greater than .07 cpd ($T = 14$ days).

A.5 July to August 1971

The low-passed time series of u and v wind stress components, surf temperature at Daytona Beach, and bottom temperatures at BY1, BY2 for the period 1 July to 18 August 1971 are shown in Figure A.11. This period corresponds to the time of largest negative temperature anomalies during the year. The record was the shortest of those which contained coincident measurements at both BY1 and BY2. The sample interval was 8 hours and the record length was 144 points (48 days).

All three temperature records were remarkably similar and all contained the large temperature depression in the middle of the record, the partial recovery from day 35 to 45, and the beginning of another sharp decrease at the end of the record. The alongshore stress was positive (upwelling favorable) for nearly the entire record length with superimposed 3-to-7 day oscillations. Similar periodicities were apparent for the u component; however, positive (negative) values were associated with decreasing (increasing) temperature as expected by simple upwelling theory. The large increase in both stress components at the end of the

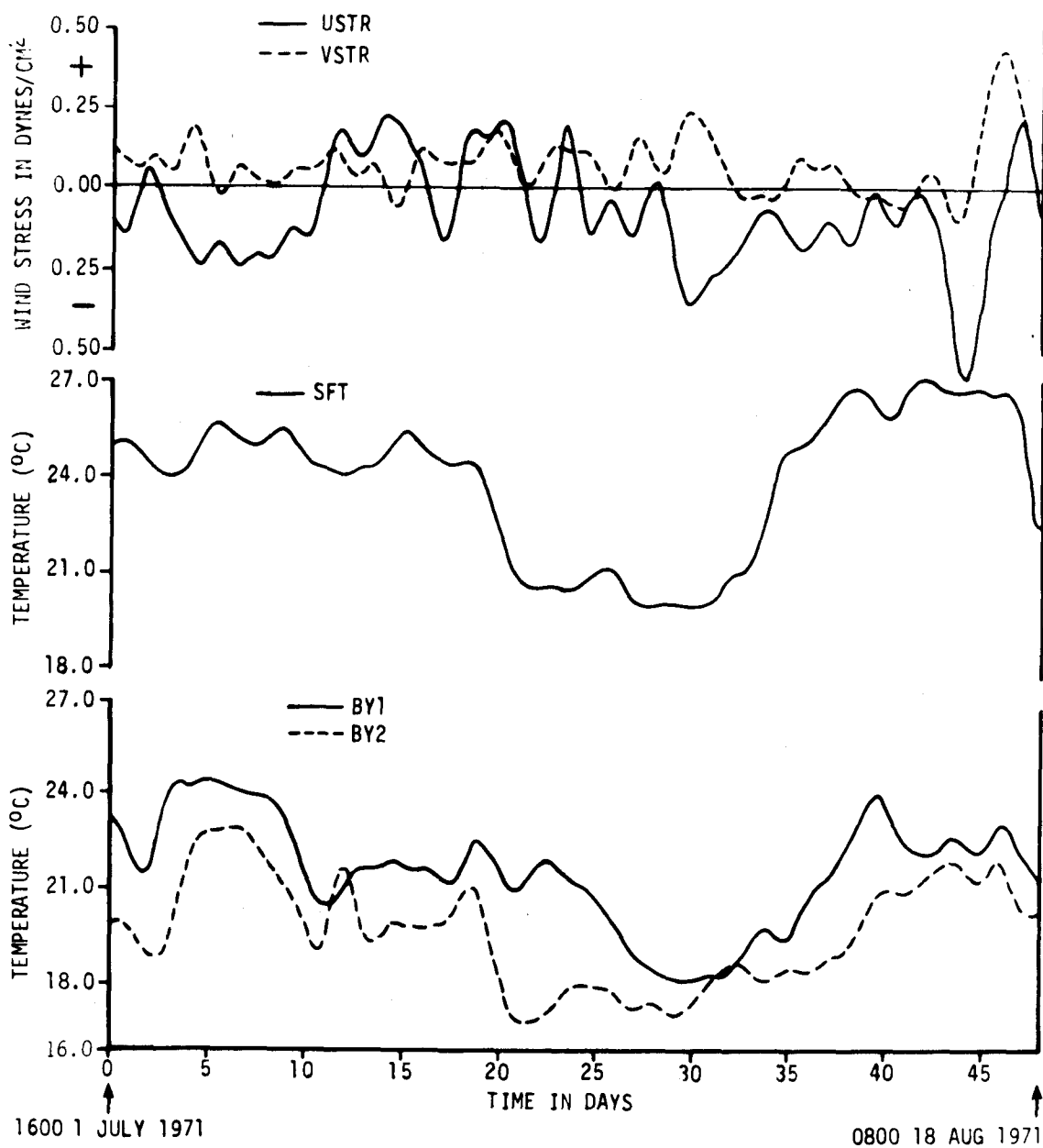


Figure A.11. Low passed u and v wind stress components (USTR, VSTR), surf temperature at Daytona Beach (SFT), and bottom temperatures at BY1 and BY2 for 1 July to 18 August 1971.

record was consistent with the beginning of the sharp temperature decrease at that time.

The sample statistics for each time series and the correlation coefficients are shown in Table A.4. Although the records were from mid-summer, the mean bottom temperature at BY2 (19.7°C) was nearly the same as the mean temperature during 21 March to 18 May (Table A.3) and 1.1°C colder than the 16 November 1970 to 18 January 1971 record (Table A.2). Although the mean bottom temperature at BY1 was about 2°C warmer than that recorded during 21 March to 18 May, 1971, the minimum temperature (18.1°C) was nearly as low as that for the spring (17.7°C). The mean surf temperature (23.9°C) was high, reflecting the seasonal heating, but reached a minimum of 19.9°C which was nearly as cold as the overall mean for spring conditions (Table A.3). The standard deviations for the temperature records were larger from July to August than for either the winter (Table A.2) or spring (Table A.3). The mean wind stress was toward the northwest but of very small magnitude (0.1 dyne/cm^2).

The correlation coefficients (Table A.4) among the temperature records were all high (>0.83). In addition, the correlations between USTR and the temperatures were high and negative, especially between USTR and by1 (-0.80). The negative sign is consistent with upwelling theory indicating decreasing temperatures associated with positive values of both stress components. The larger absolute values of the correlation coefficients associated with USTR indicate that the offshore stress may be the controlling factor so long as the v-component remains positive, which is typical of summer wind conditions.

TABLE A.4. Statistics for low-passed u and v wind stress components (USTR, VSTR), surf temperature at Daytona Beach (SFT), and bottom temperatures at BY1 and BY2 for 1 July to 18 August 1971. Record length = 144. $\Delta t = 8$ hours.

Data Set		Maximum	Minimum	Mean	Standard Deviation
USTR (dynes/cm ²)		0.23	-0.62	-0.08	0.16
VSTR (dynes/cm ²)		0.43	-0.11	0.07	0.09
SFT (°C)		27.1	19.9	23.9	2.3
BY1 (°C)		24.4	18.1	21.6	1.7
BY2 (°C)		23.0	16.8	19.7	1.7
1	2	Correlation Coefficient		Time Lag (days) (+ indicates Column 1 Leads Column 2)	
USTR vs.	SFT	-.63**		+ 1.3	
	BY1	-.80**		+ 1.0	
	BY2	-.63**		+ 1.0	
VSTR vs.	SFT	-.33		+ 1.0	
	BY1	-.39*		+ 2.6	
	BY2	-.51**		+ 1.3	
SFT	BY1	+.88**		+ 1.3	
	BY2	+.83**		+ 0.6	
BY1 vs.	BY2	+.85**		+ 1.0	

*SIGNIFICANT AT 95% LEVEL

**SIGNIFICANT AT 99% LEVEL

The autospectra for all five series are shown in Figure A.12. Computations were for 27 lags with an effective bandwidth of .069 cpd and 13.3 DOF. As in all previous calculations, most of the energy in the temperature spectra was concentrated in the very low frequency range. The SFT and BY1 spectra had very small peaks centered at a frequency of 0.22 cpd ($T = 4.5$ days). The BY2 spectrum had no pronounced peaks. The spectrum for USTR had a maximum centered at a frequency of .056 cpd ($T = 18$ days), while that for VSTR had a maximum at 2.3 and 9 days with a somewhat smaller peak at 3.6 days.

The coherence squared and phase for SFT and BY1 vs. USTR and VSTR are shown in Figure A.13. The surf temperature was coherent with both stress components at a frequency of 0.11 cpd ($T = 9.0$ days) and also at 0.22 cpd ($T = 4.5$ days) which was probably the second harmonic of the former period. Negative phase indicates that the temperature was leading the offshore stress. Positive phase showed just the opposite for the alongshore stress. The BY1 temperature was coherent with USTR for all periods greater than 6 days and the stress led the temperature. The temperature for BY1 was coherent with VSTR for all periods between 9 and 18 days. Positive phase for the latter indicates the stress was also leading the temperature at those frequencies. The dominance of the fortnightly and longer period band was demonstrated by Brooks (1975) to be typical for the Florida area in summer months.

The same plots for BY2 vs. USTR and VSTR, for SFT vs. BY1 and BY2, and for BY2 vs. BY1 are shown in Figure A.14. The coherence was above the 95% significance level for BY2 vs. VSTR for all frequencies between .056 cpd ($T = 18$ days) and .278 cpd ($T = 3.6$ days). The alongshore

AUTOSPECTRA, 1 JULY TO 18 AUGUST 1971

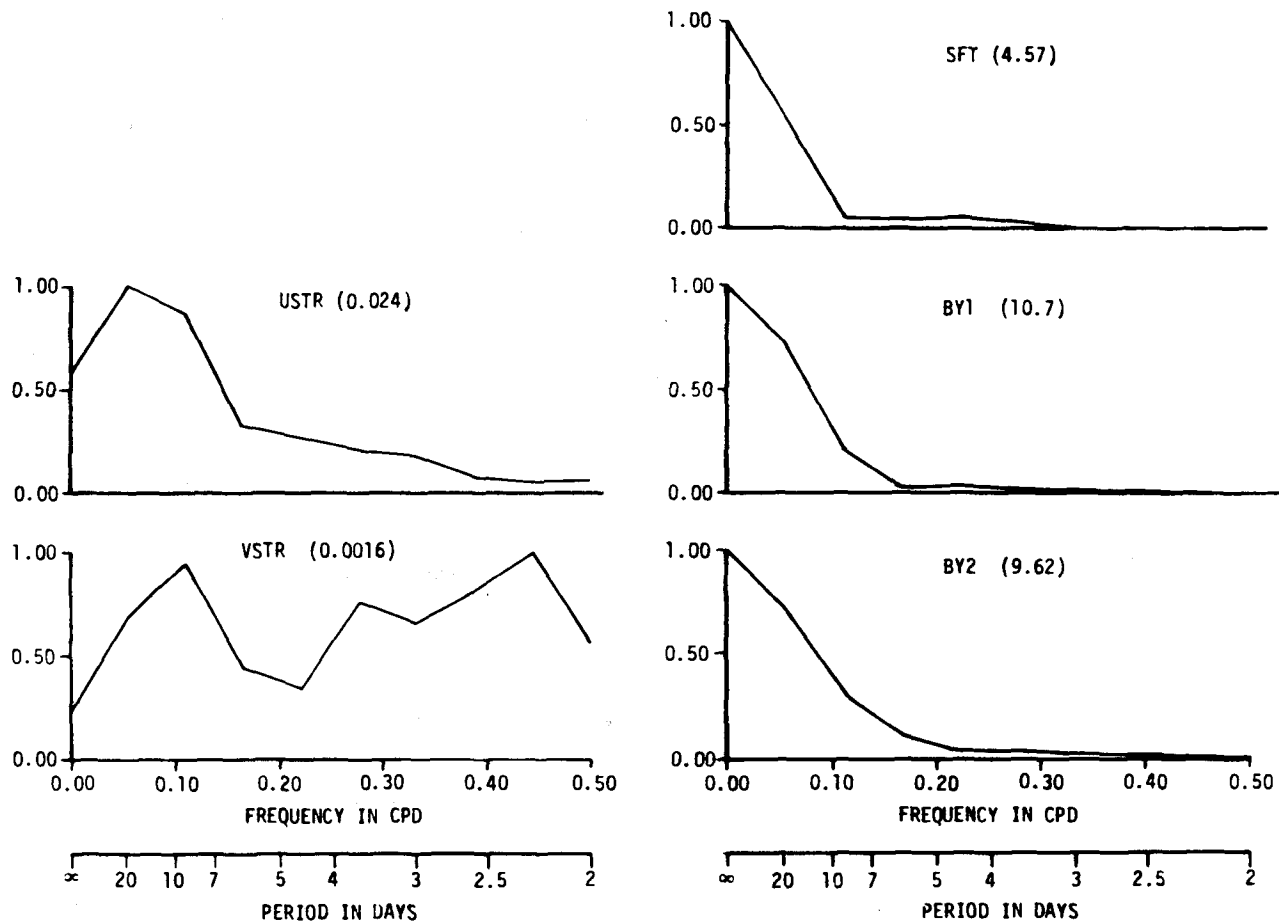


Figure A.12. Autospectra for USTR, VSTR, SFT, BY1 and BY2; 1 July to 18 August 1971. $N = 144$, $\Delta t = 8$ hours, $M = 27$, $BW_e = 0.069$ cpd, $DOF = 13.3$.

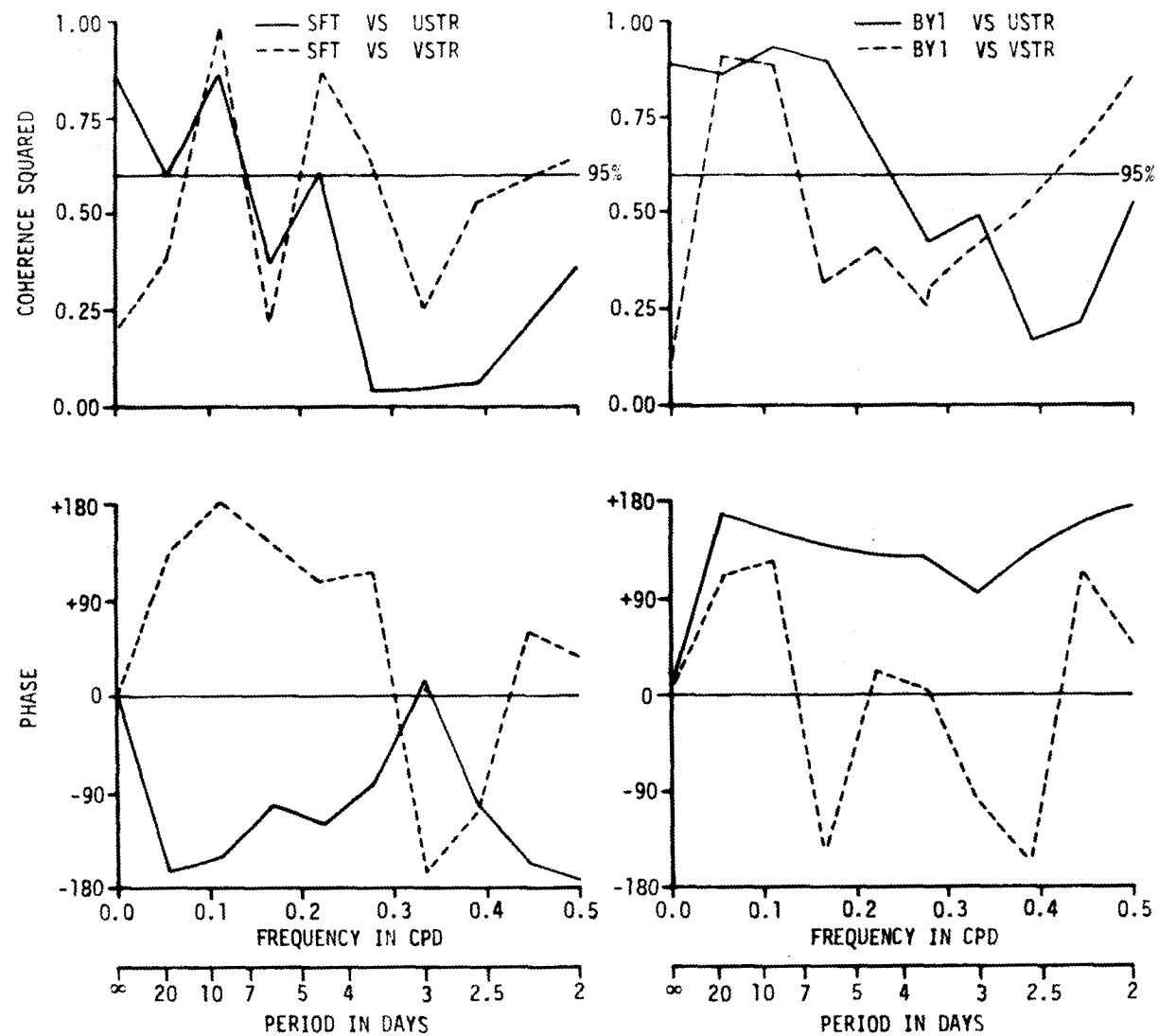


Figure A.13. Coherence squared and phase for SFT and BY1 vs. USTR and VSTR; 1 July to 18 August 1971. $N = 144$, $\Delta t = 8$ hours, $M = 27$, $BW_e = 0.069$ cpd, $DOF = 13.3$.

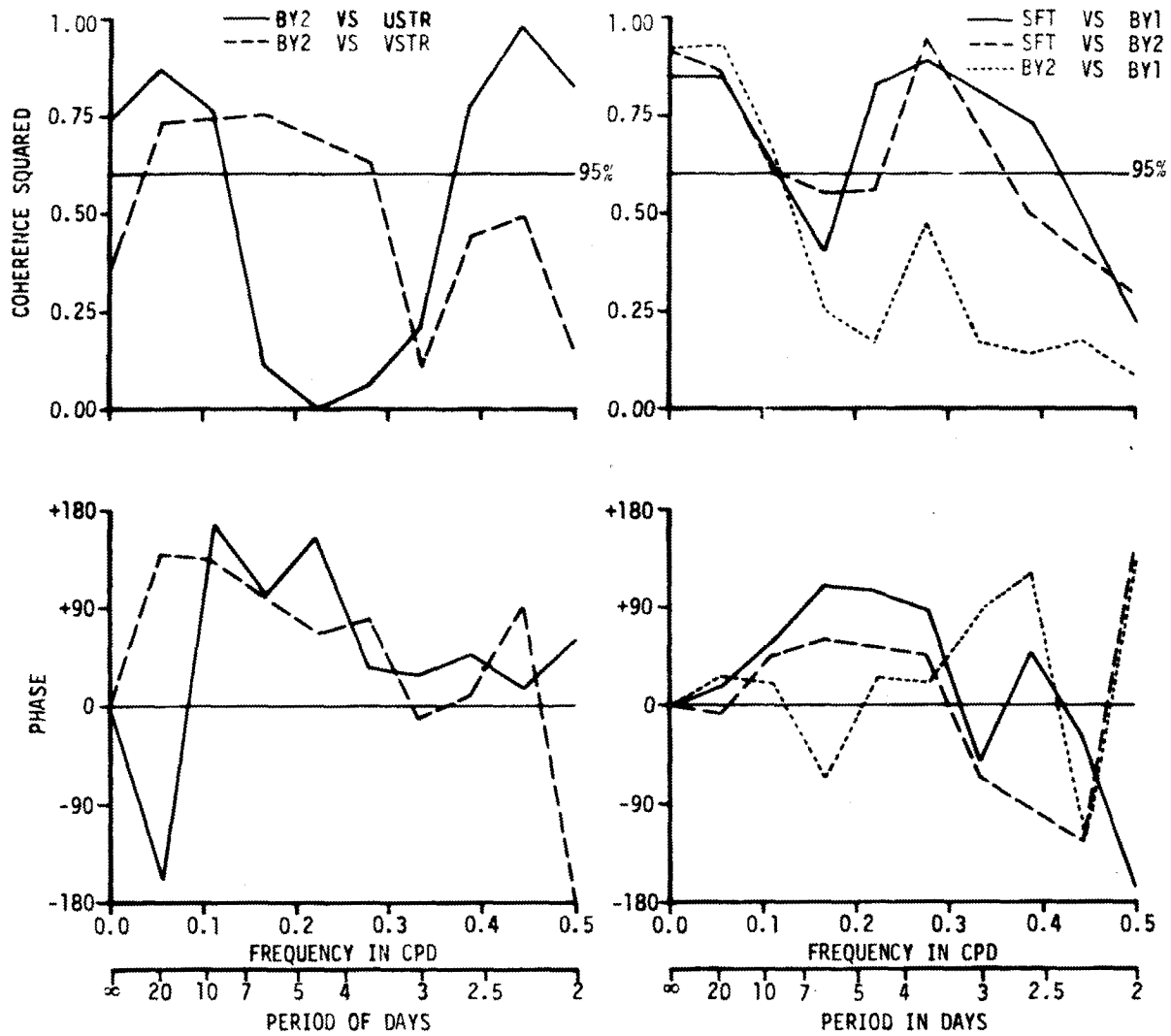


Figure A.14. Coherence squared and phase for BY2 vs. USTR and VSTR; SFT vs. BY1 and BY2; and BY2 vs. BY1: 1 July to 18 August 1971. $N = 144$, $\Delta t = 8$ hours, $M = 27$, $BW_e = 0.069$ cpd, $DOF = 13.3$.

stress led the temperature since the phase remained positive for this frequency band. High coherence also existed between BY2 and USTR in the 2.0-to 2.5-day band with the stress leading. The SFT was coherent with BY1 and BY2 for the 9-to-18 day band and all three records were nearly in phase. These results are consistent with simple upwelling theory as described in Chapter 3.4.4. SFT was also coherent with BY1 and BY2 over a band from 0.2 to 0.4 cpd, centered at a period of 3.6 days. The phase was positive indicating that the bottom temperatures led the surf temperatures. BY2 and BY1 were significantly coherent only at periods greater than 9 days and nearly in phase. There was a hint of coherence between the buoy temperatures at the 3.6 day period which was significant at the 80% level.

For July to August, the predominant coherence between the wind stress and temperature was in the 9-to 18-day period band with some indications of significant coherence at periods of about 4.5 and 3.6 days. In the longer period band, the phase relationships among the temperatures and between the temperatures and the alongshore wind stress component were consistent with that expected for the subsurface onshore-offshore compensation flow required by simple wind-driven coastal upwelling. Similar energetic period bands have been reported from temperature and velocity time series in the Florida Current near Miami (D'Ángelo, et al., 1977). They found that the most energetic band was 8 to 25 days with smaller but significant peaks in the period ranges from 4 to 5 days, and 2 to 3 days. The shorter period variations (4 to 5, 2 to 3 days) were interpreted to be wind driven or initiated by atmospheric forcing but the class of waves to which they belong is not known.

Brooks and Mooers (1977 b) have interpreted the longer period fluctuations to be associated with barotropic continental shelf waves.

APPENDIX B

RESULTS SIGNIFICANT TO CALICO SCALLOP

The original purpose of the acquisition effort for the basic data presented in this thesis was to monitor the bottom habitat of the calico scallop, Argopecten Gibbus. Large concentrations of the species occur on the continental shelf near Cape Canaveral in depths from 9 to 74 m (Drummond, 1969) and support a substantial commercial fishery. The greatest concentrations of calico scallops are found near coastal projections such as Cape Canaveral and Cape San Blas, Florida; and Cape Hatteras (Bullis and Thompson, 1965) and Cape Lookout, N.C. (Allen and Costello, 1972). A general description of the calico scallop biology and fishery can be found in Allen and Costello (1972). The results presented in this thesis believed to be of significance to the calico scallop resource are discussed separately in terms of currents and temperature.

B.1 Current Effects

After spawning, the larval scallops rely almost totally on currents for transport until they are old enough to set. Thus, the flow field is believed to have a significant effect on the overall distribution of scallop beds. Bullis and Cummins (1961) suggested that the Cape Canaveral projection causes "interruption and eddying" that produces "repetitive settling of scallop larvae." They believed that such eddies were responsible for keeping the larvae from being swept away from the area, thereby creating a permanent resource.

The results of the bottom current measurements presented in Chapter 5.1 support the hypothesis that scallop larvae would be likely to remain within the general area. Laboratory experiments have shown that calico scallops remain in the larval stage for about 16 days (Costello, et al., 1972). The cyclic flow shown in the progressive vector diagram of Figure 5.2 demonstrates that, for a 16 day larval drift period, the total displacement can be quite small. For example, in the 16 day period from 5 June to 21 June 1970, the total displacement was about 7 km. At the other extreme, the total displacement between 12 June and 28 June was about 40 km, a distance well within the limits of the known scallop grounds. The specific cause of the cyclic flow is not known; however, meanders of the Florida Current, perhaps due to continental shelf waves, are suspected. Any eddying effects of Cape Canaveral cannot be evaluated with this data set, although Chapter 5.2.3 suggests that the cape can exert significant influence on the coastal flow field.

The scallops have been observed to occur in irregularly distributed, long, narrow beds oriented parallel to the coastline (Bullis and Cummins, 1961). Some beds have been reported off Cape Canaveral which were more than 800 m long and several hundred meters wide (Roe, et al., 1971). The beds were reported to be generally elliptical in shape. From dye observations in the coastal waters off Cape Canaveral, Carter and Okubo (1965) developed a model for tracer diffusion in a vertically and horizontally sheared flow which predicts just such elliptically shaped patches. It would seem likely that the calico scallop larvae would drift and diffuse in a sheared flow similar to that predicted for dyes; hence, after setting, narrow elongated beds of adult scallops

oriented parallel to the flow (alongshore in the mean) would be expected.

B.2 Temperature Effects

Temperature has been shown to have a significant effect on calico scallop reproduction and survival (Waller, 1969). Rising water temperature is known to trigger spawning. Specifically, Costello, et al. (1972) induced spawning in laboratory scallops several times in less than one hour by raising the water temperature from 20°C to 25°C. It is still not known whether the effect is primarily dependent on a rapid temperature change or on the absolute temperature.

The daily mean bottom temperatures at BY1 and BY2 were patched to provide a continuous record from 27 August 1970 to 24 August 1971. The relative distribution of the temperature observations (Table B.1) for the nearly year-long record indicates that the temperature was above 25°C only about 9% of the time, and was above 20°C about 56% of the year. The minimum survivable temperature for the calico scallop is believed to be 15°C (G. Miller, personal communication). Results indicate that the bottom temperature at the biological buoy site never reached the lethal level; however, 44% of the observations were below the 20°C level presumed necessary for spawning.

The general depth range for the scallop beds off Cape Canaveral is about 20 to 60 m. Results from the XBT surveys showed that the meandering of the Florida Current can inject cold offshore water onto the shelf along the bottom. Figure 4.4 is an example of such an intrusion during late July 1971. The 15°C isotherm intersected the bottom at about 50 m depth, near the offshore edge of the scallop beds. An even more extreme

TABLE B.1. Percentage distribution of the daily mean bottom temperature observations by temperature interval for BY1; 27 August 1970 to 24 August 1971.

Temperature Range	16.0-16.9	17.0-17.9	18.0-18.9	19.0-19.9	20.0-20.9	21.0-21.9	22.0-22.9	23.0-23.9	24.0-24.9	25.0-25.9	26.0-26.9	>27.0
% Observations	3.3	3.9	15.5	21.3	6.9	14.4	12.5	7.2	6.1	4.7	4.2	0.0
Cumulative % < max. temp. in interval	3.3	7.2	22.7	44.0	51.0	65.4	77.8	85.0	91.1	95.8	100.0	---
Cumulative % > min. temp. in interval	100.0	96.7	92.8	77.3	56.0	49.0	34.6	22.2	15.0	8.9	4.2	0.0

case occurred during June 1971, (not shown) when a pool of bottom water less than 15°C existed along XBT Transect 3 from about 40 m to 55 m depth. Even if lethal temperatures are not reached during such summer intrusions, the bottom temperature depression is probably sufficient to preclude spawning. A counter effect to the low bottom temperatures resulting from the intrusions may be that the nutrient concentration over the shelf is significantly increased. Recently, Atkinson, et al. (1978) showed that an intrusion of the Gulf Stream onto the shelf near St. Augustine, Florida coincided with significant increases in nitrate and chlorophyll concentrations. The bottom layer was found to be so dense with a bloom of Phaeocystis pouchetti (up to 3.1×10^6 cells/l) that zooplankton sampling was not possible. Thus, competing influences of decreasing temperature and increased food supply may complicate any conclusions about the individual effect of each on scallop growth rates from field studies alone.

Appendix C

INDIVIDUAL XBT SECTIONS

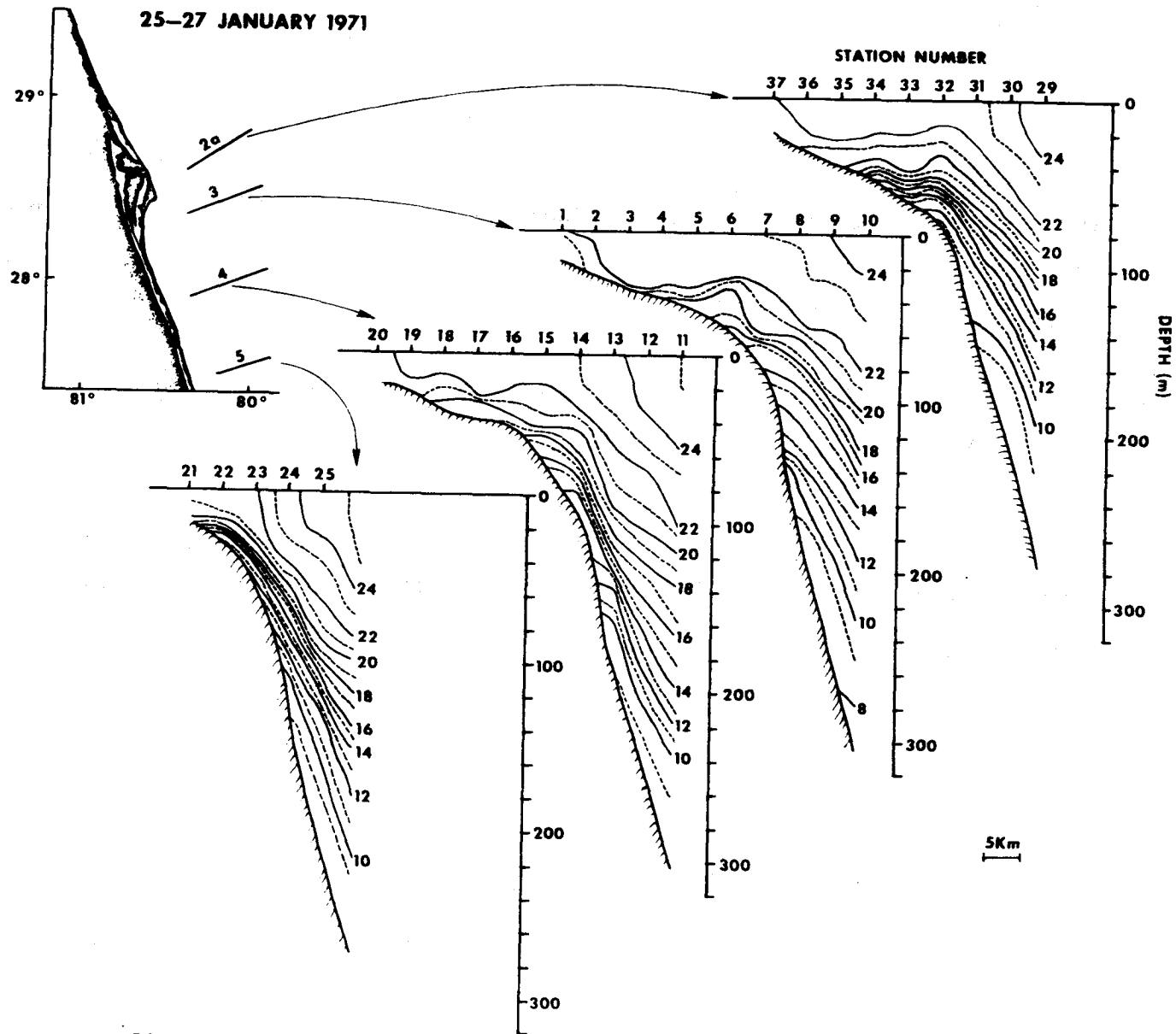


Figure C.1. Vertical XBT temperature sections, 25-27 January 1971.

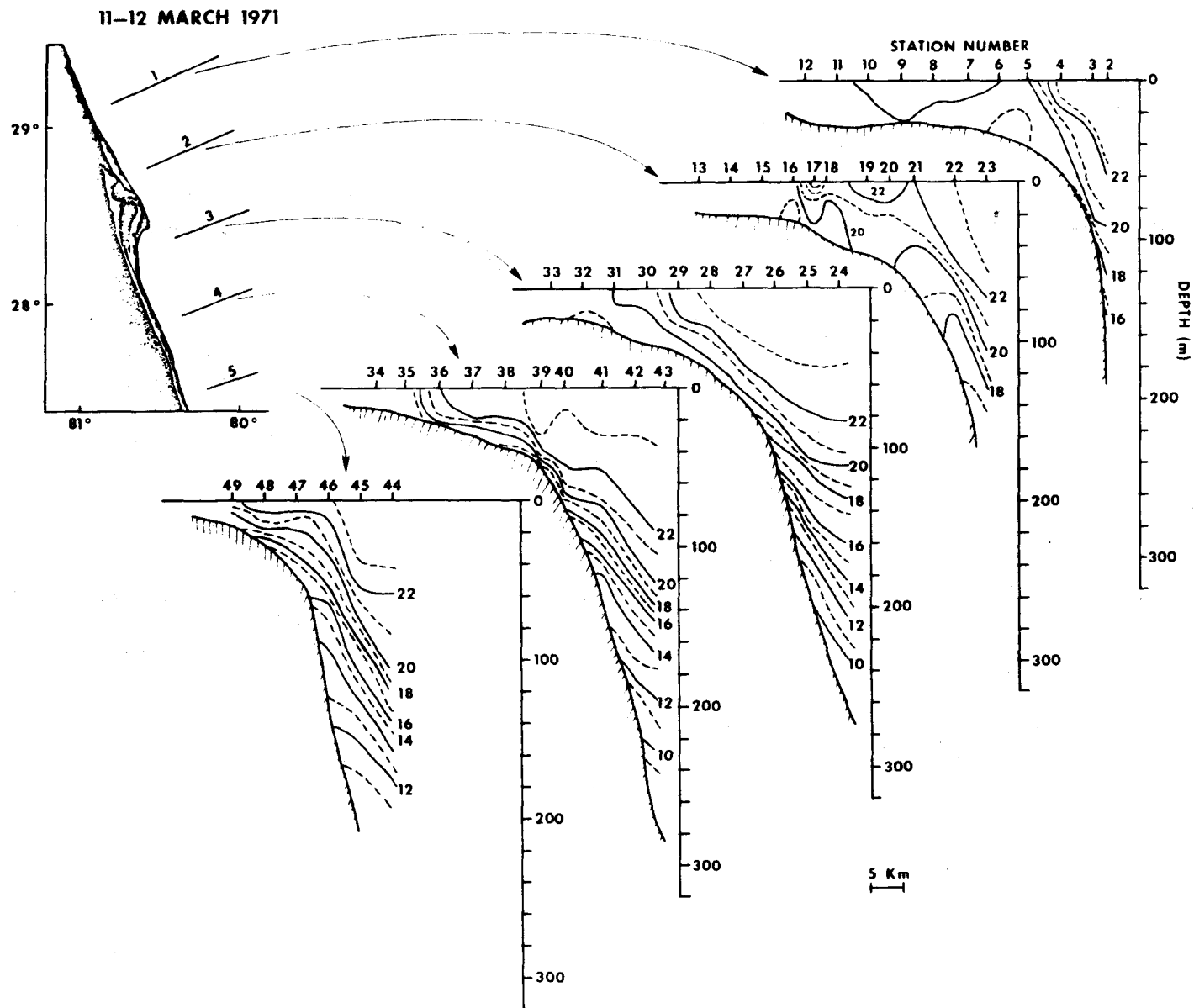


Figure C.2. Vertical XBT temperature sections, 11-12 March 1971.

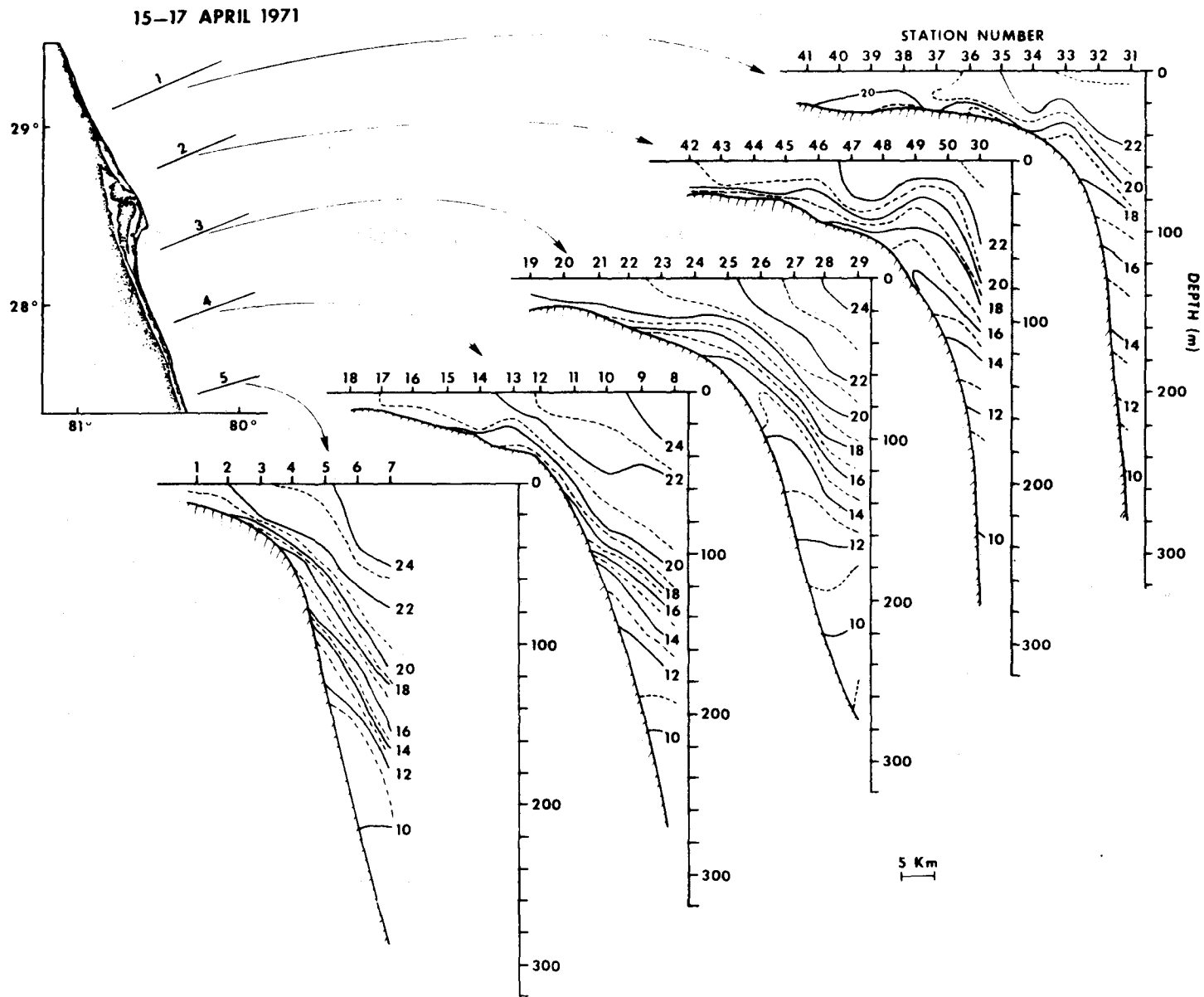


Figure C.3. Vertical XBT temperature sections, 15-17 April 1971.

20-21 MAY 1971

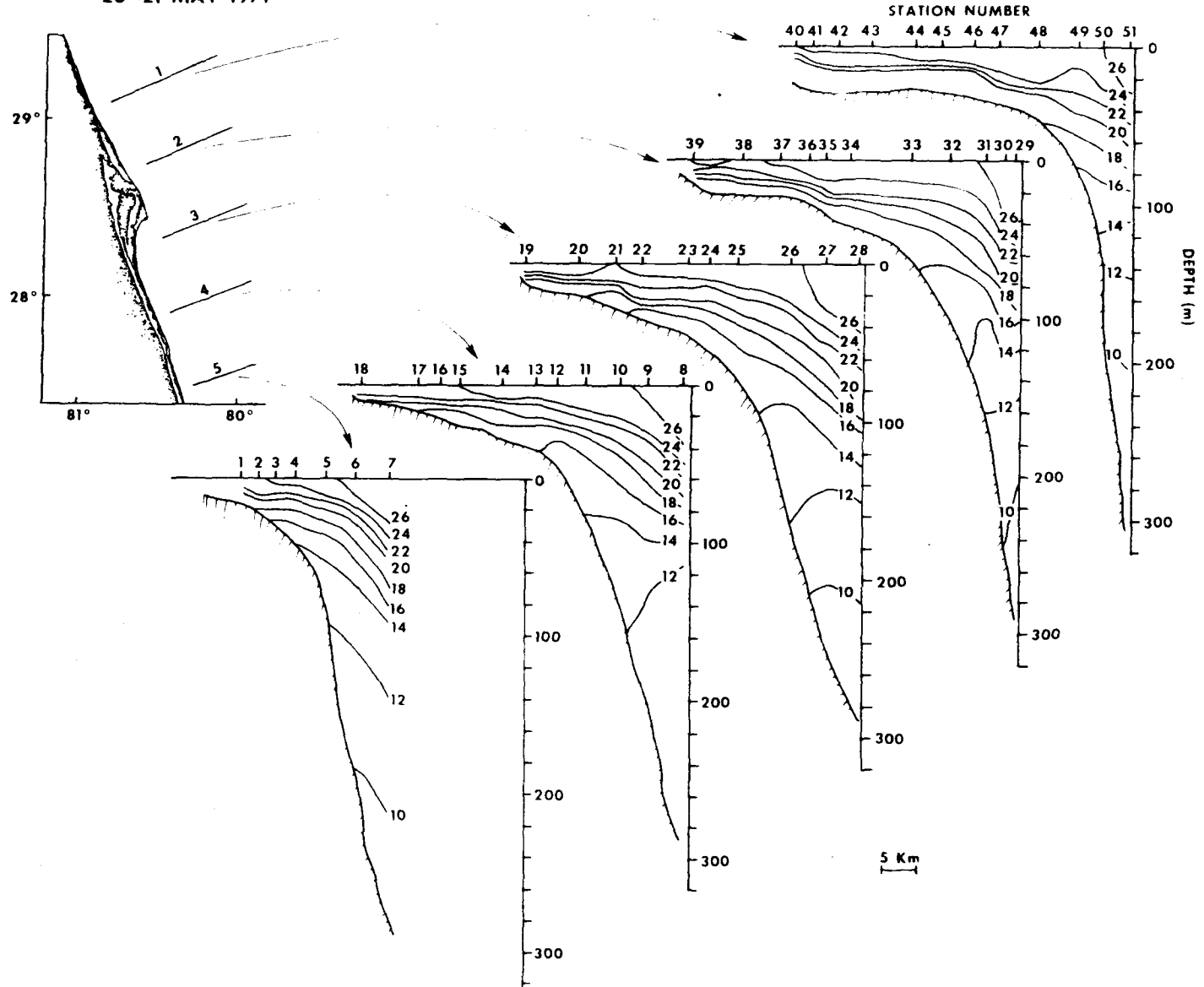


Figure C.4. Vertical XBT temperature sections, 20-21 May 1971.

28-29 JUNE 1971

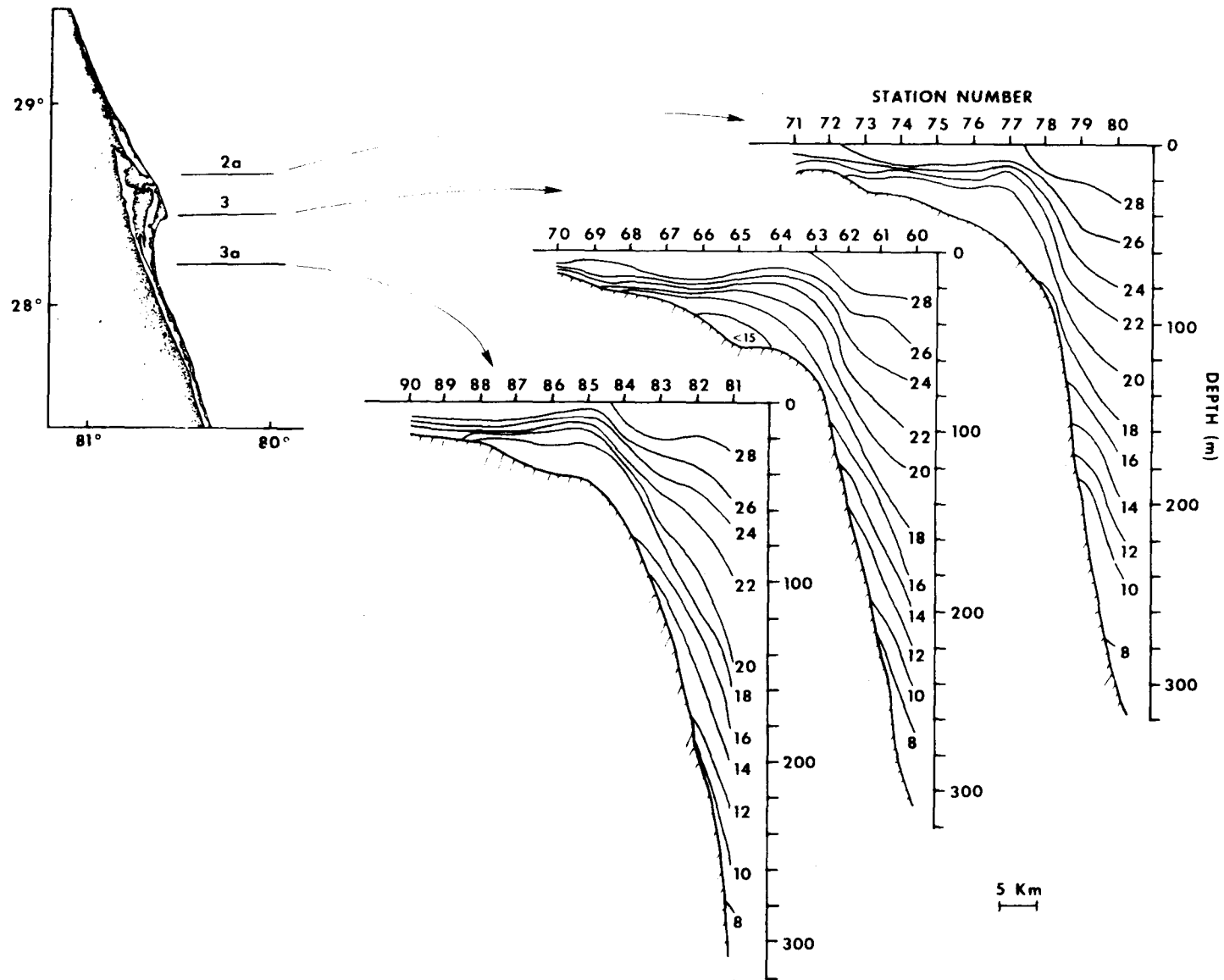


Figure C.5. Vertical XBT temperature sections, 28-29 June 1971.

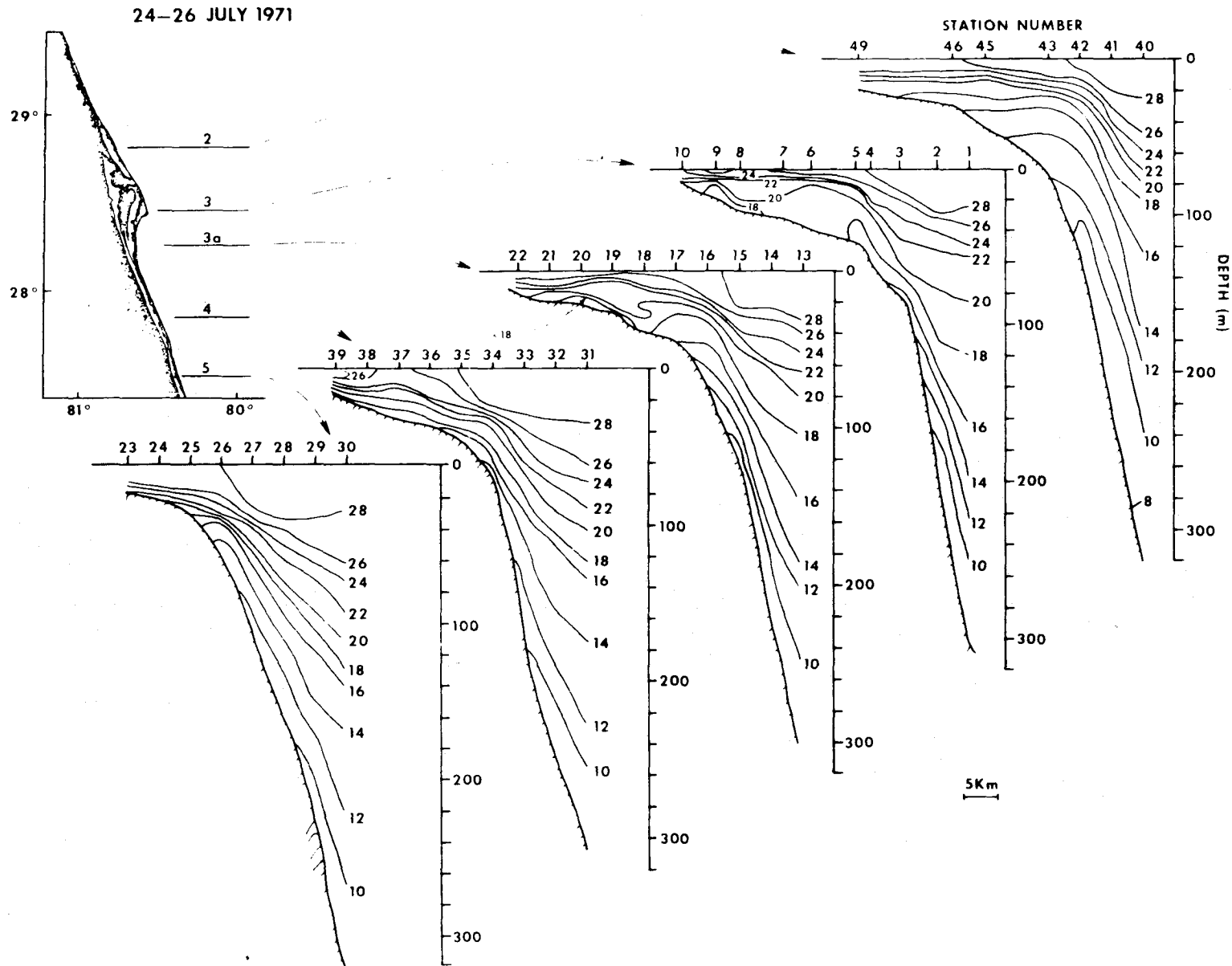


Figure C.6. Vertical XBT temperature sections, 24-26 July 1971.

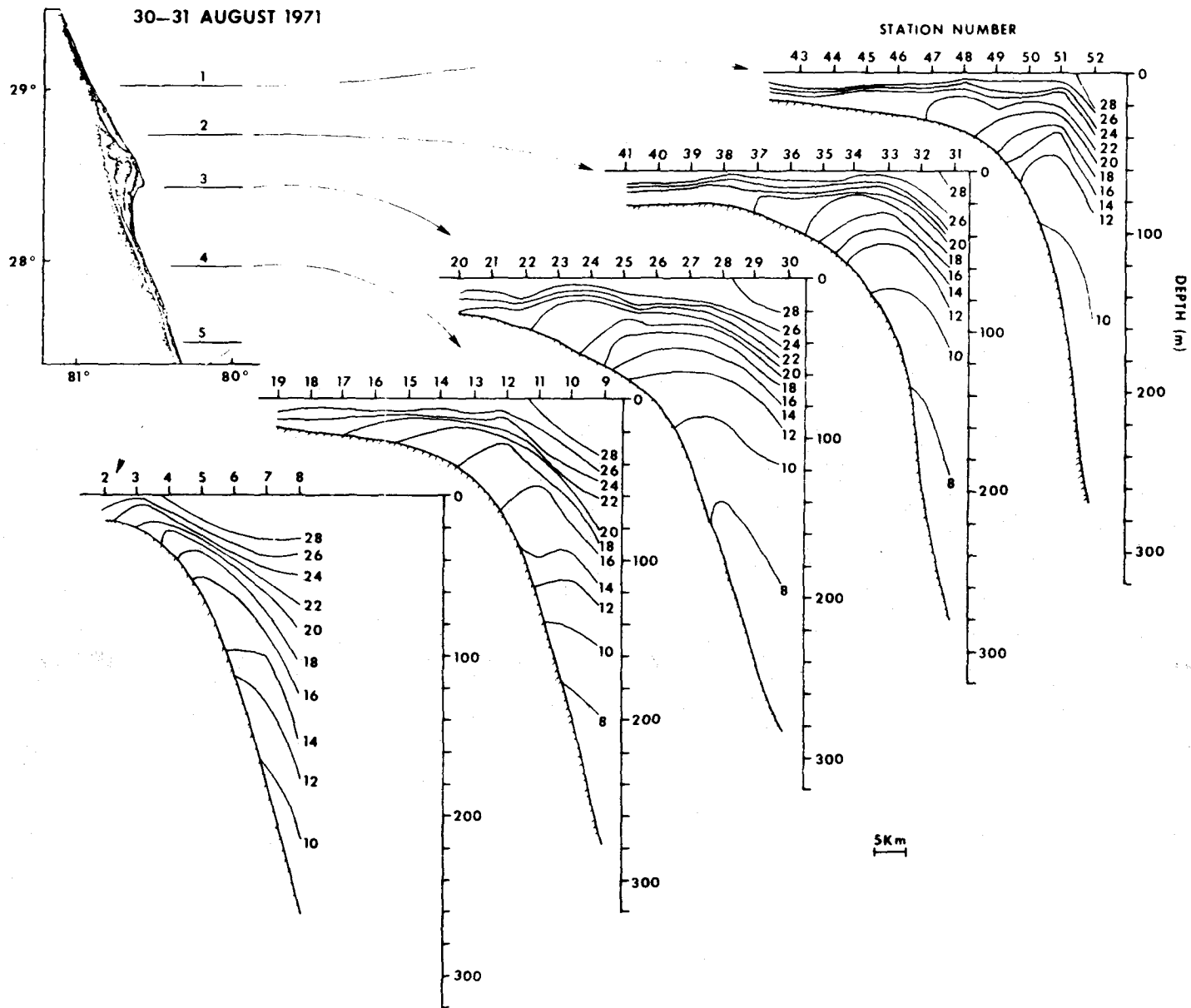


Figure C.7. Vertical XBT temperature sections, 30-31 August 1971.

2-3 NOVEMBER 1971

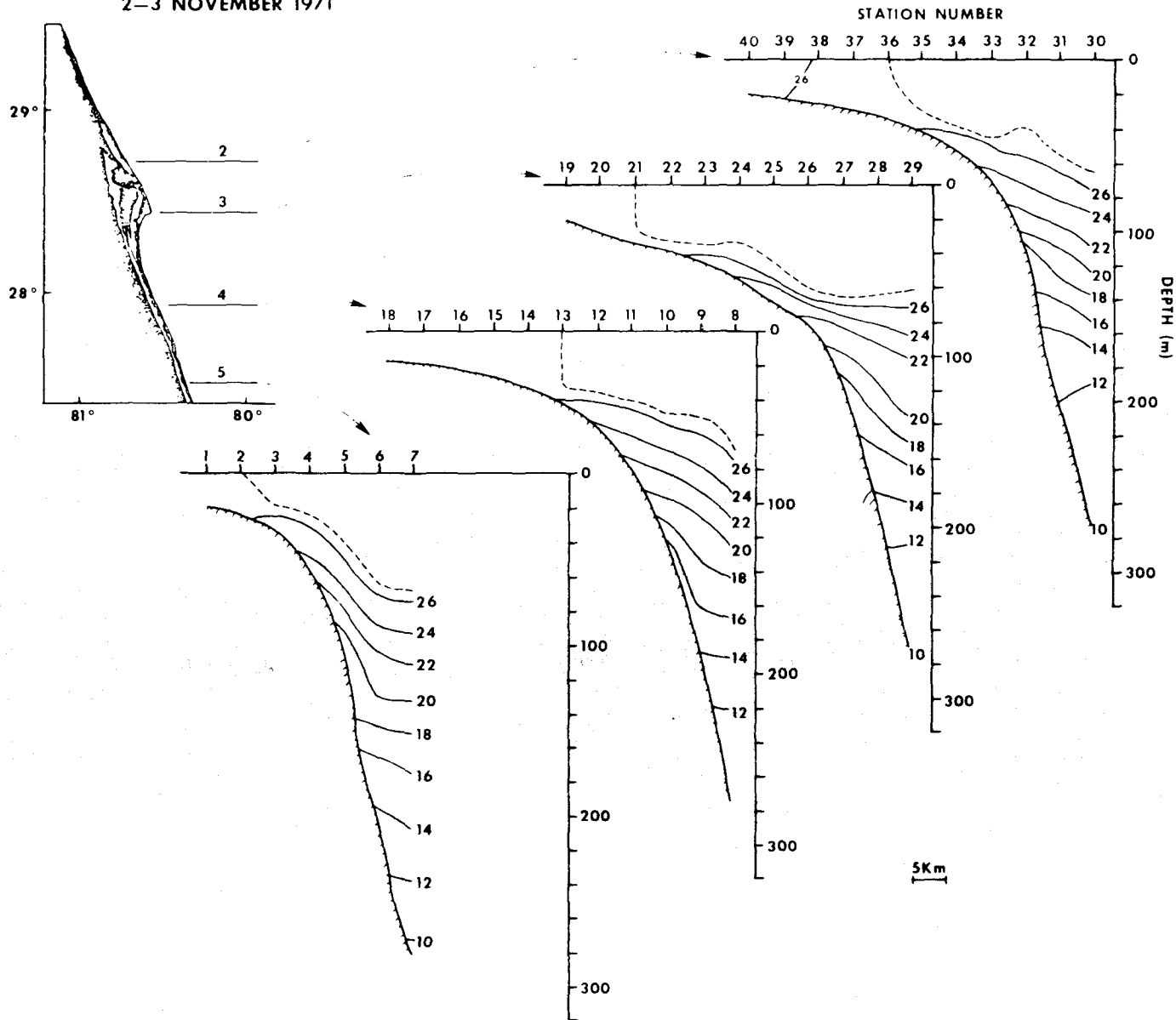


Figure C.8. Vertical XBT temperature sections, 2-3 November 1971.

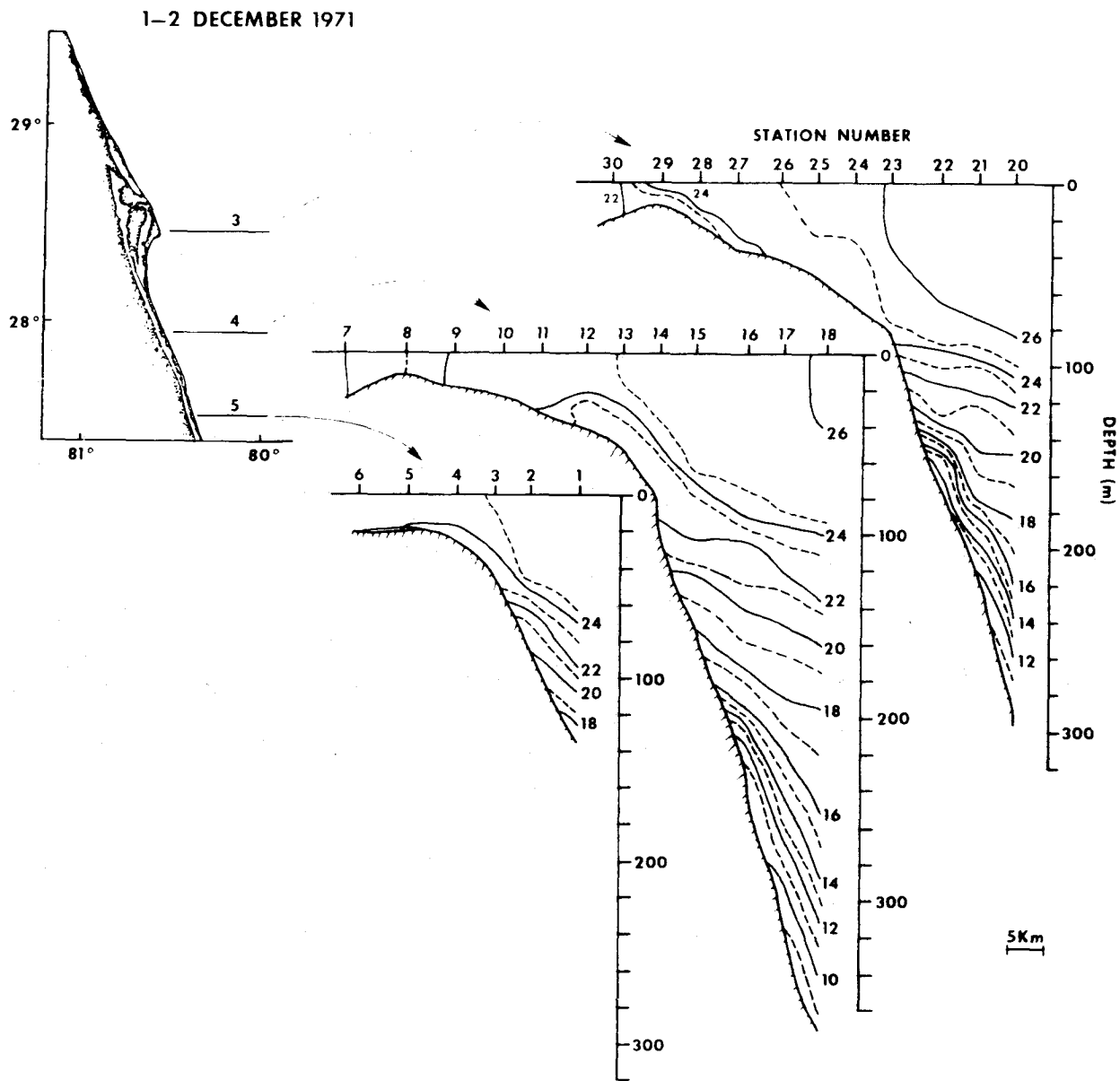


Figure C.9. Vertical XBT temperature sections, 1-2 December 1971.

Appendix D

TABULARIZED DAILY SURF TEMPERATURE
AND
DAILY MEAN BOTTOM TEMPERATURES

Table D.1. Daily surf temperature (°C) at Sun Glow Fishing Pier, Daytona Beach, Florida for 1971.

<u>DAY</u>	<u>JAN</u>	<u>FEB</u>	<u>MAR</u>	<u>APR</u>	<u>MAY</u>	<u>JUN</u>	<u>JUL</u>	<u>AUG</u>	<u>SEP</u>	<u>OCT</u>	<u>NOV</u>	<u>DEC</u>
1	16.7	15.6	17.2	16.1	19.4	22.8	25.0	20.0	25.6	25.6	24.4	18.9
2	14.4	12.8	18.3	16.7	20.6	24.4	25.0	21.1	26.7	25.0	23.9	20.0
3	17.2	15.6	18.3	16.1	22.2	23.9	24.4	21.1	27.2	25.6	23.9	18.9
4	16.7	16.7	16.7	16.7	19.4	24.4	23.9	23.9	26.7	25.6	22.8	17.8
5	18.3	15.0	16.7	17.8	19.4	24.4	24.4	25.0	27.2	26.7	21.1	19.4
6	18.3	15.0	17.2	16.7	20.0	24.4	25.6	25.0	25.6	27.2	22.2	18.9
7	17.8	15.6	18.3	16.1	20.6	25.6	25.6	26.1	25.6	26.1	22.2	18.3
8	16.7	16.7	17.8	15.0	20.6	22.8	25.0	26.7	27.8	26.1	22.2	18.3
9	16.7	14.4	17.2	16.7	21.1	22.2	25.0	26.7	27.2	26.1	20.6	18.9
10	17.2	13.9	16.7	17.2	22.2	22.2	25.6	25.6	27.2	26.1	20.6	19.4
11	16.1	13.9	17.2	17.2	22.8	22.2	24.4	26.7	26.7	24.4	18.3	18.9
12	16.7	15.0	17.2	18.9	22.8	23.3	24.4	27.2	27.2	23.9	18.9	19.4
13	16.7	15.6	18.3	17.8	22.8	22.8	23.9	26.7	26.1	24.4	18.9	18.9
14	16.1	13.9	18.3	17.8	23.3	23.3	24.4	26.7	26.1	25.0	19.4	20.0
15	17.2	13.9	20.0	18.9	22.2	23.3	24.4	26.7	25.6	25.0	18.9	20.0
16	15.6	14.4	18.9	18.9	21.1	23.3	25.6	26.7	26.1	25.6	20.0	20.6
17	13.9	15.0	18.3	18.9	22.2	23.3	25.0	25.6	25.6	26.1	20.6	20.6
18	14.4	16.1	16.7	18.9	22.2	24.4	24.4	21.1	26.1	25.6	20.6	20.0
19	15.0	16.7	17.8	20.0	22.8	25.6	24.4	22.2	26.1	25.6	21.1	17.8
20	11.1	16.7	16.7	20.0	22.2	25.0	24.4	22.8	26.7	23.3	20.6	18.9
21	12.2	15.6	15.6	18.9	20.0	25.6	22.2	23.9	26.1	23.9	19.4	19.4
22	13.3	16.1	17.8	19.4	22.2	25.6	20.6	22.8	26.1	24.4	18.3	19.4
23	13.3	16.1	16.7	18.9	22.8	25.6	20.6	21.1	27.2	23.9	17.2	18.9
24	15.0	15.6	18.3	18.9	23.3	23.3	20.6	20.6	26.7	23.9	20.0	18.9
25	15.6	15.6	17.8	18.9	21.7	25.0	20.6	22.8	26.7	24.4	17.8	19.4
26	15.6	16.1	18.3	20.0	20.0	23.3	21.1	22.8	26.7	23.3	16.7	18.3
27	15.6	17.2	16.7	20.0	20.0	23.3	21.1	24.4	26.7	23.9	18.3	18.9
28	12.8	17.8	18.3	20.0	20.0	24.4	20.0	23.3	26.7	23.3	18.3	18.9
29	13.3		17.8	20.0	20.0	25.6	20.0	24.4	26.1	23.9	18.3	18.3
30	14.4		16.7	20.6	21.1	25.0	20.0	25.6	25.0	23.9	19.4	18.3
31	15.0		16.1		22.8		20.0	25.6		23.9		19.4

Table D.2. Daily mean bottom temperatures ($^{\circ}\text{C}$) at BY1 for 1970. Missing data are due to instrument loss or malfunction.

<u>DAY</u>	<u>M O N T H</u>									
	<u>MAR</u>	<u>APR</u>	<u>MAY</u>	<u>JUN</u>	<u>JUL</u>	<u>AUG</u>	<u>SEP</u>	<u>OCT</u>	<u>NOV</u>	<u>DEC</u>
1		18.0	19.2	23.3	25.6		21.9	25.9	24.1	18.6
2		18.5	19.4	24.3	25.7		21.8	25.8	23.6	18.6
3		18.3	19.3	24.5	25.5		21.7	25.9	23.6	18.7
4		18.5	20.5	23.1	25.9		21.8	26.1	23.5	18.8
5		18.2	20.9	22.8	25.4		22.8	26.1	22.8	19.0
6		18.1	20.7	22.6	23.4		22.9	26.4	22.5	19.0
7		18.0	21.0	22.8	23.1		22.9	26.4	22.3	19.0
8		18.2	20.9	22.8	22.8		23.1	26.2	22.1	19.1
9		18.3	21.5	23.5	22.8		23.0	26.1	22.1	18.9
10		18.2	22.3	24.0	22.7		23.2	26.2	22.0	18.9
11		18.5	21.9	23.7	22.9		23.6	26.3	22.3	19.0
12		18.1	22.4	23.9	21.8		23.7	26.4	23.7	19.1
13		18.2	21.5	23.7	20.7		23.6	26.6	22.7	19.0
14		18.3	21.2	23.9	21.8		23.7	26.6	22.7	19.0
15		18.4	20.8	24.6	22.6		23.7	26.7	22.4	19.1
16		19.1	20.6	24.6			23.7	26.9	22.7	19.0
17		19.5	20.6	24.9			24.1	26.8	22.5	19.0
18		19.8	21.0	24.9			24.0	26.1	22.0	19.0
19		19.6	21.8	25.0			24.5	25.9	22.0	19.0
20		20.2	21.4	25.2			24.8	25.5	21.9	19.0
21		20.1	21.4	25.5			25.1	25.3	21.8	19.0
22		20.1	21.5	25.6			25.1	25.2	21.7	20.7
23		19.6	21.4	24.8			25.7	25.1	21.8	20.7
24		19.2	22.0	24.8			25.7	25.0	21.7	21.3
25		19.4	22.7	24.6			25.6	25.2	20.8	22.4
26		19.2	23.4	23.3			24.8	24.9	19.5	22.9
27		19.4	22.9	21.4		23.5	24.7	24.7	18.9	22.5
28	18.2	19.4	22.7	21.6		22.9	25.9	24.3	18.7	21.8
29	18.1	19.3	23.2	25.4		22.8	26.3	24.2	18.4	21.0
30	18.3	19.5	23.4	25.5		22.3	25.8	24.3	18.3	21.1
31	18.1		23.3			21.9		24.5		20.8

Table D.3. Daily mean bottom temperatures (°C) at BY1 for 1971. Missing data are due to instrument loss or malfunction.

<u>DAY</u>	<u>M O N T H</u>							
	<u>1 9 7 1</u>							
	<u>JAN</u>	<u>FEB</u>	<u>MAR</u>	<u>APR</u>	<u>MAY</u>	<u>JUN</u>	<u>JUL</u>	<u>AUG</u>
1	20.1	18.3	20.9	18.6	20.2		23.1	18.3
2	19.9	18.8	21.1	19.0	20.7		22.5	18.4
3	19.8	18.4	21.4	19.0	20.9		21.5	19.3
4	19.9	19.0	21.2	19.0	21.4		23.8	19.8
5	19.9	19.0	21.1	18.9	21.3		24.3	19.4
6	19.9	18.5	20.3	18.8	21.3		24.3	20.9
7	20.1	18.7	20.4	18.6	21.5		24.3	21.2
8	20.0	19.1	19.9	18.7	22.1		24.1	22.1
9	19.6	18.9	19.8	19.1	22.0		23.9	23.5
10	19.1	18.4	19.5	19.4	21.2		23.2	23.7
11	19.0	18.1	19.2	19.3	20.7		21.6	22.5
12	19.0	17.9	19.2	19.5	20.6		20.5	22.2
13	19.3	17.9	19.3	19.9	21.4		20.8	22.2
14	19.9	16.9	19.4	19.8	21.4		21.7	22.5
15	19.6	16.3	19.3	19.8	19.6		21.7	22.3
16	19.9	16.4	19.3	20.0	18.1		21.9	22.8
17	19.8	16.4	19.5	20.2	17.7		21.7	22.2
18	18.7	16.6	19.4	19.4	17.7		21.4	21.4
19	18.2	16.7	19.4	19.1	17.7		21.5	21.0
20	17.9	16.6	19.1	-	17.4		22.5	20.9
21	17.0	17.4	19.0	18.6	17.6		21.6	21.0
22	16.8	16.9	19.7	18.9	18.3		21.1	21.1
23	16.7	17.7	19.3	19.2			21.7	
24	16.9	18.2	19.4	18.5			21.7	
25	16.8	19.0	19.3	18.4			21.3	
26	17.6	19.6	19.5	18.7			20.7	
27	17.9	20.6	18.8	18.8		21.5	19.9	
28	18.3	20.9	18.6	18.9		21.1	19.1	
29	18.6		18.8	18.8		22.4	18.5	
30	19.3		18.9	18.8		23.1	18.1	
31	19.0		18.5				18.2	

Table D.4. Daily mean bottom temperatures ($^{\circ}\text{C}$) at BY2 for 1970 and 1971. Missing data are due to instrument loss or malfunction.

<u>DAY</u>	<u>1 9 7 0</u>		<u>M O N T H</u>						<u>1 9 7 1</u>	
	<u>NOV</u>	<u>DEC</u>	<u>JAN</u>	<u>FEB</u>	<u>MAR</u>	<u>APR</u>	<u>MAY</u>	<u>JUN</u>	<u>JUL</u>	<u>AUG</u>
1		19.5	20.4			19.3	19.5	21.1	19.9	17.9
2		19.2	20.7			20.6	21.4	21.4	19.9	18.3
3		18.9	20.6			20.7	21.5	21.5	19.3	19.0
4		18.9	20.7			20.5	22.0	21.7	19.0	18.2
5		20.3	21.3			20.4	22.0	21.9	20.6	18.4
6		21.0	20.6			20.3	22.0	22.5	22.5	18.7
7		20.7	20.8			20.2	21.7	22.9	22.8	18.3
8		19.6	20.5			20.4	21.4	22.3	22.9	18.8
9		19.6	20.5			20.3	20.6	22.0	22.3	19.3
10		19.7	19.9			20.5	20.4	21.9	21.1	20.8
11		20.0	19.8			20.4	20.3	22.0	20.5	20.6
12	22.7	20.0	20.1			20.3	20.2	22.9	19.4	21.0
13	23.3	19.9	21.2			20.2	20.9	23.9	20.5	21.4
14	22.9	20.4	21.8			20.5	18.4	23.4	20.6	21.8
15	23.2	19.4	21.5			19.5	17.5	22.9	19.5	21.0
16	22.7	19.3	21.1			19.4	17.2	22.9	19.8	22.0
17	22.8	19.1	20.5		19.9	19.3	17.1	23.0	19.8	21.1
18	22.4	18.9	20.4		19.3	18.8	16.9	23.5	19.8	20.3
19	21.7	19.3	20.1		19.5	18.1	16.9	23.9	20.2	20.3
20	21.9	21.3	18.8		21.0	18.2	17.0	24.0	20.9	20.2
21	23.3	23.1	18.2		19.3	19.2	17.0	24.6	19.7	20.2
22	22.5	22.9	19.0		19.2	18.8	17.3	24.8	17.4	20.6
23	21.7	22.9			19.1	18.2	18.0	24.9	16.8	19.8
24	21.3	23.4			18.6	17.9	18.0	24.4	17.1	18.9
25	20.4	22.9			19.6	18.0	18.2	22.9	17.8	
26	19.8	22.7			19.6	18.0	18.3	21.7	18.0	
27	19.6	22.1			19.4	18.0	18.5	19.8	17.8	
28	19.8	21.8			19.2	18.1	18.8	19.5	17.2	
29	20.7	21.8			19.4	18.3	19.0	19.5	17.4	
30	19.9	21.5			19.4	18.4	19.8	19.8	17.2	
31		21.1			19.2		20.7		17.1	

Table D.5. Daily mean bottom temperatures (°C) at CM1 and CM2 during June, July, 1971.

<u>DATE</u>	<u>CM1</u>	<u>CM2</u>
June 26	18.3	15.8
27	17.9	16.0
28	17.7	17.1
29	17.0	18.7
30	18.1	18.0
July 1	18.7	16.1
2	18.7	15.5
3	18.1	14.4
4	19.0	15.5
5	22.2	16.4
6	21.7	15.7
7	21.6	16.6
8	21.1	18.0
9	19.6	17.7
10	18.9	18.1
11	18.9	21.1
12	20.5	21.4
13	21.7	19.6
14	21.6	18.3
15	21.8	16.1
16	21.8	15.4
17	21.8	14.5
18	21.9	15.1
19	21.2	15.6
20	20.2	12.6
21	19.1	12.0
22	18.8	14.5
23	17.2	18.2

BIBLIOGRAPHY

- Allen, Donald M., and T. J. Costello (1972) The calico scallop, Argopecten Gibbus. NOAA Tech. Rep., NMFS SSRF-659, 19 pp.
- Allen, J. S. (1973) Upwelling and coastal jets in a continuously stratified ocean. *J. Phys. Oceanogr.* 3, 245-257.
- Allen, J. S. (1975) Coastal trapped waves in a stratified ocean. *J. Phys. Oceanogr.*, 5, 300-325.
- Allen, J. S. (1976) Continental shelf waves and alongshore variations in bottom topography and coastline. *J. Phys. Oceanogr.*, 6, 864-878.
- Allen, J. S. and P. K. Kundu (1978) On the momentum and mass balance on the Oregon Shelf. *J. Phys. Oceanogr.*, 8, 13-27.
- Arthur, R. S. (1965) On the calculation of vertical motion in eastern boundary currents from determinations of horizontal motion. *J. Geophys. Res.*, 70(12), 2799-2803.
- Atkinson, Larry P. (1977) Modes of Gulf Stream intrusion into the South Atlantic Bight shelf waters. *Geophys. Res. Ltrs.*, 4(12), 583-586.
- Atkinson, Larry P., Gustav-Adolf Paffenhöffer, and William M. Dunstan (1978) The chemical and biological effect of a Gulf Stream intrusion off St. Augustine, Florida. *Bull. Mar. Sci.*, 28(4), 667-679.
- Blackman, R. B. and J. W. Tukey (1958) The Measurement of Power Spectra. Dover Publ. Inc., New York, 190 pp.

- Blanton, Jackson (1971) Exchange of Gulf Stream water with North Carolina shelf water in Onslow Bay during stratified conditions. *Deep-Sea Res.*, 18, 167-178.
- Blanton, Jackson and L. J. Pietrafesa (1978) Flushing of the continental shelf south of Cape Hatteras by the Gulf Stream. *Geophys. Res. Ltrs.*, 5(6), 495-498.
- Brooks, D. A. (1975) Wind-forced continental shelf waves in the Florida Current. UM-RSMAS Techn. Rep. #75026, 268 pp.
- Brooks, D. A. (1978) Subtidal sea level fluctuations and their relation to atmospheric forcing along the North Carolina Coast. *J. Phys. Oceanogr.*, 8, 481-493.
- Brooks, D. A. and C. N. K. Mooers (1977 a) Free, stable continental shelf waves in a sheared, barotropic boundary current. *J. Phys. Oceanogr.*, 7, 380-388.
- Brooks, D. A. and C. N. K. Mooers (1977 b) Wind-forced continental shelf waves in the Florida Current. *J. Geophys. Res.*, 82, 2569-2576.
- Bullis, H. R., Jr., and R. Cummins, Jr. (1961) An interim report of the Cape Canaveral calico scallop bed. *Comm. Fish. Rev.*, 23(10), 1-8.
- Bullis, H. R., Jr., and J. R. Thompson (1965) Collections by the exploratory fishing vessels Oregon, Silver Bay, Combat, and Pelican made during 1956 to 1960 in the southwestern North Atlantic. U.S. Fish Wildl. Serv., Spec. Sci. Rep. Fish., 510, 130 pp.

- Bumpus, Dean F. (1955) The circulation over the continental shelf south of Cape Hatteras. *Trans. Am. Geophys. Un.*, 36, 601-611.
- Bumpus, Dean F. (1964) Report on non-tidal drift experiments off Cape Canaveral during 1962. *Woods Hole Oceanogr. Inst. Ref. No. 64-6*, 15 pp.
- Bumpus, Dean F. and E. Lowe Pierce (1955) The hydrography and the distribution of chaetognaths over the continental shelf off North Carolina. *Pap. Mar. Biol. Oceanogr. Suppl. Deep-Sea Res.*, 3, 92-109.
- Carter, H. H. and Akira Okubo (1965) A study of the physical process of movement and dispersion in the Cape Kennedy area. *Cheas. Bay Inst., Johns Hopkins Univ., Ref. 65-2*, 150 pp.
- Costello, T. J., J. Harold Hudson, John L. Dupuy and Samuel Rivkin (1972) Larval culture of the calico scallop, Argopecten Gibbus. *Proc. Nat. Shellfish. Assoc.*, 63, 72-76.
- Davis, John C. (1973) Statistics and Data Analysis in Geology. John Wiley and Sons, Inc., New York, 550 pp.
- Drummond, S. B. (1969) Explorations for calico scallop, Pecten gibbus, in the area off Cape Kennedy, Florida, 1960-66. *Fish. Ind. Res.*, 5, 85-101.
- Dúing, Walter O. (1975) Synoptic studies of transients in the Florida Current. *J. Mar. Res.*, 33(1), 53-73.

- Dúing, Walter O. and Donald Johnson (1971) High resolution current profiling in the Straits of Florida. Sci. Rep., Univ. Miami, ML71085, 19 pp.
- Dúing, Walter O. and D. R. Johnson (1972) High resolution current profiling in the Straits of Florida. Deep-Sea Res., 19, 259-274.
- Dúing, Walter O., Christopher N. K. Mooers, and Thomas N. Lee (1977) Low-frequency variability in the Florida Current and relations to atmospheric forcing from 1972 to 1974. J. Mar. Res., 34(1), 129-161.
- Fuglister, F. C. (1951 a) Annual variations in current speeds in the Gulf Stream. J. Mar. Res., 10, 119-127.
- Fuglister, F. C. (1951 b) Multiple currents in the Gulf Stream system. Tellus, 3, 230-233.
- Gill, A. E., and A. J. Clarke (1974) Wind-induced upwelling, coastal currents and sea-level changes. Deep-Sea Res., 21, 325-345.
- Green, C. K. (1944) Summer upwelling, northeast coast of Florida. Science, 100, 546-547.
- Hurlbert, H. E. and J. D. Thompson (1973) Coastal upwelling on a β -plane. J. Phys. Oceanogr., 3, 16-32.
- Jenkins, Gwilym, M. and Donald G. Watts (1968) Spectral Analysis and Its Applications. Holden-Day, San Francisco, 525 pp.

- Johnson, Walter R. (1976) Cyclesonde measurements in the upwelling region off Oregon. Univ. Miami, Rosenstiel School Mar. Atmos. Sci., TR76-1.
- Kundu, P. K., J. S. Allen and R. L. Smith (1974) Modal decomposition of the velocity field near the Oregon Coast. *J. Phys. Oceanogr.*, 5, 683-704.
- Kutzbach, J. E. (1967) Empirical eigenvectors of sea level, pressure, surface temperature, and precipitation complexes over North America. *J. App. Met.*, 6, 791-802.
- Lee, Thomas N. (1975) Florida Current spin-off eddies. *Deep-Sea Res.*, 22, 753-765.
- Lee, Thomas N. and Dennis A. Mayer (1977) Low-frequency current variability and spin-off eddies along the shelf off southeast Florida. *J. Mar. Res.*, 35(1), 193-220.
- Lee, Thomas N. and C. N. K. Mooers (1977) Near-bottom temperature and current variability over the Miami Slope and Terrace. *Bull. Mar. Sci.*, 27(4), 758-775.
- Lorenz, E. N. (1956) Empirical orthogonal functions and statistical weather prediction. Science Report No. 1, Contract AF19 (604)-1566, Dep. of Meteorology, MIT, 49 pp.
- Mooers, C. N. K. and J. S. Allen (1973) Final Report of the Coastal Upwelling Ecosystems Analysis Summer 1973 Theoretical Workshop. School of Oceanography, Oregon State University.

- Mooers, C. N. K. and D. A. Brooks (1977) Fluctuations in the Florida Current, summer 1970. *Deep-Sea Res.*, 24(5), 399-425.
- Mysak, L. A. and B. V. Hamon (1969) Low-frequency sea level behavior and continental shelf waves off North Carolina. *J. Geophys. Res.*, 74, 1397-1405.
- Niiler, P. P. and L. A. Mysak (1971) Barotropic waves along an eastern continental shelf. *Geophys. Fluid Dyn.*, 2, 273-288.
- Niiler, P. P. and W. S. Richardson (1973) Seasonal variability of the Florida Current. *J. Mar. Res.*, 31(3), 144-167.
- O'Brien, J. J. and H. E. Hurlbert (1972) A numerical model of coastal upwelling. *J. Phys. Oceanogr.*, 2, 14-20.
- Orlanski, I. (1969) The influence of bottom topography on the stability of jets in a baroclinic fluid. *J. Atmos. Sci.*, 26, 1216-1232.
- Orlanski, I. and M. D. Cox (1973) Baroclinic instability in ocean currents. *Geophys. Fluid Dyn.*, 4, 297-332.
- Parr, A. E. (1937) Report on hydrographic observations at a series of anchor stations across the straits of Florida. *Bull. Bingham oceanogr. Coll.*, 6(3), 62 pp.
- Partagas, J. F. P. and C. N. K. Mooers (1975) A sub-synoptic study of winter cold fronts in Florida. *Month. Wea. Rev.*, 103(8), 742-744.
- Roe, R. B., R. Cummins, Jr., and H. R. Bullis, Jr. (1971) Calico scallop distribution, abundance, and yield off eastern Florida, 1967-1968. *Nat'l. Mar. Fish. Serv., Fish. Bull.*, 69, 399-409.

- Schott, F. and W. Dúing (1976) Continental shelf waves in the Florida Current. *J. Phys. Oceanogr.*, 6, 451-460.
- Schmitz, W. J. and W. S. Richardson (1968) On the transport of the Florida Current. *Deep-Sea Res.*, 15, 679-693.
- Smith, R. L. (1968) Upwelling. *Oceanogr. Marine Biol. Ann. Rev.*, 6, 11-46.
- Smith, R. L. (1974) A description of current, wind, and sea-level variations during coastal upwelling off the Oregon coast, July - August 1972. *J. Geophys. Res.*, 79, 435-443.
- Stefánsson, Unstein, Larry P. Atkinson and Dean F. Bumpus (1971) Hydrographic properties and circulation of the North Carolina shelf and slope waters. *Deep-Sea Res.*, 18, 383-420.
- Stone, R. B. and T. R. Azarovitz (1968) An occurrence of unusually cold water off the Florida coast. *Underwater Naturalist*, 5(2), 14-17.
- Taylor, C. B. and H. B. Stewart, Jr. (1959) Summer upwelling along the east coast of Florida. *J. Geophys. Res.*, 64(1), 33-40.
- von Arx, W. S., D. F. Bumpus, and W. S. Richardson (1955) On the fine-structure of the Gulf Stream front. *Deep-Sea Res.*, 3, 46-65.
- von Arx, W. S. (1962) An Introduction to Physical Oceanography. Addison-Wesley, Reading, Mass., 422 pp.
- Wagner, L. P. (1957) Note on the Daytona Beach cold water. *Tech. Rep. Marine Lab., Univ. Miami Ref. 57-9*, 81-82.

- Walin, G. (1972) Some observations of temperature fluctuations in the coastal region of the Baltic. *Tellus*, 24, 187-198.
- Waller, T. R. (1969) The evolution of the Argopecten gibbus stock (Mollusca: Bivalvia), with emphasis on the Tertiary and Quaternary species of eastern North America. *Paleontol. Soc., Mem.* 3, 125 pp.
- Wang, Dong-Ping and Christopher N. K. Mooers (1976) Coastal-trapped waves in a continuously stratified ocean. *J. Phys. Oceanogr.*, 6, 853-863.
- Webster, Ferris (1961) A description of Gulf Stream meanders off Onslow Bay. *Deep-Sea Res.*, 8, 130-143.
- Witte, J., C. N. K. Mooers, and P. Niiler (1977) A model shelf dynamics program. Report to the National Science Foundation, Office of IDOE, NOVA/NYIT Univ. Press, 73 pp.